

AD-A019 324

APPLICATION OF A NEAR-OPTIMAL CLOSED LOOP CONTROL LAW TO
A PURSUIT-EVASION GAME BETWEEN TWO SPACECRAFT

Gary D. Bohn

Air Force Institute of Technology
Wright-Patterson Air Force Base, Ohio

December 1975

DISTRIBUTED BY:

NTIS

National Technical Information Service
U. S. DEPARTMENT OF COMMERCE

UNCLASSIFIED

SECURITY CLASSIFICATION OF THIS PAGE(When Data Entered)

correction and the state error are tested. Three coplanar trajectories and two non-coplanar trajectories are tested using various vehicle characteristics.

The control law is shown to provide the pursuer an effective means to take advantage of non-optimal play by his opponent; thereby reducing the final range below the original TPBVP solution.

Plots comparing the TPBVP solutions and the trajectories resulting from application of the control law against several non-optimal evaders are presented.

i(a)

UNCLASSIFIED

SECURITY CLASSIFICATION OF THIS PAGE(When Data Entered)

GA/MC/75D-2 ✓

①

APPLICATION OF A NEAR-OPTIMAL CLOSED
LOOP CONTROL LAW TO A PURSUIT-EVASION
GAME BETWEEN TWO SPACECRAFT

THESIS

GA/MC/75D-2 ✓

Gary D. Bohn
Captain USAF

A

Approved for public release; distribution unlimited

i(A)

APPLICATION OF A NEAR-OPTIMAL CLOSED
LOOP CONTROL LAW TO A PURSUIT-EVASION
GAME BETWEEN TWO SPACECRAFT

THESIS

Presented to the Faculty of the School of Engineering
of the Air Force Institute of Technology
Air University
in Partial Fulfillment of the
Requirements for the Degree of
Master of Science

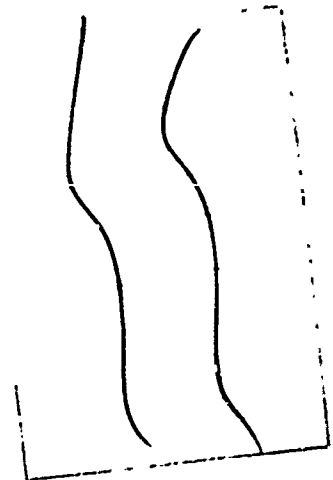
by

Gary D. Bohn, B.S.E.E.

Captain USAF

Graduate Astronautics

December 1975



Approved for public release; distribution unlimited.

1 (c)

Preface

This report addresses the implementation of a pseudo-closed loop control law to a spacecraft intercept problem formulated as a differential game. Although it is recognized that a solution to the two-point boundary value problem is required to initiate this control law, methods to obtain solutions are not discussed in this report. My purpose is to validate the control law for a more realistic problem than has been previously demonstrated.

I wish to express my sincere appreciation to Prof. Gerald M. Anderson of the Air Force Institute of Technology for his advice and assistance in this effort.

Gary D. Bohn

Contents

Preface	11
List of Figures	v
List of Tables	ix
List of Symbols	x
Abstract	xii
I. Introduction	1
Background	1
Statement of the Problem	1
II. Equations of Motion	4
Coplanar Equations of Motion	4
Three Dimensional Equations of Motion	7
III. Differential Game Formulation	11
Coplanar Game	11
Three Dimensional Game	16
IV. Pseudo-Closed Loop Control Law	27
Backward Sweep Method	27
Transition Matrix Method	30
Implementation of the Control Law	31
Linearized TPBVP Coefficients and Terminal Conditions	32
V. Results	34
Coplanar Model	34
Three Dimensional Model	37
General Comments	39
VI. Conclusions	52
Bibliography	54
Appendix A: Coefficients for the Linearized TPBVP	55
Coplanar Model	56
Three Dimensional Model	59

Appendix B: Terminal Conditions for the Control Laws	66
Coplanar Model	66
Three Dimensional Model	68
Appendix C: Plots for Trajectory 1	71
Appendix D: Plots for Trajectory 2	93
Appendix E: Plots for Trajectory 3	101
Appendix F: Plots for Trajectory 4	109
Appendix G: Plots for Trajectory 5	115
Vita	124

List of Figures

<u>Figure</u>		<u>Page</u>
1	Coplanar Orbital Geometry	4
2	Three Dimensional Orbital Reference Frame .	8
3	Body Fixed Reference Frame	9
4	Coplanar Range	12
5	Three Dimensional Range	18
6	Control Law Implementation	33
C-1	Trajectory 1, Backward Sweep Method. V = 3.0, Sampling Interval = 0.012 TU. . .	72
C-2	Trajectory 1, Backward Sweep Method. V = 2.0, Sampling Interval = 0.012 TU. . .	73
C-3	Trajectory 1, Backward Sweep Method. V = 1.0, Sampling Interval = 0.008 TU. . .	74
C-4	Trajectory 1, Backward Sweep Method. V = 0.0, Sampling Interval = 0.012 TU. . .	75
C-5	Trajectory 1, Backward Sweep Method. V = -1.0, Sampling Interval = 0.012 TU. . .	76
C-6	Trajectory 1, Backward Sweep Method. V = -2.0, Sampling Interval = 0.012 TU. . .	77
C-7	Trajectory 1, Backward Sweep Method. V = -3.0, Sampling Interval = 0.012 TU. . .	78
C-8	Trajectory 1, Transition Matrix Method. V = 3.0, Sampling Interval = 0.012 TU. . .	79
C-9	Trajectory 1, Transition Matrix Method. V = 2.0, Sampling Interval = 0.012 TU. . .	80
C-10	Trajectory 1, Transition Matrix Method. V = 1.0, Sampling Interval = 0.012 TU. . .	81
C-11	Trajectory 1, Transition Matrix Method. V = 0.0, Sampling Interval = 0.012 TU. . .	82
C-12	Trajectory 1, Transition Matrix Method. V = -1.0, Sampling Interval = 0.012 TU. . .	83

C-13	Trajectory 1, Transition Matrix Method. V = -2.0, Sampling Interval = 0.012 TU. . .	84
C-14	Trajectory 1, Transition Matrix Method. V = -3.0, Sampling Interval = 0.012 TU. . .	85
C-15	Trajectory 1, Backward Sweep Method. V = 3.0, Sampling Interval = 0.016 TU. . .	86
C-16	Trajectory 1, Backward Sweep Method. V = 2.0, Sampling Interval = 0.016 TU. . .	87
C-17	Trajectory 1, Backward Sweep Method. V = 1.0, Sampling Interval = 0.016 TU. . .	88
C-18	Trajectory 1, Backward Sweep Method. V = 0.0, Sampling Interval = 0.016 TU. . .	89
C-19	Trajectory 1, Backward Sweep Method. V = -1.0, Sampling Interval = 0.016 TU. . .	90
C-20	Trajectory 1, Backward Sweep Method. V = -2.0, Sampling Interval = 0.016 TU. . .	91
C-21	Trajectory 1, Backward Sweep Method. V = -3.0, Sampling Interval = 0.016 TU. . .	92
D-1	Trajectory 2, Backward Sweep Method. V = 3.0, Sampling Interval = 0.012 TU. . .	94
D-2	Trajectory 2, Backward Sweep Method. V = 2.0, Sampling Interval = 0.012 TU. . .	95
D-3	Trajectory 2, Backward Sweep Method. V = 1.0, Sampling Interval = 0.012 TU. . .	96
D-4	Trajectory 2, Backward Sweep Method. V = 0.0, Sampling Interval = 0.012 TU. . .	97
D-5	Trajectory 2, Backward Sweep Method. V = -1.0, Sampling Interval = 0.012 TU. . .	98
D-6	Trajectory 2, Backward Sweep Method. V = -2.0, Sampling Interval = 0.012 TU. . .	99
D-7	Trajectory 2, Backward Sweep Method. V = -3.0, Sampling Interval = 0.012 TU. . .	100
E-1	Trajectory 3, Transition Matrix Method. V = 3.0, Sampling Interval = 0.012 TU. . .	102

E-2	Trajectory 3, Transition Matrix Method. V = 2.0, Sampling Interval = 0.012 TU. . .	103
E-3	Trajectory 3, Transition Matrix Method. V = 1.0, Sampling Interval = 0.012 TU. . .	104
E-4	Trajectory 3, Transition Matrix Method. V = 0.0, Sampling Interval = 0.012 TU. . .	105
E-5	Trajectory 3, Transition Matrix Method. V = -1.0, Sampling Interval = 0.012 TU. . .	106
E-6	Trajectory 3, Transition Matrix Method. V = -2.0, Sampling Interval = 0.012 TU. . .	107
E-7	Trajectory 3, Transition Matrix Method. V = -3.0, Sampling Interval = 0.012 TU. . .	108
F-1	Trajectory 4, Backward Sweep Method. V ₁ = 0.0, V ₂ = 1.0, Sampling Interval = 0.024 TU.	110
F-2	Trajectory 4, Backward Sweep Method. V ₁ = 0.0, V ₂ = -1.0, Sampling Interval = 0.024 TU.	111
F-3	Trajectory 4, Backward Sweep Method. V ₁ = 3.14, V ₂ = 1.0, Sampling Interval = 0.024 TU.	112
F-4	Trajectory 4, Backward Sweep Method. V ₁ = 3.14, V ₂ = -1.0, Sampling Interval = 0.024 TU.	113
F-5	Trajectory 4, Backward Sweep Method. V ₁ = 1.571, V ₂ = 0.0, Sampling Interval = 0.024 TU.	114
G-1	Trajectory 5, Backward Sweep Method. V ₁ = 0.0, V ₂ = 1.0, Sampling Interval = 0.012 TU.	116
G-2	Trajectory 5, Backward Sweep Method. V ₁ = 0.0, V ₂ = -1.0, Sampling Interval = 0.024 TU.	117
G-3	Trajectory 5, Backward Sweep Method. V ₁ = 1.571, V ₂ = 1.0, Sampling Interval = 0.016 TU.	118

G-4	Trajectory 5, Backward Sweep Method. $V_1 = 1.571, V_2 = -1.0$, Sampling Interval = 0.024 TU.	119
G-5	Trajectory 5, Backward Sweep Method. $V_1 = 3.14, V_2 = 1.0$, Sampling Interval = 0.024 TU.	120
G-6	Trajectory 5, Backward Sweep Method. $V_1 = 3.14, V_2 = -1.0$, Sampling Interval = 0.024 TU.	121
G-7	Trajectory 5, Backward Sweep Method. $V_1 = 4.71, V_2 = 1.0$, Sampling Interval = 0.024 TU.	122
G-8	Trajectory 5, Backward Sweep Method. $V_1 = 4.71, V_2 = -1.0$, Sampling Interval = 0.024 TU.	123

List of Tables

<u>Table</u>		<u>Page</u>
I	Test Cases	35
II	Final range for Non-Optimal Evader (Coplanar)	38
III	Final Range for Non-Optimal Evader (Non-coplanar)	40
IV	Predicted Final Range At Each Sampling Time (Trajectory 1, Transition Matrix Method, Sampling Interval = 0.012 TU.) . .	43
V	Predicted Final Range At Each Sampling Time (Trajectory 1, Backward Sweep Method, Sampling Interval = 0.012 TU.)	44
VI	Predicted Final Range At Each Sampling Time (Trajectory 1, Backward Sweep Method, Sampling Interval = 0.016 TU.)	45
VII	Predicted Final Range At Each Sampling Time (Trajectory 1, Backward Sweep Method, V = 1.0, Sampling Interval = 0.008 TU.) . .	46
VIII	Predicted Final Range At Each Sampling Time (Trajectory 2, Backward Sweep Method, Sampling Interval = 0.012 TU.)	47
IX	Predicted Final Range At Each Sampling Time (Trajectory 3, Transition Matrix Method, Sampling Interval = 0.012 TU.) . .	48
X	Predicted Final Range At Each Sampling Time (Trajectory 4, Backward Sweep Method, Sampling Interval = 0.024 TU.)	49
XI	Predicted Final Range At Each Sampling Time (Trajectory 5, Backward Sweep Method, Sampling Interval = 0.024 TU.)	50
XII	Predicted Final Range At Each Sampling Time (Trajectory 5, Backward Sweep Method, V ₁ = 0.0, V ₂ = 1.0, Sampling Interval = 0.012 TU.)	51
XIII	Predicted Final Range At Each Sampling Time (Trajectory 5, Backward Sweep Method, V ₁ = 1.571, V ₂ = 1.0, Sampling Interval = 0.016 TU.)	51

List of Symbols

<u>Symbol</u>	<u>Definition</u>
C	Normalized thrust
D	Range between vehicles
F	Thrust
f_x	Matrix of partial derivatives of state differential equation vector with respect to states
f_λ	Matrix of partial derivatives of state differential equation vector with respect to costates
g_x	Matrix of partial derivatives of costate differential equation vector with respect to states
g_λ	Matrix of partial derivatives of costate differential equation vector with respect to costates
H	Hamiltonian function
J	Payoff function
L	Path (integral) payoff
m	Vehicle mass
r	Radius from earth's center
r_0	Radius of spherical earth
t	Time
u	Pursuer's control angle
v	Evader's control angle
V_0	Velocity of circular orbit at earth's surface
V_r	Radial velocity
V_θ	Transverse velocity (θ)

<u>Symbol</u>	<u>Definition</u>
v_ϕ	Transverse velocity (ϕ)
x	State variable
α	Control angle
δx	State error
$\delta \lambda$	Costate correction
θ	Angular position of spacecraft measured from inertial \hat{e}_z axis
λ	Costates of x
v	Constant Lagrange multiplier associated with the terminal surface
μ	Earth gravitation constant
τ	Characteristic time unit (TU)
ϕ	Angular position of spacecraft in the reference plane, measured from the inertial \hat{e}_x axis
Φ	For control law formulation, the terminal payoff function (the same as J for this problem)
Φ	State transition matrix
ψ	Terminal surface

Subscripts

e	Denotes evader
f	Final conditions
k	Sampling time index
o	Initial conditions
p	Denotes pursuer

Abstract

A near-optimal closed loop control law for zero-sum perfect information differential games is tested on a free final time, minimax range, pursuit-evasion game between two constant thrust spacecraft.

The control law is based on a periodic first order update to the costate vector. This costate correction is generated from the state error from a reference TPBVP solution. Two nearly equivalent methods to obtain the relationship between the costate correction and the state error are tested. Three coplanar trajectories and two non-coplanar trajectories are tested using various vehicle characteristics.

The control law is shown to provide the pursuer an effective means to take advantage of non-optimal play by his opponent; thereby reducing the final range below the original TPBVP solution.

Plots comparing the TPBVP solutions and the trajectories resulting from application of the control law against several non-optimal evaders are presented.

APPLICATION OF A NEAR-OPTIMAL CLOSED LOOP
CONTROL LAW TO A PURSUIT-EVASION
GAME BETWEEN TWO SPACECRAFT

I. Introduction

Background

The theory of zero-sum perfect information differential games has been successfully applied to a large number of problems in which two players have diametrically opposed goals. One serious drawback to the application of differential games, however, is that closed loop control laws, by which one player could take advantage of non-optimal play by his opponent, have not been developed for realistic, non-linear problems. To date, closed loop control laws have been developed only for linear-quadratic problems (Ref 3) and for simple problems of low state dimension (Ref 5).

Anderson (Refs 1,2) has proposed two methods to generate near-optimal closed loop solutions to non-linear differential games. However, he has applied these methods only to simple problems with low state dimension. The success of these methods on realistic non-linear problems with large state dimension has yet to be demonstrated.

Statement of the Problem

Scope. This study applies these two near-optimal closed loop control laws to a free final time, minimax range

pursuit-evasion game between two spacecraft. Both coplanar and three dimensional models are used.

Assumptions. Both vehicles thrust continuously with constant thrust, the thrust of both vehicles being the same. If either vehicle ceased thrusting, the problem becomes a one player game, the advantage passing to the player which is still thrusting. A simple intercept or avoidance problem results.

Two-body dynamics with an inverse square gravitational field are used. The central attracting body is considered to be a homogeneous sphere, and the vehicles are considered to be point masses. All perturbative forces, other than thrust, are neglected.

The payoff is the separation between the vehicles at final time. The pursuer's goal is to minimize final range; the evader's goal to maximize this same quantity. Each player has perfect information on the current state of the system and the performance capabilities of his opponent. Each controls his thrust direction to achieve his desired goal.

The mass of each vehicle decreases at a constant rate proportional to the vehicles' thrust. Minimum range is assumed to occur prior to either vehicle exhausting its available fuel.

There are no barriers or ill-defined surfaces. That is, it is assumed that the solution in the small is valid.

Approach. The two-point boundary value problem (TPBVP)

describing the coplanar free final time, minimax range differential game will be formulated and solved, using a variety of vehicle thrust-to-weight ratios and different final ranges.

Using a TPBVP solution as a nominal trajectory, both control laws will be extensively tested, using various non-optimal controls for the evader, in order to demonstrate the equivalence of the two methods. In addition, the effect of different sampling intervals will also be investigated. Each control law will then be tested on other nominal trajectories, allowing the evader to use several non-optimal controls.

Finally, the model will be expanded to allow both players to thrust out of the plane of their trajectories, and to allow a non-coplanar intercept. Two nominal trajectories will be investigated here; the first, in which both vehicles are initially moving in the same reference plane, and the last, in which the pursuer is initially out of the reference plane of the evader.

II. Equations of Motion

Coplanar Equations of Motion

The equations of motion for two-body orbital dynamics are

$$\ddot{r} - r\dot{\phi}^2 = -\frac{\mu}{r^2} + \frac{F\sin\alpha}{m} \quad (1)$$

$$r\ddot{\phi} + 2\dot{r}\dot{\phi} = \frac{F\cos\alpha}{m} \quad (2)$$

where the thrust angle α is measured from the local horizontal as shown in Fig. 1. Additionally, since the thrust is constant, the mass is allowed to vary by

$$m = m_0 + \dot{m}t \quad (3)$$

$$\dot{m} = \frac{-F}{I_{sp}g_e} \quad (4)$$

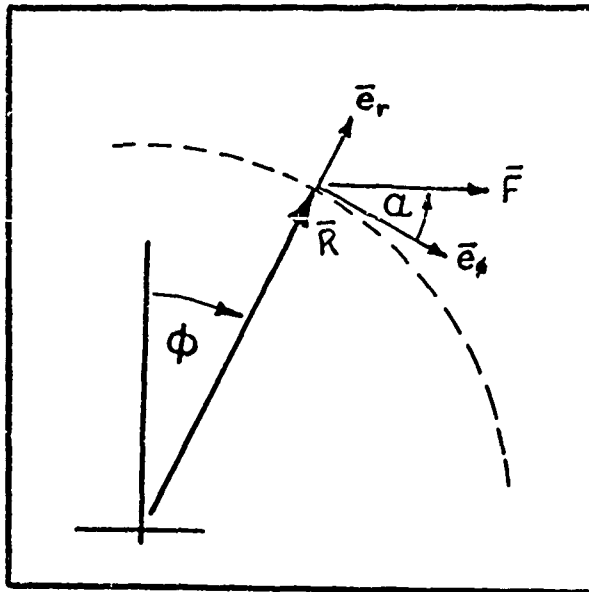


Fig. 1. Coplanar Orbital Geometry.

Rewriting Eqs. (1) and (2) in terms of the radial and transverse velocities, V_r and V_ϕ , gives

$$\dot{V}_r - \frac{V_\phi^2}{r} = -\frac{\mu}{r^2} + \frac{F \sin \alpha}{m} \quad (5)$$

$$\dot{V}_\phi + \frac{V_r V_\phi}{r} = \frac{F \cos \alpha}{m} \quad (6)$$

where

$$V_r = \dot{r} \quad (7)$$

$$V_\phi = r \dot{\phi} \quad (8)$$

It is desirable to normalize the equations of motion so that all parameters are the same order of magnitude. This is done by defining the state variables

$$X_1 = \frac{r}{r_0} \quad (9)$$

$$X_2 = \frac{V_r}{V_0} \quad (10)$$

$$X_3 = \phi \quad (11)$$

$$X_4 = \frac{V_\phi}{V_0} \quad (12)$$

where r_0 is the radius of a circular orbit at the surface of the earth, and V_0 is the transverse velocity of that circular orbit.

The non-dimensional time unit is introduced

$$\tau = \frac{V_0 t}{r_0} \quad (13)$$

The time derivatives must be converted to tau derivatives by

$$\frac{d(\cdot)}{d\tau} = \frac{d(\cdot)}{dt} \left(\frac{dt}{d\tau} \right) = \left(\frac{r_0}{V_0} \right) \frac{d(\cdot)}{dt} \quad (14)$$

The vehicle mass and mass flow rate are also normalized relative to the initial mass so that

$$m = 1 + \dot{m}\tau \quad (15)$$

$$\dot{m} = - \frac{r_0 F}{V_0 m_0 I_{sp} g_e} \quad (16)$$

Using Eqs. (9) thru (12) and Eq. (14), the normalized state differential equations become¹

$$X_1' = X_2 \quad (17)$$

$$X_2' = \frac{X_4^2}{X_1} - \frac{1}{X_1^2} + \frac{C \sin \alpha}{m} \quad (18)$$

$$X_3' = \frac{X_4}{X_1} \quad (19)$$

$$X_4' = - \frac{X_2 X_4}{X_1} + \frac{C \cos \alpha}{m} \quad (20)$$

¹ Tau derivatives will be indicated by a prime (') to avoid confusion with time derivatives.

where

$$c = \frac{r_0 F}{V_0^2 m_0} \quad (21)$$

These equations of motion apply to both vehicles.

Three Dimensional Equations of Motion

If the pursuer and the evader are not initially in the same plane, or if the thrust direction is not restricted to lie in the orbital plane of the vehicle, then three dimensional equations of motion must be used.

Using the spherical coordinate system indicated in Fig. 2, the three dimensional equations of motion for two body dynamics are

$$\ddot{r} - r\dot{\theta}^2 - r\dot{\phi}^2 \sin^2 \theta = -\frac{\mu}{r^2} + \frac{F \sin \alpha_1}{m} \quad (22)$$

$$r\ddot{\theta} + 2\dot{r}\dot{\theta} - r\dot{\phi}^2 \cos \theta \sin \theta = \frac{F \cos \alpha_1 \cos \alpha_2}{m} \quad (23)$$

$$r\ddot{\phi} \sin \theta + 2r\dot{\theta}\dot{\phi} \cos \theta + 2\dot{r}\dot{\phi} \sin \theta = \frac{F \sin \alpha_1 \cos \alpha_2}{m} \quad (24)$$

where the thrust angles α_1 and α_2 are measured as depicted in Fig. 3.

If the vehicles lie in the same reference plane ($\theta = \pi/2$), and the thrust direction is restricted to lie in the plane of the orbit, these equations reduce to the coplanar equations of motion, Eqs. (1) and (2).

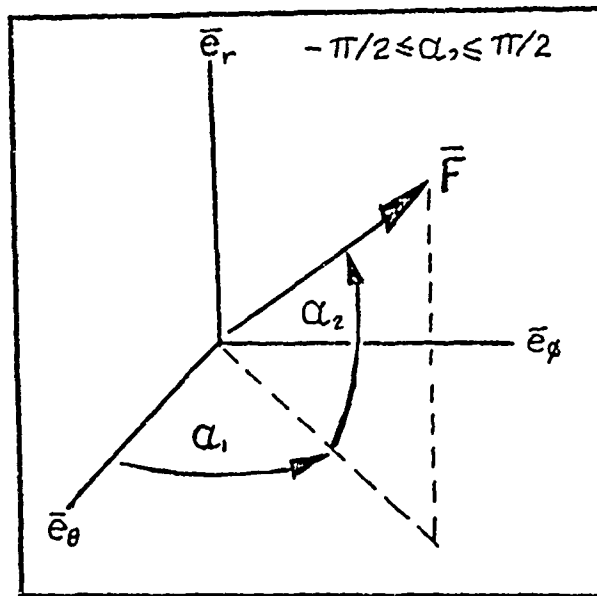


Fig. 3. Body-Fixed Reference Frame.

Using the defining relationship given by Eqs. (13) and (14), and the normalized state variables

$$X_1 = \frac{r}{r_0} \quad (31)$$

$$X_2 = \frac{V_r}{V_0} \quad (32)$$

$$X_3 = \theta \quad (33)$$

$$X_4 = \frac{V_\theta}{V_0} \quad (34)$$

$$X_5 = \phi \quad (35)$$

$$X_6 = \frac{V_\phi}{V_0} \quad (36)$$

the state differential equations are

$$X_1' = X_2 \quad (37)$$

$$X_2' = \frac{X_4^2}{X_1} + \frac{X_6^2 \sin^2 X_3}{X_1} - \frac{1}{X_1} + \frac{C \sin \alpha_2}{m} \quad (38)$$

$$X_3' = \frac{X_4}{X_1} \quad (39)$$

$$X_4' = -\frac{X_2 X_4}{X_1} + \frac{X_6^2}{X_1} \cos X_3 \sin X_3 + \frac{C \cos \alpha_1 \cos \alpha_2}{m} \quad (40)$$

$$X_5' = \frac{X_6}{X_1} \quad (41)$$

$$X_6' = -\frac{X_2 X_6}{X_1} - \frac{2 X_4 X_6 \cos X_3}{X_1 \sin X_3} + \frac{C \sin \alpha_1 \cos \alpha_2}{m \sin X_3} \quad (42)$$

where C is defined by Eq. (21) and the mass varies by Eqs. (15) and (16).

Again, the motion of each vehicle is governed by these equations.

III. Differential Game Formulation

The pursuit-evasion differential game presented here is free-time, with final range as the payoff. The solution to the differential game is required prior to initiating the control law. The formulation follows that of Bryson and Ho (Ref. 3).

Coplanar Game

Both the pursuer (P) and the evader (E) have identical state equations given by Eqs. (17) thru (20). Thus

$$\dot{X}_{1p} = X_{2p} \quad (43)$$

$$\dot{X}_{2p} = \frac{X_{4p}^2}{X_{1p}} - \frac{1}{X_{1p}^2} + \frac{C_p \sin u}{m_p} \quad (44)$$

$$\dot{X}_{3p} = \frac{X_{4p}}{X_{1p}} \quad (45)$$

$$\dot{X}_{4p} = -\frac{X_{2p} X_{4p}}{X_{1p}} + \frac{C_p \cos u}{m_p} \quad (46)$$

$$\dot{X}_{1e} = X_{2e} \quad (47)$$

$$\dot{X}_{2e} = \frac{X_{4e}^2}{X_{1e}} - \frac{1}{X_{1e}^2} + \frac{C_e \sin v}{m_e} \quad (48)$$

$$\dot{X}_{3e} = \frac{X_{4e}}{X_{1e}} \quad (49)$$

$$\dot{X}_{4e} = -\frac{X_{2e} X_{4e}}{X_{1e}} + \frac{C_e \cos v}{m_e} \quad (50)$$

where u and v are the thrust angles for the pursuer and evader, respectively. The mass of each vehicle varies according to Eqs. (15) and (16)

The desired result for any intercept problem is to hit the target vehicle, or at least to get as close as possible, at which time the warhead is detonated. The target vehicle should attempt to escape the interceptor; that is, to maximize the range at closest approach. Thus, the final range is a natural choice for the payoff for this game. The distance between the two players is given by the law of cosines (Fig. 4). For simplicity, the square of the final range is used, scaled by a factor of one-half.

$$J = \frac{1}{2} \left[X_{1P}^2 + X_{1E}^2 - 2 X_{1P} X_{1E} \cos (\phi_P - \phi_E) \right] \quad (51)$$

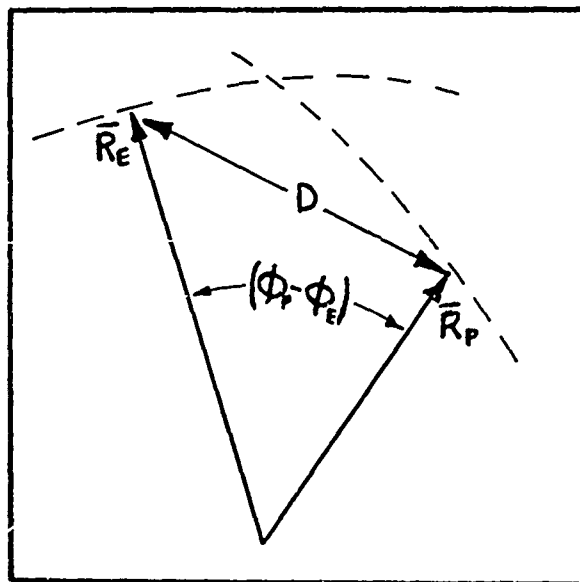


Fig. 4. Coplanar Range

Since there is no path cost, the Hamiltonian (H) is formed by adjoining the costates to the state equations.

$$\begin{aligned}
 H &= \lambda_p^T f_p + \lambda_e^T f_e \\
 H &= \lambda_{1p} X_{2p} + \lambda_{2p} \left(\frac{X_{4p}^2}{X_{1p}} - \frac{1}{X_{1p}^2} + \frac{C_p \sin u}{m_p} \right) \\
 &\quad + \lambda_{3p} \left(\frac{X_{4p}}{X_{1p}} \right) + \lambda_{4p} \left(-\frac{X_{2p} X_{4p}}{X_{1p}} + \frac{C_p \cos u}{m_p} \right) \\
 &\quad + \lambda_{1e} X_{2e} + \lambda_{2e} \left(\frac{X_{4e}^2}{X_{1e}} - \frac{1}{X_{1e}^2} + \frac{C_e \sin v}{m_e} \right) \\
 &\quad + \lambda_{3e} \left(\frac{X_{4e}}{X_{1e}} \right) + \lambda_{4e} \left(-\frac{X_{2e} X_{4e}}{X_{1e}} + \frac{C_e \cos v}{m_e} \right) \quad (52)
 \end{aligned}$$

The costate differential equations are given by

$$\lambda'^T = -H_x = g(x, \lambda, \tau) \quad (53)$$

which yields

$$\lambda'_{1p} = \frac{\lambda_{2p} X_{4p}^2}{X_{1p}^2} - \frac{2\lambda_{2p}}{X_{1p}^3} + \frac{\lambda_{3p} X_{4p}}{X_{1p}^2} - \frac{\lambda_{4p} X_{2p} X_{4p}}{X_{1p}^2} \quad (54)$$

$$\lambda'_{2p} = -\lambda_{1p} + \frac{\lambda_{4p} X_{4p}}{X_{1p}} \quad (55)$$

$$\lambda'_{3p} = 0 \quad (56)$$

$$\lambda'_{4p} = -\frac{2\lambda_{2p} X_{4p}}{X_{1p}} - \frac{\lambda_{3p}}{X_{1p}} + \frac{\lambda_{4p} X_{2p}}{X_{1p}} \quad (57)$$

$$\lambda'_{1e} = \frac{\lambda_{2e} X_{4e}^2}{X_{1e}^2} - \frac{2\lambda_{2e}}{X_{1e}^3} + \frac{\lambda_{3e} X_{4e}}{X_{1e}^2} - \frac{\lambda_{4e} X_{2e} X_{4e}}{X_{1e}^2} \quad (58)$$

$$\lambda'_{2e} = -\lambda_{1e} + \frac{\lambda_{4e} X_{4e}}{X_{1e}} \quad (59)$$

$$\lambda'_{3e} = 0 \quad (60)$$

$$\lambda'_{4e} = -\frac{2\lambda_{2e} X_{4e}}{X_{1e}} - \frac{\lambda_{3e}}{X_{1e}} + \frac{\lambda_{4e} X_{2e}}{X_{1e}} \quad (61)$$

The expressions for the pursuer's optimal control angle are found by minimizing the Hamiltonian with respect to u :

$$H_u = \frac{\lambda_{2p} C_p \cos u}{m_p} - \frac{\lambda_{4p} C_p \sin u}{m_p} = 0 \quad (62)$$

which yields

$$\tan u = \frac{\lambda_{2p}}{\lambda_{4p}} \quad (63)$$

The sufficiency condition

$$H_{uu} = -\frac{\lambda_{2p} C_p \sin u}{m_p} - \frac{\lambda_{4p} C_p \cos u}{m_p} > 0 \quad (64)$$

requires that

$$\sin u = -\frac{\lambda_{2p}}{\sqrt{\lambda_{2p}^2 + \lambda_{4p}^2}} \quad (65)$$

$$\cos u = -\frac{\lambda_{4p}}{\sqrt{\lambda_{2p}^2 + \lambda_{4p}^2}} \quad (66)$$

The evader's optimal control is found by maximizing the Hamiltonian with respect to v . An expression similar to Eq. (63) results, except that the sufficiency condition ($H_{vv} < 0$) requires that

$$\sin V = \frac{\lambda_{2e}}{\sqrt{\lambda_{2e}^2 + \lambda_{4e}^2}} \quad (67)$$

$$\cos V = \frac{\lambda_{4e}}{\sqrt{\lambda_{2e}^2 + \lambda_{4e}^2}} \quad (68)$$

The transversality conditions give the value of the costates at final time

$$\lambda^T(\tau_f) = \phi_x(\tau_f) = \left(\frac{\partial J}{\partial x} \right)_{\tau_f} \quad (69)$$

$$\lambda_{1p}(\tau_f) = (x_{1p} - x_{1e} \cos(x_{3p} - x_{3e}))_{\tau_f} \quad (70)$$

$$\lambda_{2p}(\tau_f) = 0 \quad (71)$$

$$\lambda_{3p}(\tau_f) = (x_{1p} x_{1e} \sin(x_{3p} - x_{3e}))_{\tau_f} \quad (72)$$

$$\lambda_{4p}(\tau_f) = 0 \quad (73)$$

$$\lambda_{1e}(\tau_f) = (x_{1e} - x_{1p} \cos(x_{3p} - x_{3e}))_{\tau_f} \quad (74)$$

$$\lambda_{2e}(\tau_f) = 0 \quad (75)$$

$$\lambda_{3e}(\tau_f) = (-x_{1p} x_{1e} \sin(x_{3p} - x_{3e}))_{\tau_f} \quad (76)$$

$$\lambda_{4e}(\tau_f) = 0 \quad (77)$$

An additional requirement for the free time problem is that the Hamiltonian be zero at final time. Substituting

the expressions (70) thru (77) into Eq. (52) at final time gives

$$\begin{aligned}
 H(\tau_f) = 0 = & \left[X_{1p} X_{2p} + X_{1e} X_{2e} \right. \\
 & - (X_{2p} X_{1e} + X_{1p} X_{2e}) \cos (X_{3p} - X_{3e}) \\
 & \left. + (X_{4p} X_{1e} - X_{1p} X_{4e}) \sin (X_{3p} - X_{3e}) \right] \tau_f \quad (78)
 \end{aligned}$$

This is the same condition as requiring the range-squared rate to be zero at closest approach. Differentiating Eq. (51) and setting the result equal to zero gives

$$\begin{aligned}
 0 = & X_{1p} X'_{1p} + X_{1e} X'_{1e} \\
 & - (X'_{1p} X_{1e} + X_{1p} X'_{1e}) \cos (X_{3p} - X_{3e}) \\
 & + X_{1p} X_{1e} (X'_{3p} - X'_{3e}) \sin (X_{3p} - X_{3e}) \quad (79)
 \end{aligned}$$

Substituting Eqs. (43) thru (50) gives

$$\begin{aligned}
 0 = & X_{1p} X_{2p} + X_{1e} X_{2e} \\
 & - (X_{2p} X_{1e} + X_{1p} X_{2e}) \cos (X_{3p} - X_{3e}) \\
 & + (X_{4p} X_{1e} - X_{1p} X_{4e}) \sin (X_{3p} - X_{3e}) \quad (80)
 \end{aligned}$$

which, when evaluated at final time, is the same as Eq. (78).

The two-point boundary value problem (TPBVP) for the coplanar model is given by Eqs. (43) thru (50), (54) thru (61), (70) thru (78), plus the initial values of the states.

Three Dimensional Game

As in the coplanar game, the pursuer and evader have the same state equations.

$$X'_{1p} = X_{2p} \quad (81)$$

$$X'_{2p} = \frac{X_{4p}^2}{X_{1p}} + \frac{X_{6p}^2 \sin^2 X_{3p}}{X_{1p}} - \frac{1}{X_{1p}^2} + \frac{C_p \sin u_2}{m_p} \quad (82)$$

$$X'_{3p} = \frac{X_{4p}}{X_{1p}} \quad (83)$$

$$X'_{4p} = -\frac{X_{2p} X_{4p}}{X_{1p}} + \frac{X_{6p}^2 \sin X_{3p} \cos X_{3p}}{X_{1p}} + \frac{C_p \cos u_1 \cos u_2}{m_p} \quad (84)$$

$$X'_{5p} = \frac{X_{6p}}{X_{1p}} \quad (85)$$

$$X'_{6p} = -\frac{X_{2p} X_{6p}}{X_{1p}} - \frac{2 X_{4p} X_{6p} \cos X_{3p}}{X_{1p} \sin X_{3p}} + \frac{C_p \sin u_1 \cos u_2}{m_p \sin X_{3p}} \quad (86)$$

$$X'_{1e} = X_{2e} \quad (87)$$

$$X'_{2e} = \frac{X_{4e}^2}{X_{1e}} + \frac{X_{6e}^2 \sin^2 X_{3e}}{X_{1e}} - \frac{1}{X_{1e}^2} + \frac{C_e \sin v_2}{m_e} \quad (88)$$

$$X'_{3e} = \frac{X_{4e}}{X_{1e}} \quad (89)$$

$$X'_{4e} = -\frac{X_{2e} X_{4e}}{X_{1e}} + \frac{X_{6e}^2 \sin X_{3e} \cos X_{3e}}{X_{1e}} + \frac{C_e \cos v_1 \cos v_2}{m_e} \quad (90)$$

$$X'_{5e} = \frac{X_{6e}}{X_{1e}} \quad (91)$$

$$X'_{6e} = -\frac{X_{2e} X_{6e}}{X_{1e}} - \frac{2 X_{4e} X_{6e} \cos X_{3e}}{X_{1e} \sin X_{3e}} + \frac{C_e \sin v_1 \cos v_2}{m_e \sin X_{3e}} \quad (92)$$

where u_1 , u_2 , v_1 , and v_2 are the thrust angles for the pursuer and evader, respectively.

Again, the payoff is one-half the square of the final range between the two players. However, a straight-forward application of the law of cosines cannot be used in this case, since, in general, the plane defined by the position vectors does not lie in the ϕ - or θ -plane (Fig. 5). Recognizing that the law of cosines may be written as

$$D^2 = r_p^2 + r_e^2 - 2(\bar{r}_p \cdot \bar{r}_e) \quad (93)$$

reveals the clue to determining the range between the vehicles.

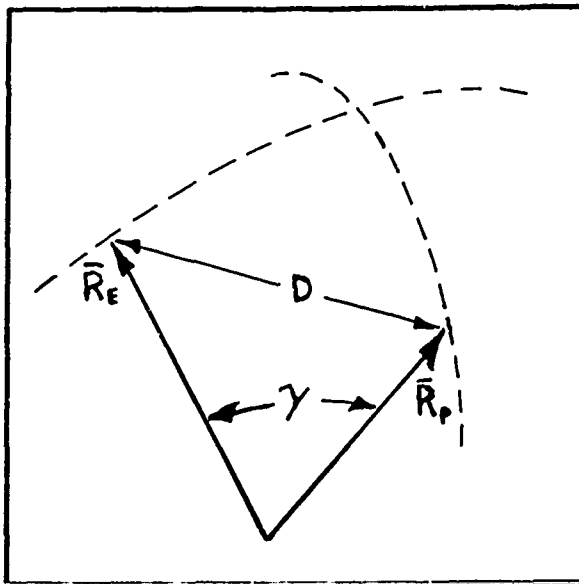


Fig. 5. Three Dimensional Range

By reference to Fig. 2, it can be seen that the components of the position vector in the inertial reference frame $(\bar{e}_x, \bar{e}_y, \bar{e}_z)$ are

$$\bar{r}_{xyz} = r \begin{bmatrix} \cos \phi \sin \theta \\ \sin \phi \sin \theta \\ \cos \theta \end{bmatrix} \quad (94)$$

Performing the dot product in Eq. (93), the payoff becomes

$$J = \frac{1}{2} \left[\chi_{1p}^2 + \chi_{1e}^2 - 2 \left(\chi_{1p} \chi_{1e} \sin \chi_{3p} \sin \chi_{3e} \cos (\chi_{5p} - \chi_{5e}) + \cos \chi_{3p} \cos \chi_{3e} \right) \right]_{t_f} \quad (95)$$

The Hamiltonian is

$$\begin{aligned} H = & \lambda_{1p} \chi_{2p} + \lambda_{2p} \left(\frac{\chi_{4p}^2}{\chi_{1p}} + \frac{\chi_{6p}^2 \sin^2 \chi_{3p}}{\chi_{1p}} - \frac{1}{\chi_{1p}^2} + \frac{C_p \sin u_2}{m_p} \right) \\ & + \lambda_{3p} \left(\frac{\chi_{4p}}{\chi_{1p}} \right) + \lambda_{4p} \left(-\frac{\chi_{2p} \chi_{4p}}{\chi_{1p}} + \frac{\chi_{6p}^2 \sin \chi_{3p} \cos \chi_{3p}}{\chi_{1p}} \right. \\ & \left. + \frac{C_p \cos u_1 \cos u_2}{m_p} \right) + \lambda_{5p} \left(\frac{\chi_{6p}}{\chi_{1p}} \right) + \lambda_{6p} \left(-\frac{\chi_{2p} \chi_{6p}}{\chi_{1p}} \right. \\ & \left. - \frac{2 \chi_{4p} \chi_{6p} \cos \chi_{3p}}{\chi_{1p} \sin \chi_{3p}} + \frac{C_p \sin u_1 \cos u_2}{m_p \sin \chi_{3p}} \right) + \lambda_{1e} \chi_{2e} \\ & + \lambda_{2e} \left(\frac{\chi_{4e}^2}{\chi_{1e}} + \frac{\chi_{6e}^2 \sin^2 \chi_{3e} \cos \chi_{3e}}{\chi_{1e}} - \frac{1}{\chi_{1e}^2} + \frac{C_e \sin v_2}{m_e} \right) \\ & + \lambda_{3e} \left(\frac{\chi_{4e}}{\chi_{1e}} \right) + \lambda_{4e} \left(-\frac{\chi_{2e} \chi_{4e}}{\chi_{1e}} + \frac{\chi_{6e}^2 \sin \chi_{3e} \cos \chi_{3e}}{\chi_{1e}} \right. \\ & \left. + \frac{C_e \cos v_1 \cos v_2}{m_e} \right) + \lambda_{5e} \left(\frac{\chi_{6e}}{\chi_{1e}} \right) + \lambda_{6e} \left(-\frac{\chi_{2e} \chi_{6e}}{\chi_{1e}} \right) \end{aligned}$$

$$- \frac{2 X_{4e} X_{6e} \cos X_{3e}}{X_{1e} \sin X_{3e}} + \frac{C_e \sin V_1 \cos V_2}{m_e \sin X_{3e}} \quad (96)$$

The costate differential equations are

$$\dot{\lambda}'^T = -H_x = g(x, \lambda, \tau) \quad (97)$$

$$\begin{aligned} \dot{\lambda}'_{1p} = & \frac{1}{X_{1p}^2} \left[\lambda_{2p} (X_{4p}^2 + X_{6p}^2 \sin^2 X_{3p} - \frac{2}{X_{1p}}) - \lambda_{4p} (X_{2p} X_{4p} \right. \\ & \left. - X_{6p}^2 \cos X_{3p} \sin X_{3p}) - \lambda_{6p} (X_{2p} X_{6p} + 2 X_{4p} X_{6p} \cot X_{3p}) \right. \\ & \left. + \lambda_{3p} X_{4p} + \lambda_{5p} X_{6p} \right] \quad (98) \end{aligned}$$

$$\dot{\lambda}'_{2p} = -\lambda_{1p} + \frac{\lambda_{4p} X_{4p}}{X_{1p}} + \frac{\lambda_{6p} X_{6p}}{X_{1p}} \quad (99)$$

$$\begin{aligned} \dot{\lambda}'_{3p} = & - \frac{\lambda_{2p} X_{6p}^2 \sin 2X_{3p}}{X_{1p}} - \frac{\lambda_{4p} X_{6p}^2 \cos 2X_{3p}}{X_{1p}} \\ & - \frac{2 \lambda_{6p} X_{4p} X_{6p}}{X_{1p} \sin^2 X_{3p}} - \frac{C_p \lambda_{6p}^2 \cos X_{3p}}{m_p \sin^3 X_{3p} [\lambda_{2p}^2 + \lambda_{4p}^2 + (\lambda_{6p} / \sin X_{3p})^2]} \quad (100) \end{aligned}$$

$$\dot{\lambda}'_{4p} = - \frac{2 \lambda_{2p} X_{4p}}{X_{1p}} - \frac{\lambda_{3p}}{X_{1p}} + \frac{\lambda_{4p} X_{2p}}{X_{1p}} + \frac{2 \lambda_{6p} X_{6p} \cos X_{3p}}{X_{1p} \sin X_{3p}} \quad (101)$$

$$\dot{\lambda}'_{5p} = 0 \quad (102)$$

$$\begin{aligned} \dot{\lambda}'_{6p} = & - \frac{1}{X_{1p}} \left[2 \lambda_{2p} X_{6p} \sin^2 X_{3p} + \lambda_{4p} X_{6p} \sin 2X_{3p} \right. \\ & \left. + \lambda_{5p} - \frac{2 \lambda_{6p} X_{4p} \cos X_{3p}}{\sin X_{3p}} - \lambda_{6p} X_{2p} \right] \quad (103) \end{aligned}$$

$$\begin{aligned} \lambda'_{1e} = & \frac{1}{\chi_{1e}^2} \left[\lambda_{2e} \left(\chi_{4e}^2 + \chi_{6e}^2 \sin^2 \chi_{3e} - \frac{2}{\chi_{1e}} \right) + \lambda_{3e} \chi_{4e} \right. \\ & - \lambda_{4e} \left(\chi_{2e} \chi_{4e} - \chi_{6e}^2 \cos \chi_{3e} \sin \chi_{3e} \right) + \lambda_{5e} \chi_{6e} \\ & \left. - \lambda_{6e} \left(\chi_{2e} \chi_{6e} + 2 \chi_{4e} \chi_{6e} \cot \chi_{3e} \right) \right] \end{aligned} \quad (104)$$

$$\lambda'_{2e} = -\lambda_{1e} + \frac{\lambda_{4e} \chi_{4e}}{\chi_{1e}} + \frac{\lambda_{6e} \chi_{6e}}{\chi_{1e}} \quad (105)$$

$$\begin{aligned} \lambda'_{3e} = & -\frac{\lambda_{2e} \chi_{6e}^2 \sin 2\chi_{3e}}{\chi_{1e}} - \frac{\lambda_{4e} \chi_{6e}^2 \cos 2\chi_{3e}}{\chi_{1e}} \\ & - \frac{2\lambda_{6e} \chi_{4e} \chi_{6e}}{\chi_{1e} \sin^2 \chi_{3e}} + \frac{C_e \lambda_{6e}^2 \cos \chi_{3e}}{m_e \sin^3 \chi_{3e} [\lambda_{2e}^2 + \lambda_{4e}^2 + (\lambda_{6e} / \sin \chi_{3e})^2]} \end{aligned} \quad (106)$$

$$\lambda'_{4e} = -\frac{1}{\chi_{1e}} \left[2\lambda_{2e} \chi_{4e} + \lambda_{3e} - \lambda_{4e} \chi_{2e} - \frac{2\lambda_{6e} \chi_{6e} \cos \chi_{3e}}{\sin \chi_{3e}} \right] \quad (107)$$

$$\lambda'_{5e} = 0 \quad (108)$$

$$\begin{aligned} \lambda'_{6e} = & -\frac{1}{\chi_{1e}} \left[2\lambda_{2e} \chi_{6e} \sin^2 \chi_{3e} + \lambda_{4e} \chi_{6e} \sin 2\chi_{3e} \right. \\ & \left. + \lambda_{5e} - \lambda_{6e} \chi_{2e} - \frac{2\lambda_{6e} \chi_{4e} \cos \chi_{3e}}{\sin \chi_{3e}} \right] \end{aligned} \quad (109)$$

Applying the optimality conditions

$$H_{u_1} = 0 = - \frac{\lambda_{4p} C_p \cos u_2 \sin u_1}{m_p} + \frac{\lambda_{6p} C_p \cos u_2 \cos u_1}{m_p \sin \chi_{3p}} \quad (110)$$

$$H_{u_2} = 0 = \frac{C_p}{m_p} \left(\lambda_{2p} \cos u_2 - \lambda_{4p} \cos u_1 \sin u_2 - \frac{\lambda_{6p} \sin u_1 \sin u_2}{\sin \chi_{3p}} \right) \quad (111)$$

from which

$$\tan u_1 = \frac{\lambda_{6p}}{\lambda_{4p} \sin \chi_{3p}} \quad (112)$$

$$\tan u_2 = \lambda_{2p} \left(\lambda_{4p} \cos u_1 + \frac{\lambda_{6p} \sin u_1}{\sin \chi_{3p}} \right)^{-1} \quad (113)$$

The sufficiency conditions require the matrix H_{uu} be positive definite

$$H_{u_1 u_1} = \frac{C_p}{m_p} \cos u_2 \left(-\lambda_{4p} \cos u_1 - \frac{\lambda_{6p} \sin u_1}{\sin \chi_{3p}} \right) > 0 \quad (114)$$

From Fig. 3,

$$-\frac{\pi}{2} \leq u_2 \leq \frac{\pi}{2} \quad (115)$$

so that

$$\cos u_2 \geq 0 \quad (116)$$

Thus, from Eqs. (110) and (114)

$$\cos u_1 = \frac{-\lambda_{4p}}{\sqrt{\lambda_{4p}^2 + (\lambda_{6p}/\sin \chi_{3p})^2}} \quad (117)$$

$$\sin u_1 = \frac{-\lambda_{6p}/\sin \chi_{3p}}{\sqrt{\lambda_{4p}^2 + (\lambda_{6p}/\sin \chi_{3p})^2}} \quad (118)$$

In addition,

$$H_{u_2 u_2} = -\lambda_{2p} \sin u_2 - \cos u_2 \left(\lambda_{4p} \cos u_1 + \frac{\lambda_{6p} \sin u_1}{\sin \chi_{3p}} \right) > 0 \quad (119)$$

Using Eqs. (113) and (114), the requirement for the inequality in Eq. (119) to hold is that

$$\sin u_2 = \frac{-\lambda_{2p}}{\sqrt{\lambda_{2p}^2 + \lambda_{4p}^2 + (\lambda_{6p} / \sin \chi_{3p})^2}} \quad (120)$$

It follows that

$$\cos u_2 = \frac{\sqrt{\lambda_{4p}^2 + (\lambda_{6p} / \sin \chi_{3p})^2}}{\sqrt{\lambda_{2p}^2 + \lambda_{4p}^2 + (\lambda_{6p} / \sin \chi_{3p})^2}} \quad (121)$$

An additional requirement for the matrix H_{uu} to be positive definite is that

$$\text{Det } H_{uu} > 0$$

Using Eqs. (117), (118) and (120), it can be easily shown that

$$H_{u_1 u_2} = H_{u_2 u_1} \equiv 0 \quad (122)$$

Thus, the matrix is positive definite.

Following the same procedure to find the evader's control

$$H_{v_1} = 0 = -\frac{\lambda_{4e} C_e \sin v_1 \cos v_2}{m_e} - \frac{\lambda_{6e} C_e \cos v_1 \cos v_2}{m_e \sin \chi_{3e}} \quad (123)$$

$$H_{v_2} = 0 = \frac{C_e}{m_e} \left(\lambda_{2e} \cos v_2 - \lambda_{4e} \cos v_1 \sin v_2 - \frac{\lambda_{6e} \sin v_2 \sin v_1}{\sin \chi_{3e}} \right) \quad (124)$$

$$\tan v_1 = \frac{\lambda_{6e}/\sin \chi_{3e}}{\lambda_{4e}} \quad (125)$$

$$\tan v_2 = \lambda_{2e} \left(\lambda_{4e} \cos v_1 + \frac{\lambda_{6e} \sin v_1}{\sin \chi_{3e}} \right)^{-1} \quad (126)$$

Since the evader is maximizing the payoff, the sufficiency conditions require that H_{vv} be negative definite.

This requires

$$H_{v_1 v_1} = \cos v_2 \left(-\lambda_{4e} \cos v_1 - \frac{\lambda_{6e} \sin v_1}{\sin \chi_{3e}} \right) < 0 \quad (127)$$

As with u_2 , v_2 is restricted to

$$-\frac{\pi}{2} \leq v_2 \leq \frac{\pi}{2} \quad (128)$$

so that

$$\cos v_2 \geq 0 \quad (129)$$

and, from Eq. (127)

$$\cos v_1 = \frac{\lambda_{4e}}{\sqrt{\lambda_{4e}^2 + (\lambda_{6e}/\sin \chi_{3e})^2}} \quad (130)$$

$$\sin v_1 = \frac{\lambda_{6e}/\sin \chi_{3e}}{\sqrt{\lambda_{4e}^2 + (\lambda_{6e}/\sin \chi_{3e})^2}} \quad (131)$$

Again, using Eqs. (130) and (131), it can be shown that

$$H_{v_1 v_2} = H_{v_2 v_1} \equiv 0 \quad (132)$$

so that, for H_{VV} to be negative definite requires

$$H_{V_2 V_2} = -\lambda_{2e} \sin V_2 + \cos V_2 \left(-\lambda_{4e} \cos V_1 - \frac{\lambda_{6e} \sin V_1}{\sin \chi_{3e}} \right) < 0 \quad (133)$$

Using Eqs. (125) and (127)

$$\sin V_2 = \frac{\lambda_{2e}}{\sqrt{\lambda_{2e}^2 + \lambda_{4e}^2 + (\lambda_{6e} / \sin \chi_{3e})^2}} \quad (134)$$

$$\cos V_2 = \frac{\sqrt{\lambda_{4e}^2 + (\lambda_{6e} / \sin \chi_{3e})^2}}{\sqrt{\lambda_{2e}^2 + \lambda_{4e}^2 + (\lambda_{6e} / \sin \chi_{3e})^2}} \quad (135)$$

The values of the costates at final time are given by the transversality conditions

$$\lambda^T(\tau_f) = \dot{\phi}_x(\tau_f) = \left(\frac{\partial J}{\partial x} \right)_{\tau_f} \quad (136)$$

$$\lambda_{1p}(\tau_f) = \left(\lambda_{1p} - \lambda_{1e} [\sin \chi_{3p} \sin \chi_{3e} \cos(\chi_{5p} - \chi_{5e}) + \cos \chi_{3p} \cos \chi_{3e}] \right)_{\tau_f} \quad (137)$$

$$\lambda_{2p}(\tau_f) = 0 \quad (138)$$

$$\lambda_{3p}(\tau_f) = \left(-\lambda_{1p} \lambda_{1e} \cos \chi_{3p} \sin \chi_{3e} \cos(\chi_{5p} - \chi_{5e}) - \sin \chi_{3p} \cos \chi_{3e} \right)_{\tau_f} \quad (139)$$

$$\lambda_{4p}(\tau_f) = 0 \quad (140)$$

$$\lambda_{5p}(\tau_f) = \left(\lambda_{1p} \lambda_{1e} \sin \chi_{3p} \sin \chi_{3e} \sin(\chi_{5p} - \chi_{5e}) \right)_{\tau_f} \quad (141)$$

$$\lambda_{6p}(\tau_f) = 0 \quad (142)$$

$$\lambda_{1e}(\tau_f) = \left(\lambda_{1e} - \lambda_{1p} [\sin \chi_{3p} \sin \chi_{3e} \cos(\chi_{5p} - \chi_{5e}) + \cos \chi_{3p} \cos \chi_{3e}] \right)_{\tau_f} \quad (143)$$

$$\lambda_{2e}(\tau_f) = 0 \quad (144)$$

$$\lambda_{3e}(\tau_f) = \left(-\lambda_{1e} \lambda_{1p} \cos \chi_{3e} \sin \chi_{3p} \cos(\chi_{5p} - \chi_{5e}) - \sin \chi_{3e} \cos \chi_{3p} \right) \tau_f \quad (145)$$

$$\lambda_{4e}(\tau_f) = 0 \quad (146)$$

$$\lambda_{5e}(\tau_f) = \left(-\lambda_{1p} \lambda_{1e} \sin \chi_{3p} \sin \chi_{3e} \sin(\chi_{5p} - \chi_{5e}) \right) \tau_f \quad (147)$$

$$\lambda_{6e}(\tau_f) = 0 \quad (148)$$

As before, the Hamiltonian must be zero at final time.

Using Eq. (96) and Eqs. (137) thru (148)

$$\begin{aligned} H(\tau_f) = 0 = & \left(\lambda_{1p} \lambda_{2p} + \lambda_{1e} \lambda_{2e} \right. \\ & - (\lambda_{1e} \lambda_{2p} + \lambda_{1p} \lambda_{2e}) [\sin \chi_{3p} \sin \chi_{3e} \cos(\chi_{5p} - \chi_{5e}) \\ & + \cos \chi_{3p} \cos \chi_{3e}] - \lambda_{4p} \lambda_{1e} [\cos \chi_{3p} \sin \chi_{3e} \cos(\chi_{5p} - \chi_{5e}) \\ & - \sin \chi_{3p} \cos \chi_{3e}] + (\lambda_{4p} \lambda_{1e} - \lambda_{1p} \lambda_{4e}) \sin \chi_{3p} \sin \chi_{3e} \sin(\chi_{5p} - \chi_{5e}) \\ & \left. - \lambda_{1p} \lambda_{4e} [\sin \chi_{3p} \cos \chi_{3e} \cos(\chi_{5p} - \chi_{5e}) - \cos \chi_{3p} \sin \chi_{3e}] \right) \tau_f \quad (149) \end{aligned}$$

As in the coplanar case, the stopping condition that the range-squared rate be zero at closest approach gives the same expression as Eq. (149).

For the three dimensional game, the TPBVP is given by Eqs. (81) thru (92), (98) thru (109), (137) thru (149), and the initial values of the states.

IV. Pseudo-Closed Loop Control Law

The pseudo-closed loop control law used in this report is based on a periodic first order update to the costate vector. At each sampling time, this update is generated from the difference between the actual states and the states of a reference trajectory. The reference trajectory assumes optimal play by both players from the sampling time to final time.

For the error in the state vector at time t_k given by

$$\delta X(t_k) = X(t_k) - X_{ref}(t_k) \quad (150)$$

the costate vector is updated by

$$\lambda(t_k) = \lambda_{ref}(t_k) + \delta\lambda(t_k) \quad (151)$$

The correction to the costate vector is produced by

$$\delta\lambda(t_k) = C \delta X(t_k) \quad (152)$$

where C is an $n \times n$ "control" matrix.

Two nearly equivalent methods have been proposed to generate this C matrix (Refs. 1,2).

Backward Sweep Method (Ref. 1)

Assuming free final time and no control constraints, the linearized TPBVP is (Ref. 3)

$$\delta\dot{X} = f_x \delta X + f_\lambda \delta\lambda, \quad \delta X(t_0) \text{ given} \quad (153)$$

$$\delta\dot{\lambda} = g_x \delta X + g_\lambda \delta\lambda \quad (154)$$

$$\begin{bmatrix} \delta\lambda(t_f) \\ 0 \\ 0 \end{bmatrix} = \begin{bmatrix} (\phi_{xx} + v^T \psi_{xx}) & \psi_x^T & \Omega_x^T \\ \psi_x & 0 & \psi_t \\ \Omega_x & \psi_t^T & \Omega_t \end{bmatrix}_{t_f} \begin{bmatrix} \delta x(t_f) \\ d\gamma \\ dt_f \end{bmatrix} \quad (155)$$

$$(156)$$

$$(157)$$

where ψ is the terminal constraint, v is a Lagrange multiplier associated with ψ , and

$$\Omega \triangleq \left(\frac{d}{dt} (\phi + v^T \psi) + L \right) \quad (158)$$

The solution to this linearized TPBVP is assumed to have the form

$$\begin{bmatrix} \delta\lambda \\ 0 \\ 0 \end{bmatrix} = \begin{bmatrix} S(t) & R(t) & m(t) \\ R^T(t) & Q(t) & n(t) \\ m^T(t) & n^T(t) & \alpha(t) \end{bmatrix} \begin{bmatrix} \delta x \\ d\gamma \\ dt_f \end{bmatrix} \quad (159)$$

$$(160)$$

$$(161)$$

where S is an $n \times n$ matrix, R and m are n - vectors, and Q , n , and α are scalars.

For the problem considered in this report, there is no ψ , so that Eqs. (155) thru (157) reduce to

$$\begin{bmatrix} \delta\lambda(t_f) \\ 0 \end{bmatrix} = \begin{bmatrix} \phi_{xx} & \Omega_x^T \\ \Omega_x & \Omega_t \end{bmatrix} \begin{bmatrix} \delta x(t_f) \\ dt_f \end{bmatrix} \quad (162)$$

$$(163)$$

and the assumed form of the solution is

$$\begin{bmatrix} \delta\lambda \\ 0 \end{bmatrix} = \begin{bmatrix} S & m \\ m^T & \alpha \end{bmatrix} \begin{bmatrix} \delta x \\ dt_f \end{bmatrix} \quad (164)$$

$$(165)$$

For $\dot{\Omega} \neq 0$, Eq. (163) can be solved for dt_f .

$$dt_f = - \left(\frac{\Omega_x}{\Omega_t} \right)_{t_f} \delta x(t_f) \quad (166)$$

This expression is substituted into Eq. (162) to yield

$$\delta \lambda(t_f) = \left(\phi_{xx} - \frac{\Omega_x^T \Omega_x}{\Omega_t} \right)_{t_f} \delta x(t_f) \quad (167)$$

Eqs. (164) and (165) become

$$\delta \lambda = \left(S - \frac{m m^T}{\alpha} \right) \delta x = \bar{S} \delta x \quad (168)$$

Thus \bar{S} is the desired control matrix.

Differentiating Eq. (168) and substituting for $\dot{\delta x}$, $\dot{\delta \lambda}$, and $\delta \lambda$ yields

$$0 = \dot{\bar{S}} + \bar{S} f_x + \bar{S} f_\lambda \bar{S} - g_\lambda \bar{S} - g_x \quad (169)$$

with the condition at final time

$$\bar{S}(t_f) = \left(\phi_{xx} - \frac{\Omega_x^T \Omega_x}{\Omega_t} \right)_{t_f} \quad (170)$$

Between sampling times, Eqs. (169) and (170) are used to generate \bar{S} and Eq. (168) is used to obtain the costate correction, $\delta \lambda(t_k)$, as a function of the state error, $\delta x(t_k)$.

Transition Matrix Method (Ref. 2)

Again assuming free final time and no control constraints, the linearized TPBVP is given by Eqs. (153) thru (157). For problems in which there is no Ψ , and for $\dot{\Omega} \neq 0$

$$dt_f = - \left(\frac{\Omega_x}{\Omega_t} \right)_{t_f} \delta x \quad (166)$$

and

$$\delta \lambda(t_f) = A \delta x(t_f) \quad (171)$$

where

$$A = \left(\phi_{xx} - \frac{\Omega_x^T \Omega_x}{\Omega_t} \right)_{t_f} \quad (172)$$

The solution to the linearized TPBVP is written as

$$\delta x(t) = \Phi_{xx}(t, t_f) \delta x(t_f) + \Phi_{x\lambda}(t, t_f) \delta \lambda(t_f) \quad (173)$$

$$\delta \lambda(t) = \Phi_{\lambda x}(t, t_f) \delta x(t_f) + \Phi_{\lambda\lambda}(t, t_f) \delta \lambda(t_f) \quad (174)$$

Substituting Eq. (172) for $\delta \lambda(t_f)$ gives

$$\delta x(t) = X \delta x(t_f) \quad (175)$$

$$\delta \lambda(t) = \Lambda \delta x(t_f) \quad (176)$$

where

$$X = \Phi_{xx}(t, t_f) + \Phi_{x\lambda}(t, t_f) A \quad (177)$$

$$\Lambda = \Phi_{\lambda x}(t, t_f) + \Phi_{\lambda\lambda}(t, t_f) A \quad (178)$$

Solving Eq. (175) for $\delta X(t_f)$ and substituting into Eq. (176)

$$\delta \lambda(t_k) = (\Lambda X^{-1})_{t_k} \delta X(t_k) \quad (179)$$

This provides the relationship between δX and $\delta \lambda$ at time t_k , and the control matrix is ΛX^{-1} .

The state transition matrices are obtained by backward integration of

$$\dot{\Phi}_{xx} = f_x \Phi_{xx} + f_\lambda \Phi_{\lambda x}, \quad \Phi_{xx}(t_f, t_f) = I \quad (180)$$

$$\dot{\Phi}_{x\lambda} = f_x \Phi_{x\lambda} + f_\lambda \Phi_{\lambda\lambda}, \quad \Phi_{x\lambda}(t_f, t_f) = 0 \quad (181)$$

$$\dot{\Phi}_{\lambda x} = g_x \Phi_{xx} + g_\lambda \Phi_{\lambda x}, \quad \Phi_{\lambda x}(t_f, t_f) = 0 \quad (182)$$

$$\dot{\Phi}_{\lambda\lambda} = g_x \Phi_{x\lambda} + g_\lambda \Phi_{\lambda\lambda}, \quad \Phi_{\lambda\lambda}(t_f, t_f) = I \quad (183)$$

from t_f to t_k , and Eq. (179) is used to generate the correction to the costate vector.

Implementation of the Control Law

To use this pseudo-closed loop control law, a player, say the pursuer, initially plays his open loop controls for a short time, while simultaneously integrating the system state and costate equations, and the necessary equations to generate the control matrix, backward from final time. At Each sampling time, t_k , the pursuer compares the actual state of the system with the reference trajectory. Any non-optimal play by the evader will be manifested as a deviation in the states. The pursuer then updates the

costate vector by Eq. (151). Using the updated costate vector, the pursuer again plays the updated open loop control until the next sampling time. Now it is necessary for the pursuer to integrate the states and updated costates forward until the stopping condition is reached to predict the final conditions for the new trajectory. Since the solution is only updated to first order, the transversality conditions are not, in general, satisfied at the final time. Thus, the final values of the costates must be adjusted to meet the transversality conditions. Using these new terminal conditions, a new reference trajectory and control matrix are generated by backward integration, as before. The problem ends when the range rate is zero. Figure 6 presents a simplified flow diagram for the control law.

Linearized TPBVP Coefficients and Terminal Conditions

The coefficients for the linearized state and costate equations, Eqs. (153) and (154), are presented in Appendix A.

The expressions for the terminal conditions given by Eqs. (170) and (172) are given in Appendix B.

V. Results

The test cases presented in this report were numerically simulated on a CDC 6600 computer using a predictor-corrector integration scheme. Three coplanar trajectories and two non-coplanar trajectories were investigated. The trajectories used different vehicle characteristics and varying final ranges as indicated in Table I. In all cases, the predicted trajectory was integrated forward until the stopping condition was reached, and the costates were adjusted to satisfy the transversality conditions prior to integrating the reference trajectory.

Coplanar Model

A sampling interval of 0.012 TU was arbitrarily chosen to test the control laws for the coplanar trajectories. This nominally provided 16 updates along the trajectory. Both the backward sweep method and the transition matrix method effectively reduced the final range to a value less than the nominal final range, except for the case where the evader used the control $V = 1.0$. This result was not too surprising since this was very near the evader's optimal control. When the sampling interval was decreased to 0.008 TU, with $V = 1.0$, the control law was able to achieve a final range less than the nominal.

Both the backward sweep method and the transition matrix method produced similar, though not identical, results

TABLE I. TEST CASES

Trajectory	Initial Mass (slugs)	Thrust (lbf)	Isp ($\frac{\text{lbf-sec}}{\text{lbm}}$)	$\frac{\text{Final Mass}}{\text{Initial Mass}}$	Final Range From TPBVP (NM)	Remarks
1	1250	20000	300	0.74	8.27	Coplanar
2	900	20000	300	0.63	25.31	Coplanar
3	750	20000	180	0.27	25.30	Coplanar
4	1250	20000	300	0.74	8.27	Three-D Same as 1
5	1250	20000	300	0.74	16.73	Three-D

when tested on Trajectory 1. Differences can best be attributed to the additional numerical operations associated with the transition matrix method.

To reduce the computation time, the integration step size for the transition matrix method was initially double that of the backward sweep method. It was found that the control matrix so produced was not symmetric (as it should be if the two methods were indeed equivalent), the elements were not close to those of the \bar{S} matrix generated by the backward sweep method, and the transition matrix method did not perform nearly as well as the backward sweep method. When the integration step size was made identical to that of the backward sweep method, the final results improved, the control matrix became symmetrical, generally, to five significant figures (usually, to six significant figures), and the elements agreed well with the elements of the \bar{S} matrix.

Since decreasing the sampling interval to 0.008 TU improved the final range for $V = 1.0$, it was decided to increase the sampling interval to 0.016 TU to see how badly the method suffered from the use of fewer updates. (This would nominally provide 12 updates.) Again, the control law was able to decrease the final range below the nominal except in the case where $V = 1.0$. The surprising results were that in two cases, $V = 3.0$ and $V = -3.0$, the final range was less than for the smaller sampling interval. This is possibly a result of the way in which the control

law works. That is, the first order correction at the longer sampling interval may have combined in such a way as to create these anomalies in the final range.

The final ranges achieved for all the coplanar trajectories are summarized in Table II. Plots of all the coplanar trajectories are presented in Appendices C thru E. Each plot compares the TPBVP solution with that produced by the control law. A range trace for the final portion of each trajectory is also shown.

Three Dimensional Model

Because of the larger state dimension, along with the geometric increase in the number of \bar{S} matrix differential equations, the sampling interval was increased to 0.024 TU to test the control law for the three dimensional model. The transition matrix method was not tested.

Since Trajectory 4 was the same as Trajectory 1 except that both players were allowed to thrust out of the reference plane, a test case was initially run to validate the three dimensional control law. The evader's controls were set at $V_1 = 1.571$, $V_2 = 0.0$ so that the evader would remain in the reference plane. (This corresponds to the coplanar case for Trajectory 1 with the control $V = 0.0$.) The resulting final range was slightly larger than that achieved for the coplanar case with a sampling interval of 0.016 TU, as could be expected. More significant was the

TABLE II. FINAL RANGE FOR NON-OPTIMAL EVADER (COPLANAR)

Sampling Interval = 0.012 TU

Method	Final Range (NM)						
	Evader's Control (Radians)						
	3.0	2.0	1.0	0.0	-1.0	-2.0	-3.0
TRAJECTORY 1 ^a							
Transition Matrix	0.22	1.70	8.39	0.82	1.28	5.40	0.82
Backward Sweep	.72	1.81	8.33 ^b	0.82	1.51	4.65	1.53
Backward Sweep ^c	1.62	2.08	8.42	1.72	2.14	5.25	0.34
TRAJECTORY 2 ^d							
Backward Sweep	0.64	10.67	23.74	1.91	2.67	7.24	1.05
TRAJECTORY 3 ^e							
Transition Matrix	1.12	1.84	22.96	0.54	2.28	6.00	1.13

^aNominal final range = 8.27 NM.

^bA sampling interval of 0.008 TU reduced the final range to 8.20 NM.

^cSampling Interval = 0.016 TU.

^dNominal final range = 25.31 NM.

^eNominal final range = 25.30 NM.

result that the control law did not erroneously drive the pursuer out of the reference plane.

In all cases but two, the control law decreased the final range below the nominal final range. The two exceptions were for $V_1 = 0.0$, $V_2 = 1.0$; and for $V_1 = 1.571$, $V_2 = 1.0$. As before, this was not too disturbing, as the evader's optimal controls were in this quadrant. A decrease of the sampling interval to 0.016 TU was sufficient to obtain a favorable result for the latter case. However, for $V_1 = 0.0$, $V_2 = 1.0$, the sampling interval had to be decreased to 0.012 TU to obtain improvement on the final range.

Table III summarizes the final ranges achieved for the non-coplanar trajectories. Plots of the non-coplanar trajectories are presented in Appendices F and G. The nominal trajectories are presented in each case for comparison, and the range trace for the last portion of each trajectory is also given.

General Comments

Real Time Considerations. To be of practical use, this control law must be capable of being implemented in real time. This can be a formidable task for realistic problems with large state dimension. Both methods tested require the forward integration of $2n$ differential equations for the trajectory prediction. In addition, the transition matrix method requires the backward integration of $2n(2n+1)$

TABLE III. FINAL RANGE FOR NON-OPTIMAL EVADER (NON-COPLANAR)

Sampling Interval = 0.024 TU

Method	Final Range (NM)									
	Evader's Control (V_1/V_2) (Radians)									
	0.0 1.0	0.0 -1.0	1.571 0.0	1.571 1.0	1.571 -1.0	3.14 1.0	3.14 -1.0	3.14 1.0	4.71 -1.0	4.71 1.0
TRAJECTORY 4 ^a										
Backward Sweep	8.18	6.67	2.00	-----	-----	8.19	6.67	-----	-----	-----
TRAJECTORY 5 ^b										
Backward Sweep	18.78 ^c	15.07	-----	20.12 ^d	2.66	11.02	4.17	5.89	7.54	-----

^aNominal final range = 8.27 NM.

^bNominal final range = 16.73 NM.

^cA sampling interval of 0.012 TU reduced the final range to 16.15 NM.

^dA sampling interval of 0.016 TU reduced the final range to 14.86 NM.

equations to generate the reference trajectory, while the backward sweep method requires $n(n+2)$ equations to be integrated. The computational burden of the backward sweep method can be reduced to $\frac{1}{2}n(n+5)$ differential equations by taking advantage of the symmetry of the \bar{S} matrix. This is a significant reduction for large state dimension problems.

For the coplanar model considered in this report, the transition matrix method required integrating 272 equations to generate the reference trajectory, and the backward sweep method required 50 equations. This latter number could have been reduced to 52 equations. For the non-coplanar model, 168 equations were integrated to generate the reference trajectory. This could have been reduced by almost 40% to 102 equations. The transition matrix method would require the integration of 600 equations!

Using a sampling interval of 0.012 TU, the backward sweep method required a maximum computation time of 12.2 seconds to compute a reference trajectory for the coplanar model, and the transition matrix method required 24.2 seconds. This is not real time, as 0.012 TU corresponds to approximately 9.7 seconds. For the non-coplanar model, with a sampling interval of 0.024 TU (19.36 seconds), the maximum computation time was 32.03 seconds. By reducing the number of equations to be integrated for the \bar{S} matrix, both of the backward sweep models could be performed very

close to real time for the specified sampling interval.

Stability of the Backward Sweep Method. While the backward sweep method enjoys the advantage of the lesser computational burden, the \bar{S} matrix sometimes becomes infinite during the backward integration of the matrix Riccati equation, Eq. (169). For the problems considered in this report, the \bar{S} matrix originally became unbounded during the backward integration. This problem was resolved by decreasing the integration step size to one-half its original value, to 0.0005 TU. However, using this new integration step size, the backward sweep method failed on Trajectory 3.

Predicted Range at Each Update Time. Tables IV thru XIII present the predicted final range at each update time, based on optimal play by both players from the update time to final time. The predicted range did not, in general, monotonically decrease at each successive update on a given trajectory. Only in those cases where the evader's control was near-optimal did the predicted range display a monotonic decrease. This phenomenon is apparently a result of non-unique solutions which result when the evader behaves in such a way that the pursuer has sufficient control to drive the range to near-zero.

TABLE IV. PREDICTED FINAL RANGE AT EACH SAMPLING TIME

Trajectory 1, Transition Matrix Method,
Sampling Interval = 0.012 TU

(Entries rounded to two decimal places)

Sampling Time	Predicted Final Range (NM)						
	Evader's Control (Radians)						
	3.0	2.0	1.0	0.0	-1.0	-2.0	-3.0
0.012	3.57	7.39	8.53	6.29	2.53	2.15	2.68
.024	0.79	6.50	8.97	4.37	2.10	4.03	2.16
.036	0.68	5.32	8.73	2.35	0.68	4.50	0.90
.048	2.64	4.50	8.74	0.69	0.70	4.44	1.49
.060	1.43	3.52	8.69	0.70	0.59	4.88	0.54
.072	1.89	2.62	8.69	0.77	4.62	4.72	1.88
.084	0.56	2.43	8.70	0.95	3.59	4.71	1.95
.096	1.61	2.03	8.70	1.58	2.49	5.03	1.61
.108	1.52	1.40	8.70	1.69	2.21	4.95	1.47
.120	1.33	2.14	8.70	1.68	2.34	4.90	1.61
.132	1.37	2.17	8.70	1.68	0.96	5.31	0.48
.144	1.84	2.02	8.70	1.68	1.20	5.21	1.07
.156	0.77	2.19	8.70	1.68	1.08	5.12	1.44
.168	0.30	2.62	8.70	1.68	1.36	5.08	1.22
.180	0.15	1.89	8.40	1.68	1.35	5.07	1.41
.192	0.72	1.73	8.39	1.68	1.34	5.06	0.57
.204	0.19	2.59	----	----	----	----	1.46

TABLE V. PREDICTED FINAL RANGE AT EACH SAMPLING TIME

**Trajectory 1, Backward Sweep Method,
Sampling Interval = 0.012 TU**

(Entries rounded to two decimal places)

Sampling Time	Predicted Final Range (NM)						
	Evader's Control (Radians)						
	3.0	2.0	1.0	0.0	-1.0	-2.0	-3.0
0.012	3.57	7.38	8.53	6.29	2.53	0.64	2.68
.024	0.79	6.50	8.97	4.37	2.10	4.07	2.16
.036	0.68	5.32	8.72	2.35	0.68	4.03	0.90
.048	2.64	4.50	8.73	0.69	0.70	4.04	1.49
.060	1.43	3.52	8.69	0.70	0.59	4.35	0.54
.072	1.89	2.62	8.69	0.77	4.02	4.32	1.88
.084	0.56	2.43	8.70	0.95	2.59	4.25	0.22
.096	1.61	2.03	8.70	1.58	2.61	4.63	1.62
.108	1.52	1.40	8.70	1.69	1.79	4.52	1.53
.120	1.33	2.14	8.45	1.68	1.80	4.48	1.90
.132	1.37	1.09	8.44	1.68	1.80	4.89	0.88
.144	0.27	2.02	8.39	1.68	1.80	4.79	1.38
.156	0.77	1.29	8.36	1.68	1.80	4.70	1.51
.168	0.64	1.74	8.35	1.68	1.80	4.67	1.27
.180	0.50	1.19	8.34	1.68	1.80	4.66	1.50
.192	1.10	1.97	8.33	1.68	1.80	4.65	0.60
.204	0.32	1.81	----	----	----	----	1.60

TABLE VI. PREDICTED FINAL RANGE AT EACH SAMPLING TIME

Trajectory 1, Backward Sweep Method,
Sampling Interval = 0.016 TU

(Entries rounded to two decimal places)

Sampling Time	Predicted Final Range (NM)						
	Evader's Control (Radians)						
	3.0	2.0	1.0	0.0	-1.0	-2.0	-3.0
0.016	2.26	6.95	8.61	5.81	1.53	2.40	1.76
.032	1.99	5.91	9.04	3.56	3.01	4.94	3.31
.048	1.14	4.75	8.85	1.52	1.46	4.97	2.10
.064	3.75	3.19	8.81	1.60	1.73	5.16	1.61
.080	0.83	2.47	8.78	1.70	1.88	5.15	1.74
.096	1.63	2.12	8.80	1.73	2.40	5.13	1.47
.112	2.40	1.39	8.56	1.72	2.31	5.36	0.63
.128	0.96	1.96	8.53	1.72	1.27	5.29	2.15
.144	0.53	1.52	8.47	1.72	1.29	5.22	0.60
.160	0.90	1.43	8.45	1.72	1.37	5.24	1.11
.176	0.42	1.54	8.44	1.72	0.55	5.54	0.67
.192	0.46	1.07	8.43	1.72	0.66	5.52	0.89
.208	0.28	----	----	----	----	----	0.35

TABLE VII. PREDICTED FINAL RANGE AT EACH SAMPLING TIME

Trajectory 1, Backward Sweep Method,
V = 1.0, Sampling Interval = 0.008 TU

(Entries rounded to two decimal places)

Sampling Time	Final Range	Sampling Time	Final Range	Sampling Time	Final Range
0.008	8.46	0.072	8.57	0.136	8.32
.016	8.61	.080	8.57	.144	8.28
.024	8.59	.088	8.57	.152	8.25
.032	8.57	.096	8.57	.160	8.23
.040	8.57	.104	8.57	.168	8.22
.048	8.57	.112	8.57	.176	8.21
.056	8.57	.120	8.57	.184	8.20
.064	8.57	.128	8.33	.192	8.20

TABLE VIII. PREDICTED FINAL RANGE AT EACH SAMPLING TIME

Trajectory 2, Backward Sweep Method,
Sampling Interval = 0.012 TU

(Entries rounded to two decimal places)

Sampling Time	Predicted Final Range (NM)						
	Evader's Control (Radians)						
	3.0	2.0	1.0	0.0	-1.0	-2.0	-3.0
0.012	18.11	23.37	25.03	21.70	16.46	13.96	16.66
.024	14.02	23.48	24.97	20.52	10.33	3.26	11.20
.036	7.56	21.84	24.84	17.38	2.48	6.92	3.61
.048	1.89	20.39	24.75	14.38	4.72	7.07	3.88
.060	4.64	19.07	24.68	11.72	3.25	7.06	1.60
.072	1.19	17.74	24.52	8.97	1.21	7.02	1.54
.084	1.79	16.64	24.42	6.66	1.14	7.24	2.08
.096	3.71	15.51	24.36	4.61	0.73	7.16	3.58
.108	1.79	14.53	24.19	2.73	4.39	7.13	1.79
.120	2.24	13.65	24.10	1.03	3.80	7.34	1.69
.132	1.23	12.88	24.03	0.48	2.75	7.26	0.43
.144	1.31	12.21	23.97	0.97	2.63	7.21	1.63
.156	0.36	11.68	23.82	1.23	2.66	7.21	0.08
.168	0.36	11.32	23.76	1.92	2.68	7.44	0.86
.180	1.03	10.88	23.72	1.91	2.68	7.39	0.35
.192	1.63	10.66	23.70	-----	-----	7.36	1.01
.204	0.46	10.67	-----	-----	-----	-----	1.33

TABLE IX. PREDICTED FINAL RANGE AT EACH SAMPLING TIME

Trajectory 3, Transition Matrix Method,
Sampling Interval = 0.012 TU

(Entries rounded to two decimal places)

Sampling Time	Predicted Final Range (NM)						
	Evader's Control (Radians)						
	3.0	2.0	1.0	0.0	-1.0	-2.0	-3.0
0.012	16.57	22.90	25.00	20.89	14.62	11.58	14.85
.024	7.93	20.81	24.82	16.72	4.09	3.30	4.42
.036	0.93	18.77	24.75	12.67	5.57	2.60	5.44
.048	1.29	16.81	24.57	8.87	2.75	4.10	2.35
.060	2.12	15.07	24.46	5.23	0.98	4.44	2.00
.072	5.11	13.23	24.27	1.81	1.00	4.25	7.49
.084	0.57	11.47	24.15	0.64	1.03	5.03	4.37
.096	0.84	9.83	23.94	4.06	0.99	4.87	2.40
.108	3.24	8.44	23.81	0.82	1.20	5.16	0.57
.120	4.84	6.72	23.60	1.47	2.27	5.41	3.06
.132	0.38	5.60	23.46	4.47	1.94	5.70	0.84
.144	1.78	4.49	23.26	2.35	1.32	5.45	3.27
.156	5.02	3.33	23.13	2.38	2.30	5.72	0.57
.168	1.68	2.55	23.04	2.39	2.08	6.04	2.05
.180	1.91	2.60	22.99	2.39	2.27	5.83	0.93
.192	2.70	1.72	22.96	-----	-----	5.77	3.00
.204	1.45	2.28	-----	-----	-----	-----	1.15
.216	1.50	-----	-----	-----	-----	-----	1.22
.228	1.51	-----	-----	-----	-----	-----	0.63

TABLE X. PREDICTED FINAL RANGE AT EACH SAMPLING TIME

**Trajectory 4, Backward Sweep Method,
Sampling Interval = 0.024 TU**

(Entries rounded to two decimal places)

Sampling Time	Predicted Final Range (NM)				
	Evader's Control (Radians)				
	$V_1 = 0.0$		$V_1 = 1.571$	$V_1 = 3.14$	
	$V_2 = 1.0$	$V_2 = -1.0$	$V_2 = 0.0$	$V_2 = 1.0$	$V_2 = -1.0$
0.024	8.30	6.70	4.21	8.30	6.70
.048	8.74	7.19	1.67	8.75	7.18
.072	8.27	7.00	1.56	8.28	6.99
.096	8.35	6.71	5.45	8.36	6.71
.120	8.04	6.63	2.47	8.05	6.63
.144	8.08	6.66	1.69	8.09	6.65
.168	7.95	6.68	0.50	7.96	6.67
.192	7.92	6.67	----	7.93	6.67

TABLE XI. PREDICTED FINAL RANGE AT EACH SAMPLING TIME

Trajectory 5, Backward Sweep Method,
Sampling Interval = 0.024 TU

(Entries rounded to two decimal places)

Sampling Time	Predicted Final Range (NM)											
	Evader's Control (Radians)											
	V ₁ = 0.0		V ₁ = 1.0		V ₁ = 1.571		V ₁ = 3.14		V ₁ = 4.71		V ₁ = 6.28	
	V ₂ = 1.0	V ₂ = -1.0	V ₂ = 1.0	V ₂ = -1.0	V ₂ = 1.0	V ₂ = -1.0	V ₂ = 1.0	V ₂ = -1.0	V ₂ = 1.0	V ₂ = -1.0	V ₂ = 1.0	V ₂ = -1.0
0.024	15.67	11.49	15.42	8.57	12.13	3.41	11.39	6.76	11.39	6.76	11.39	6.76
.048	20.78	16.24	21.01	10.17	10.97	5.39	14.23	8.00	14.23	8.00	14.23	8.00
.072	20.14	15.64	20.76	6.93	10.82	4.79	11.66	7.89	11.66	7.89	11.66	7.89
.096	19.65	15.22	20.51	5.03	10.95	4.24	9.60	7.68	9.60	7.68	9.60	7.68
.120	19.29	15.11	20.36	3.86	10.82	4.09	7.88	7.74	7.88	7.74	7.88	7.74
.144	19.07	15.04	20.28	2.69	10.78	3.66	6.82	7.57	6.82	7.57	6.82	7.57
.168	18.86	15.02	20.24	2.49	10.78	3.60	6.09	7.75	6.09	7.75	6.09	7.75
.192	18.78	15.01	20.22	-----	10.78	-----	5.57	7.66	5.57	7.66	5.57	7.66

TABLE XII. PREDICTED FINAL RANGE AT EACH SAMPLING TIME

Trajectory 5, Backward Sweep Method, $V_1 = 0.0$,
 $V_2 = 1.0$, Sampling Interval = 0.012 TU

(Entries rounded to two decimal places)

Sampling Time	Final Range	Sampling Time	Final Range
0.012	16.14	0.108	16.75
.024	18.51	.120	16.63
.036	18.51	.132	16.44
.048	18.18	.144	16.32
.060	17.75	.156	16.30
.072	17.48	.168	16.20
.084	17.19	.180	16.13
.096	16.98	.192	16.10

TABLE XIII. PREDICTED FINAL RANGE AT EACH SAMPLING TIME

Trajectory 5, Backward Sweep Method, $V_1 = 1.571$,
 $V_2 = 1.0$, Sampling Interval = 0.016 TU

(Entries rounded to two decimal places)

Sampling Time	Final Range	Sampling Time	Final Range
0.016	15.58	0.112	15.13
.032	15.94	.128	15.09
.048	15.66	.144	15.07
.064	15.52	.160	15.05
.080	15.23	.176	14.87
.096	15.20	.192	14.86

VI. Conclusions

The control law proposed by Anderson has been applied to a free time, minimax final range pursuit-evasion game between two spacecraft. The coplanar encounter was extensively investigated using the backward sweep method and the transition matrix method. The backward sweep method was also applied to the three dimensional intercept problem.

The control law has effectively demonstrated its ability to guide the pursuer to a better solution when the evader is behaving non-optimally. The shorter sampling interval, in general, provided a greater improvement on the final range, *than what?* In addition, the two methods proposed to implement the control law have been shown to produce equivalent results.

Another significant conclusion from this investigation which must not go unmentioned, is that the control law displayed remarkable flexibility in the problems considered. The basic logic displayed in Fig. 6 was used in all computer programs used to simulate the control law. The basic program used for the backward sweep method was only altered to accommodate differences peculiar to the transition matrix method, and in the three dimensional case, to accommodate the larger state dimension. These programs were used, unaltered, to test all cases presented in this report. No "fine tuning" of any kind was necessary to adapt the programs to each particular case.

The problem of real time computation is not considered an insurmountable problem in the implementation of this control law. Special use computers, along with parallel processing could provide rapid update solutions. In an actual encounter, the costate vector should be updated as often as each new reference trajectory becomes available. This should provide better results than those achieved with the fixed update times used in this report.

One disadvantage of this control law which this report has not considered, *since point* is that a reference TPBVP *To leave* solution is required prior to starting the procedure. *til* *End!* The TPBVP solutions used for this report were generated using a general purpose algorithm developed by M. J. D. Powell (Ref. 6).

Bibliography

1. Anderson, G. M., "A Near Optimal Closed Loop Solution Method for Nonsingular Zero Sum Differential Games." Journal of Optimization Theory and Applications, 13: 303-318 (March 1974).
2. Anderson, G. M., "A Transition Matrix Method for Generating Near Optimal Closed-Loop Solutions to Non-linear Zero-Sum Differential Games." Preprint of International Federation of Automatic Control - International Federation of Operational Research Symposium on Optimization Methods, Applied Aspects, Varna, Bulgaria, October 8-11, 1974, pp 27-35.
3. Bryson, A. E. and Y. C. Ho, Applied Optimal Control. Waltham, Massachusetts: Blaisdell Company, 1969.
4. Greenwood, D. T., Principles of Dynamics. Englewood Cliffs, N. J.: Prentice-Hall, Inc., 1965.
5. Isaacs, R., Differential Games. New York, New York: John Wiley and Sons, 1965.
6. Powell, M. J. D., "A Fortran Subroutine for Solving Systems of Non-Linear Algebraic Equations." Numerical Methods for Nonlinear Algebraic Equations, edited by Philip Rabinowitz, New York: Gordon and Breach Science Publishers, 1970.

Appendix A

Coefficients for the Linearized TPBVP

The linearized state and costate differential equations may be written

$$\delta \dot{x} = f_x \delta x + f_\lambda \delta \lambda$$

$$\delta \dot{\lambda} = g_x \delta x + g_\lambda \delta \lambda$$

Since the state and costate equations are separable, the $n \times n$ coefficient matrices f_x , f_λ , g_x , and g_λ may be partitioned as follows;

$$f_x = \begin{bmatrix} f_{xp} & 0 \\ 0 & f_{xe} \end{bmatrix}$$

$$f_\lambda = \begin{bmatrix} f_{\lambda p} & 0 \\ 0 & f_{\lambda e} \end{bmatrix}$$

$$g_x = \begin{bmatrix} g_{xp} & 0 \\ 0 & g_{xe} \end{bmatrix}$$

$$g_\lambda = \begin{bmatrix} g_{\lambda p} & 0 \\ 0 & g_{\lambda e} \end{bmatrix}$$

where the elements of the sub-matrices are

$$(f_{xp})_{ij} = \frac{\partial f_{pi}}{\partial x_{pj}}$$

$$(f_{\lambda p})_{ij} = \frac{\partial f_{pi}}{\partial \lambda_{pj}}$$

$$(g_{xp})_{ij} = \frac{\partial g_{pi}}{\partial x_{pj}}$$

$$(g_{\lambda p})_{ij} = \frac{\partial g_{pi}}{\partial \lambda_{pj}}$$

and similarly for the evader coefficient sub-matrices.

Coplanar Model

The coefficient sub-matrices for the pursuer are

$$f_{xp} = \begin{bmatrix} 0 & 1 & 0 & 0 \\ \left(-\frac{\lambda_{4p}^2}{\lambda_{1p}^2} + \frac{2}{\lambda_{1p}}\right) & 0 & 0 & \left(\frac{2\lambda_{4p}}{\lambda_{1p}}\right) \\ \left(-\frac{\lambda_{4p}}{\lambda_{1p}^2}\right) & 0 & 0 & \left(\frac{1}{\lambda_{1p}}\right) \\ \left(\frac{\lambda_{2p}\lambda_{4p}}{\lambda_{1p}^2}\right) & \left(-\frac{\lambda_{4p}}{\lambda_{1p}}\right) & 0 & \left(-\frac{\lambda_{2p}}{\lambda_{1p}}\right) \end{bmatrix}$$

$$f_{\lambda p} = \begin{bmatrix} 0 & 0 & 0 & 0 \\ 0 & \left(\frac{-c_p \lambda_{4p}^2}{m_p (\lambda_{2p}^2 + \lambda_{4p}^2)^{3/2}}\right) & 0 & \left(\frac{c_p \lambda_{2p} \lambda_{4p}}{m_p (\lambda_{2p}^2 + \lambda_{4p}^2)^{3/2}}\right) \\ 0 & 0 & 0 & 0 \\ 0 & \left(\frac{c_p \lambda_{2p} \lambda_{4p}}{m_p (\lambda_{2p}^2 + \lambda_{4p}^2)^{3/2}}\right) & 0 & \left(\frac{-c_p \lambda_{2p}^2}{m_p (\lambda_{2p}^2 + \lambda_{4p}^2)^{3/2}}\right) \end{bmatrix}$$

$$g_{xp} = \begin{bmatrix} \left[\frac{2}{x_{1p}^2} \left(-\lambda_{2p} x_{4p}^2 + \frac{3\lambda_{2p}}{x_{1p}} \right) \right] & \left(-\frac{\lambda_{4p} x_{4p}}{x_{1p}^2} \right) & 0 & \left[\frac{1}{x_{1p}^2} \left(2\lambda_{2p} x_{4p} + \lambda_{3p} \right) \right] \\ \left(-\frac{\lambda_{4p} x_{4p}}{x_{1p}^2} \right) & 0 & 0 & \left(\frac{\lambda_{4p}}{x_{1p}} \right) \\ 0 & 0 & 0 & 0 \\ \left[\frac{1}{x_{1p}^2} \left(2\lambda_{2p} x_{4p} + \lambda_{3p} \right) \right] & \left(\frac{\lambda_{4p}}{x_{1p}} \right) & 0 & \left(-\frac{2\lambda_{2p}}{x_{1p}} \right) \end{bmatrix}$$

$$g_{\lambda p} = -f_{xp}^T$$

The coefficient sub-matrices for the evader are

$$f_{xe} = \begin{bmatrix} 0 & 1 & 0 & 0 \\ \left(-\frac{\lambda_{4e}}{x_{1e}^2} + \frac{2}{x_{1e}^2} \right) & 0 & 0 & \left(\frac{2\lambda_{4e}}{x_{1e}} \right) \\ \left(-\frac{\lambda_{4e}}{x_{1e}^2} \right) & 0 & 0 & \left(\frac{1}{x_{1e}} \right) \\ \left(\frac{\lambda_{2e} \lambda_{4e}}{x_{1e}^2} \right) & \left(-\frac{\lambda_{4e}}{x_{1e}} \right) & 0 & \left(-\frac{\lambda_{2e}}{x_{1e}} \right) \end{bmatrix}$$

$$f_{\lambda e} = \begin{bmatrix} 0 & 0 & 0 & 0 \\ 0 & \left(\frac{C_e \lambda_{4e}^2}{m_e (\lambda_{2e}^2 + \lambda_{4e}^2)^{3/2}} \right) & 0 & \left(\frac{-C_e \lambda_{2e} \lambda_{4e}}{m_e (\lambda_{2e}^2 + \lambda_{4e}^2)^{3/2}} \right) \\ 0 & 0 & 0 & 0 \\ 0 & \left(\frac{-C_e \lambda_{2e} \lambda_{4e}}{m_e (\lambda_{2e}^2 + \lambda_{4e}^2)^{3/2}} \right) & 0 & \left(\frac{C_e \lambda_{2e}^2}{m_e (\lambda_{2e}^2 + \lambda_{4e}^2)^{3/2}} \right) \end{bmatrix}$$

$$g_{\lambda e} = \begin{bmatrix} \left[\frac{2}{\chi_{1e}^3} \begin{pmatrix} -\lambda_{2e} \chi_{4e}^2 + \frac{3\lambda_{2e}}{\chi_{1e}} \\ -\lambda_{3e} \chi_{4e} + \lambda_{2e} \chi_{2e} \chi_{4e} \end{pmatrix} \right] & \left(\frac{-\lambda_{4e} \chi_{4e}}{\chi_{1e}^2} \right) & 0 & \left[\frac{1}{\chi_{1e}^2} \begin{pmatrix} 2\lambda_{2e} \chi_{4e} + \lambda_{3e} \\ -\lambda_{4e} \chi_{2e} \end{pmatrix} \right] \\ \left(\frac{-\lambda_{4e} \chi_{4e}}{\chi_{1e}^2} \right) & 0 & 0 & \left(\frac{\lambda_{1e}}{\chi_{1e}} \right) \\ 0 & 0 & 0 & 0 \\ \left[\frac{1}{\chi_{1e}^2} \begin{pmatrix} 2\lambda_{2e} \chi_{4e} + \lambda_{3e} \\ -\lambda_{4e} \chi_{2e} \end{pmatrix} \right] & \left(\frac{\lambda_{4e}}{\chi_{1e}} \right) & 0 & \left(\frac{-2\lambda_{2e}}{\chi_{1e}} \right) \end{bmatrix}$$

$$g_{\lambda e} = -f_{\lambda e}^T$$

Three Dimensional Model

The non-zero coefficients for the pursuer are

$$f_{x_{p12}} = 1$$

$$f_{x_{p21}} = -\frac{1}{x_{1p}^2} \left(x_{4p}^2 + x_{6p}^2 \sin^2 x_{3p} - \frac{2}{x_{1p}} \right)$$

$$f_{x_{p23}} = \frac{1}{x_{1p}} (x_{6p}^2 \sin 2x_{3p}) - \frac{c_p \lambda_{2p} \lambda_{6p}^2 \cos x_{3p}}{D_p^{3/2} \sin^3 x_{3p}}$$

$$f_{x_{p24}} = \frac{2x_{4p}}{x_{1p}}$$

$$f_{x_{p26}} = \frac{2}{x_{1p}} (x_{6p} \sin^2 x_{3p})$$

$$f_{x_{p31}} = -\frac{x_{4p}}{x_{1p}^2}$$

$$f_{x_{p34}} = \frac{1}{x_{1p}}$$

$$f_{x_{p41}} = \frac{1}{x_{1p}^2} \left(x_{2p} x_{4p} - \frac{x_{6p}^2 \sin 2x_{3p}}{2} \right)$$

$$f_{x_{p42}} = -\frac{x_{4p}}{x_{1p}}$$

$$f_{x_{p43}} = \frac{x_{6p}^2 \cos 2x_{3p}}{x_{1p}} - \frac{c_p \lambda_{4p} \lambda_{6p}^2 \cos x_{3p}}{D_p^{3/2} \sin^3 x_{3p}}$$

$$f_{x_{p44}} = -\frac{x_{2p}}{x_{1p}}$$

$$f_{x_{p46}} = \frac{1}{x_{1p}} (x_{6p} \sin 2x_{3p})$$

$$f_{x_{p51}} = -\frac{x_{6p}}{x_{1p}^2}$$

$$f_{x_{p54}} = \frac{1}{x_{1p}}$$

$$f_{x_{p61}} = \frac{1}{x_{1p}^2} \left(x_{2p} x_{6p} + 2x_{4p} x_{6p} \cot x_{3p} \right)$$

$$f_{\chi p 62} = -\frac{\chi_{6p}}{\chi_{1p}}$$

$$f_{\chi p 63} = \frac{2\chi_{4p}\chi_{6p}}{\chi_{1p}\sin^2\chi_{3p}} + \frac{C_p\lambda_{6p}\cos\chi_{3p}}{D_p^{1/2}\sin^3\chi_{3p}} \left(2 - \frac{\lambda_{6p}^2}{D_p\sin^2\chi_{3p}}\right)$$

$$f_{\chi p 64} = -\frac{2\chi_{6p}\cos\chi_{3p}}{\chi_{1p}\sin\chi_{3p}}$$

$$f_{\chi p 66} = -\frac{1}{\chi_{1p}} (\chi_{2p} + 2\chi_{4p}\cot\chi_{3p})$$

$$f_{\lambda p 22} = \frac{C_p}{D_p^{1/2}} \left(\frac{\lambda_{2p}^2}{D_p} - 1\right)$$

$$f_{\lambda p 24} = \frac{C_p\lambda_{2p}\lambda_{4p}}{D_p^{3/2}} = f_{\lambda p 42}$$

$$f_{\lambda p 26} = \frac{C_p\lambda_{2p}\chi_{6p}}{D_p^{3/2}\sin^2\chi_{3p}} = f_{\lambda p 62}$$

$$f_{\lambda p 44} = \frac{C_p}{D_p^{1/2}} \left(\frac{\lambda_{4p}^2}{D_p} - 1\right)$$

$$f_{\lambda p 46} = \frac{C_p\lambda_{4p}\chi_{6p}}{D_p^{3/2}\sin^2\chi_{3p}} = f_{\lambda p 64}$$

$$f_{\lambda p 66} = \frac{C_p}{D_p^{1/2}\sin^2\chi_{3p}} \left(\frac{\lambda_{6p}^2}{D_p\sin^2\chi_{3p}} - 1\right)$$

$$g_{\chi p 11} = -\frac{2}{\chi_{1p}^3} \left[\lambda_{2p} (\chi_{4p}^2 + \chi_{6p}^2 \sin^2\chi_{3p} - \frac{3}{\chi_{1p}}) - \lambda_{4p} (\chi_{2p}\chi_{4p} - \frac{\chi_{6p}^2 \sin 2\chi_{3p}}{2}) \right. \\ \left. - \lambda_{6p} (\chi_{2p}\chi_{6p} + 2\chi_{4p}\chi_{6p} \cot\chi_{3p}) + \lambda_{2p}\chi_{4p} + \lambda_{6p}\chi_{6p} \right]$$

$$g_{\chi p 12} = -\frac{1}{\chi_{1p}^2} (\lambda_{4p}\chi_{4p} + \lambda_{6p}\chi_{6p})$$

$$g_{\chi p 13} = \frac{1}{\chi_{1p}^2} (\lambda_{2p}\chi_{6p}^2 \sin 2\chi_{3p} + \lambda_{4p}\chi_{6p}^2 \cos 2\chi_{3p} + \frac{2\lambda_{6p}\chi_{4p}\chi_{6p}}{\sin^2\chi_{3p}})$$

$$g_{\chi p 14} = \frac{1}{\chi_{1p}^2} (2\lambda_{2p}\chi_{4p} - \lambda_{4p}\chi_{2p} - 2\lambda_{6p}\chi_{6p} \cot\chi_{3p} + \lambda_{2p})$$

$$g_{x_{p16}} = \frac{1}{\chi_{1p}^2} \left[2\lambda_{2p} \lambda_{6p} \sin^2 \chi_{3p} + \lambda_{4p} \chi_{6p} \sin 2\chi_{3p} + \lambda_{5p} - \lambda_{6p} (\chi_{2p} + 2\chi_{4p} \cot \chi_{3p}) \right]$$

$$g_{x_{p21}} = g_{x_{p12}}$$

$$g_{x_{p24}} = \frac{\lambda_{4p}}{\chi_{1p}}$$

$$g_{x_{p26}} = \frac{\lambda_{6p}}{\chi_{1p}}$$

$$g_{x_{p31}} = g_{x_{p13}}$$

$$g_{x_{p33}} = \frac{1}{\chi_{1p}} \left(-2\lambda_{2p} \chi_{6p}^2 \cos 2\chi_{3p} + 2\lambda_{4p} \chi_{6p}^2 \sin 2\chi_{3p} + 4\lambda_{6p} \chi_{4p} \chi_{6p} \cot \chi_{3p} \csc^2 \chi_{3p} \right) + \frac{c_p \lambda_{6p}^2}{D_p \nu_2 \sin^2 \chi_{3p}} \left(1 + \frac{3 \cos^2 \chi_{3p}}{\sin^2 \chi_{3p}} - \frac{\lambda_{20}^2 \cos^2 \chi_{3p}}{D_p \sin^4 \chi_{3p}} \right)$$

$$g_{x_{p34}} = -\frac{2\lambda_{6p} \chi_{6p}}{\chi_{1p} \sin^2 \chi_{3p}}$$

$$g_{x_{p36}} = -\frac{2}{\chi_{1p}} \left(\lambda_{2p} \chi_{6p} \sin 2\chi_{3p} + \lambda_{4p} \chi_{6p} \cos 2\chi_{3p} + \frac{\lambda_{6p} \chi_{4p}}{\sin^2 \chi_{3p}} \right)$$

$$g_{x_{p42}} = g_{x_{p24}}$$

$$g_{x_{p43}} = g_{x_{p34}}$$

$$g_{x_{p44}} = -\frac{2\lambda_{20}}{\chi_{1p}}$$

$$g_{x_{p46}} = \frac{2\lambda_{6p} \cos \chi_{3p}}{\chi_{1p} \sin \chi_{3p}}$$

$$g_{x_{p61}} = g_{x_{p16}}$$

$$g_{x_p 62} = g_{x_p 26}$$

$$g_{x_p 63} = g_{x_p 36}$$

$$g_{x_p 64} = g_{x_p 46}$$

$$g_{x_p 66} = -\frac{1}{x_{1p}} (2\lambda_{2p} \sin^2 \chi_{3p} + \lambda_{4p} \sin 2\chi_{3p})$$

$$g_{x_p} = -f_{x_p}^T$$

where

$$D_p = \lambda_{2p}^2 + \lambda_{4p}^2 + \left(\frac{\lambda_{4p}}{\sin \chi_{3p}} \right)^2$$

The non-zero coefficients for the evader are

$$f_{x_e 12} = 1$$

$$f_{x_e 21} = -\frac{1}{x_{1e}^2} \left(x_{4e}^2 + x_{6e}^2 \sin^2 \chi_{3e} - \frac{2}{x_{1e}} \right)$$

$$f_{x_e 23} = \frac{x_{6e}^2 \sin 2\chi_{3e}}{x_{1e}} + \frac{c_e \lambda_{2e} \lambda_{6e}^2 \cos \chi_{3e}}{D_e^{3/2} \sin^3 \chi_{3e}}$$

$$f_{x_e 24} = \frac{2x_{4e}}{x_{1e}}$$

$$f_{x_e 26} = \frac{1}{x_{1e}} (2 x_{6e} \sin^2 \chi_{3e})$$

$$f_{x_e 31} = -\frac{x_{4e}}{x_{1e}^2}$$

$$f_{x_e 34} = \frac{1}{x_{1e}}$$

$$f_{x_e 41} = \frac{1}{x_{1e}^2} \left(x_{2e} x_{4e} - \frac{x_{6e}^2 \sin 2\chi_{3e}}{2} \right)$$

$$f_{\lambda e42} = -\frac{\lambda_{4e}}{\lambda_{1e}}$$

$$f_{\lambda e43} = \frac{\lambda_{6e}^2 \cos 2\lambda_{3e}}{\lambda_{1e}} + \frac{C_e \lambda_{4e} \lambda_{6e} \cos \lambda_{3e}}{D_e^{3/2} \sin^3 \lambda_{3e}}$$

$$f_{\lambda e44} = -\frac{\lambda_{2e}}{\lambda_{1e}}$$

$$f_{\lambda e46} = \frac{\lambda_{6e} \sin 2\lambda_{3e}}{\lambda_{1e}}$$

$$f_{\lambda e51} = -\frac{\lambda_{6e}}{\lambda_{1e}^2}$$

$$f_{\lambda e56} = \frac{1}{\lambda_{1e}}$$

$$f_{\lambda e61} = \frac{1}{\lambda_{1e}^2} (\lambda_{2e} \lambda_{6e} + 2 \lambda_{4e} \lambda_{6e} \cot \lambda_{3e})$$

$$f_{\lambda e62} = -\frac{\lambda_{6e}}{\lambda_{1e}}$$

$$f_{\lambda e63} = \frac{2 \lambda_{4e} \lambda_{6e}}{\lambda_{1e} \sin^2 \lambda_{3e}} - \frac{C_e \lambda_{6e} \cos \lambda_{3e}}{D_e^{3/2} \sin^3 \lambda_{3e}} \left(2 - \frac{\lambda_{6e}^2}{D_e \sin^2 \lambda_{3e}} \right)$$

$$f_{\lambda e64} = -\frac{1}{\lambda_{1e}} (2 \lambda_{6e} \cot \lambda_{3e})$$

$$f_{\lambda e66} = -\frac{1}{\lambda_{1e}} (\lambda_{2e} + 2 \lambda_{4e} \cot \lambda_{3e})$$

$$f_{\lambda e22} = -\frac{C_e}{D_e^{3/2}} \left(\frac{\lambda_{2e}^2}{D_e} - 1 \right)$$

$$f_{\lambda e24} = -\frac{C_e \lambda_{2e} \lambda_{4e}}{D_e^{3/2}} = f_{\lambda e42}$$

$$f_{\lambda e26} = -\frac{C_e \lambda_{2e} \lambda_{6e}}{D_e^{3/2} \sin^2 \lambda_{3e}} = f_{\lambda e62}$$

$$f_{\lambda e44} = -\frac{C_e}{D_e^{3/2}} \left(\frac{\lambda_{4e}^2}{D_e} - 1 \right)$$

$$f_{\lambda e 46} = -\frac{C_e \lambda_{4e} \lambda_{6e}}{D_e^{3/2} \sin^2 \chi_{3e}} = f_{\lambda e 64}$$

$$f_{\lambda e 66} = -\frac{C_e}{D_e^{1/2} \sin^2 \chi_{3e}} \left(\frac{\lambda_{6e}^2}{D_e \sin^2 \chi_{3e}} - 1 \right)$$

$$\begin{aligned} g_{\chi e 11} = & -\frac{2}{\chi_{1e}^3} \left[\lambda_{2e} (\chi_{4e}^2 + \chi_{6e}^2 \sin^2 \chi_{3e} - \frac{3}{\chi_{1e}}) + \lambda_{3e} \chi_{4e} \right. \\ & - \lambda_{4e} \left(\chi_{2e} \chi_{4e} - \frac{\chi_{6e}^2 \sin 2\chi_{3e}}{2} \right) + \lambda_{5e} \chi_{6e} \\ & \left. - \lambda_{6e} (\chi_{2e} \chi_{6e} + 2 \chi_{4e} \chi_{6e} \cot \chi_{3e}) \right] \end{aligned}$$

$$g_{\chi e 12} = -\frac{1}{\chi_{1e}^2} (\lambda_{4e} \chi_{4e} + \lambda_{6e} \chi_{6e})$$

$$\begin{aligned} g_{\chi e 13} = & \frac{1}{\chi_{1e}^2} \left(\lambda_{2e} \chi_{6e}^2 \sin 2\chi_{3e} + \lambda_{4e} \chi_{6e}^2 \cos 2\chi_{3e} \right. \\ & \left. + \frac{2 \lambda_{6e} \chi_{4e} \chi_{6e}}{\sin^2 \chi_{3e}} \right) \end{aligned}$$

$$g_{\chi e 14} = \frac{1}{\chi_{1e}^2} (2 \lambda_{2e} \chi_{4e} + \lambda_{3e} - \lambda_{4e} \chi_{2e} - 2 \lambda_{6e} \chi_{6e} \cot \chi_{3e})$$

$$\begin{aligned} g_{\chi e 16} = & \frac{1}{\chi_{1e}^2} \left[2 \lambda_{2e} \chi_{6e}^2 \sin^2 \chi_{3e} + \lambda_{4e} \chi_{6e} \sin 2\chi_{3e} + \lambda_5 \right. \\ & \left. - \lambda_{6e} (\chi_{2e} + 2 \chi_{4e} \cot \chi_{3e}) \right] \end{aligned}$$

$$g_{\chi e 21} = g_{\chi e 12}$$

$$g_{\chi e 24} = \frac{\lambda_{4e}}{\chi_{1e}}$$

$$g_{\chi e 26} = \frac{\lambda_{6e}}{\chi_{1e}}$$

$$g_{\chi e 31} = g_{\chi e 13}$$

$$\begin{aligned} g_{\chi e 33} = & \frac{2}{\chi_1} \left(-\lambda_{2e} \chi_{6e}^2 \cos 2\chi_{3e} + \lambda_{4e} \chi_{6e}^2 \sin 2\chi_{3e} + 2 \lambda_{6e} \chi_{4e} \chi_{6e} \cot \chi_{3e} \right) \\ & - \frac{C_e \lambda_{6e}^2}{D_e^{1/2} \sin^2 \chi_{3e}} \left(1 + \frac{3 \cos^2 \chi_{3e}}{\sin^2 \chi_{3e}} - \frac{\lambda_{6e}^2 \cos^2 \chi_{3e}}{D_e \sin^4 \chi_{3e}} \right) \end{aligned}$$

$$g_{xe34} = -\frac{2\lambda_{6e}\lambda_{4e}}{\lambda_{1e}\sin^2\chi_{3e}}$$

$$g_{xe36} = -\frac{2}{\lambda_{1e}}\lambda_{2e}\lambda_{6e}\sin 2\chi_{3e} + \lambda_{4e}\lambda_{6e}\cos 2\chi_{3e} + \frac{\lambda_{6e}\lambda_{4e}}{\sin^2\chi_{3e}}$$

$$g_{xe41} = g_{xe14}$$

$$g_{xe43} = g_{xe34}$$

$$g_{xe44} = -\frac{2\lambda_{2e}}{\lambda_{1e}}$$

$$g_{xe46} = \frac{1}{\lambda_{1e}}2\lambda_{6e}\cot\chi_{3e}$$

$$g_{xe61} = g_{xe16}$$

$$g_{xe62} = g_{xe26}$$

$$g_{xe63} = g_{xe36}$$

$$g_{xe64} = g_{xe46}$$

$$g_{xe66} = -\frac{1}{\lambda_{1e}}2\lambda_{2e}\sin^2\chi_{3e} + \lambda_{4e}\sin 2\chi_{3e}$$

$$g_{\lambda e} = -f_{\lambda e}^T$$

where

$$D_e = \lambda_{2e}^2 + \lambda_{4e}^2 + \frac{\lambda_{6e}}{\sin\chi_{3e}}$$

Appendix B

Terminal Conditions for the Control Laws

The terminal condition given by

$$(\phi_{xx} - \dot{\Omega}^{-1} \Omega_x^T \Omega_x)_{T_f}$$

must be evaluated at final time prior to the backward integration for both control laws.

Coplanar Model

The non-zero elements of the ϕ_{xx} matrix are

$$\phi_{xx11} = 1$$

$$\phi_{xx13} = (X_{ie} A)_{T_f} = \phi_{xx31}$$

$$\phi_{xx15} = -B_{T_f} = \phi_{xx51}$$

$$\phi_{xx17} = -(X_{ie} A)_{T_f} = \phi_{xx71}$$

$$\phi_{xx33} = (X_{ip} X_{ie} B)_{T_f}$$

$$\phi_{xx35} = (X_{ip} A)_{T_f} = \phi_{xx53}$$

$$\phi_{xx37} = -(X_{ip} X_{ie} B)_{T_f} = \phi_{xx73}$$

$$\phi_{xx55} = 1$$

$$\phi_{xx57} = -(X_{ip} A)_{T_f} = \phi_{xx75}$$

$$\phi_{xx77} = (X_{ip} X_{ie} B)_{T_f}$$

$$\Omega_{x1} = (x_{2p} - x_{2e}B - x_{4e}A) \tau_f$$

$$\Omega_{x2} = (x_{1p} - x_{1e}B) \tau_f$$

$$\Omega_{x3} = [(x_{2p}x_{1e} + x_{1p}x_{2e})A + (x_{4p}x_{1e} - x_{1p}x_{4e})B] \tau_f$$

$$\Omega_{x4} = (x_{1e}A) \tau_f$$

$$\Omega_{x5} = (x_{2e} - x_{2p}B + x_{4p}A) \tau_f$$

$$\Omega_{x6} = (x_{1e} - x_{1p}B) \tau_f$$

$$\Omega_{x7} = [(x_{2p}x_{1e} + x_{1p}x_{2e})A - (x_{4p}x_{1e} - x_{1p}x_{4e})B] \tau_f$$

$$\Omega_{x8} = -(x_{1p}A) \tau_f$$

where

$$A = \sin(x_{3p} - x_{3e})$$

$$B = \cos(x_{3p} - x_{3e})$$

$$\dot{\Omega}_{\tau_f} = \left(\frac{\partial \Omega}{\partial \tau} + \frac{\partial \Omega}{\partial x} \dot{x} \right) \tau_f = (\Omega_x \dot{f}) \tau_f$$

(This scalar product was performed by matrix multiplication within the computer program.)

Three Dimensional Model

The non-zero elements of the ϕ_{xx} matrix are

$$\phi_{xx11} = 1$$

$$\phi_{xx13} = -[X_{ie} (CA \cdot SB \cdot CC - SA \cdot CB)]_{T_f} = \phi_{xx31}$$

$$\phi_{xx15} = (X_{ie} SA \cdot SB \cdot SC)_{T_f} = \phi_{xx51}$$

$$\phi_{xx17} = (-SA \cdot SB \cdot CC - CA \cdot CB)_{T_f} = \phi_{xx71}$$

$$\phi_{xx19} = -[X_{ie} (SA \cdot CB \cdot CC - CA \cdot SB)]_{T_f} = \phi_{xx91}$$

$$\phi_{xx1,11} = -(X_{ie} SA \cdot SB \cdot SC)_{T_f} = \phi_{xx11,1}$$

$$\phi_{xx23} = [X_{ip} X_{ie} (SA \cdot SB \cdot CC + CA \cdot CB)]_{T_f}$$

$$\phi_{xx35} = (X_{ip} X_{ie} CA \cdot SB \cdot SC)_{T_f} = \phi_{xx53}$$

$$\phi_{xx37} = -[X_{ip} (CA \cdot SB \cdot CC - SA \cdot CB)]_{T_f} = \phi_{xx73}$$

$$\phi_{xx39} = -[X_{ip} X_{ie} (CA \cdot CB \cdot CC + SA \cdot SB)]_{T_f} = \phi_{xx93}$$

$$\phi_{xx3,11} = -(X_{ip} X_{ie} CA \cdot SB \cdot SC)_{T_f} = \phi_{xx11,3}$$

$$\phi_{xx55} = (X_{ip} X_{ie} SA \cdot SB \cdot CC)_{T_f}$$

$$\phi_{xx57} = (X_{ip} SA \cdot SB \cdot SC)_{T_f} = \phi_{xx75}$$

$$\phi_{xx59} = (X_{ip} X_{ie} SA \cdot CB \cdot SC)_{T_f} = \phi_{xx95}$$

$$\phi_{xx5,11} = -(X_{ip} X_{ie} SA \cdot SB \cdot CC)_{T_f} = \phi_{xx11,5}$$

$$\phi_{xx7,7} = 1$$

$$\phi_{xx79} = -[X_{ip} (SA \cdot CB \cdot CC - CA \cdot SB)]_{T_f} = \phi_{xx97}$$

$$\phi_{xx7,11} = -(X_{ip} SA \cdot SB \cdot SC)_{T_f} = \phi_{xx11,7}$$

$$\Phi_{x99} = [X_{1p} X_{1e} (SA \cdot SB \cdot CC + CA \cdot CB)]_{T_f}$$

$$\Phi_{x9,11} = -(X_{1p} X_{1e} SA \cdot CB \cdot SC)_{T_f} = \Phi_{x11,9}$$

$$\Phi_{x11,11} = (X_{1p} X_{1e} SA \cdot SB \cdot CC)_{T_f}$$

$$\Omega_{x1} = [X_{2p} - X_{2e} (SA \cdot SB \cdot CC + CA \cdot CB) - X_{4e} (SA \cdot CB \cdot CC - CA \cdot SB) - X_{6e} (CA \cdot SB \cdot SC)]_{T_f}$$

$$\Omega_{x2} = [X_{1p} - X_{1e} (SA \cdot SB \cdot CC + CA \cdot CB)]_{T_f}$$

$$\Omega_{x3} = [- (X_{1e} X_{2p} + X_{1p} X_{2e}) (CA \cdot SB \cdot CC - SA \cdot CB) + X_{4p} X_{1e} (SA \cdot SB \cdot CC + CA \cdot CB) - X_{1p} X_{4e} (CA \cdot CB \cdot CC + SA \cdot SB) + (X_{6p} X_{1e} - X_{1p} X_{6e}) (CA \cdot SB \cdot SC)]_{T_f}$$

$$\Omega_{x4} = [-X_{1e} (CA \cdot SB \cdot CC - SA \cdot CB)]_{T_f}$$

$$\Omega_{x5} = [(X_{1e} X_{2p} + X_{1p} X_{2e}) SA \cdot SB \cdot SC + X_{4p} X_{1e} CA \cdot SB \cdot SC + X_{1p} X_{4e} SA \cdot CB \cdot SC + (X_{6p} X_{1e} - X_{1p} X_{6e}) SA \cdot SB \cdot CC]_{T_f}$$

$$\Omega_{x6} = (X_{1e} SA \cdot SB \cdot SC)_{T_f}$$

$$\Omega_{x7} = [X_{2e} - X_{2p} (SA \cdot SB \cdot CC + CA \cdot CB) - X_{4p} (CA \cdot SB \cdot CC - SA \cdot CB) + X_{6p} SA \cdot SB \cdot SC]_{T_f}$$

$$\Omega_{x8} = [X_{1e} - X_{1p} (SA \cdot SB \cdot CC + CA \cdot CB)]_{T_f}$$

$$\begin{aligned} \Omega_{x9} = & \left[(X_{1e} X_{2p} + X_{1p} X_{2e}) (SA \cdot CB \cdot CC - CA \cdot SB) \right. \\ & - X_{4p} X_{1e} (CA \cdot CB \cdot CC + SA \cdot SB) \\ & + X_{1p} X_{4e} (SA \cdot SB \cdot CC + CA \cdot CB) \\ & \left. + (X_{6p} X_{1e} - X_{1p} X_{6e}) SA \cdot CB \cdot SC \right]_{T_f} \end{aligned}$$

$$\Omega_{x10} = \left[-X_{1p} (SA \cdot CB \cdot CC - CA \cdot SB) \right]_{T_f}$$

$$\begin{aligned} \Omega_{x11} = & \left[- (X_{1e} X_{2p} + X_{1p} X_{2e}) SA \cdot SB \cdot SC \right. \\ & - X_{4p} X_{1e} CA \cdot SB \cdot SC - X_{1p} X_{4e} SA \cdot CB \cdot SC \\ & \left. - (X_{6p} X_{1e} - X_{1p} X_{6e}) SA \cdot SB \cdot CC \right]_{T_f} \end{aligned}$$

$$\Omega_{x12} = -X_{1p} SA \cdot SB \cdot SC \Big|_{T_f}$$

where

$$SA = \sin X_{3p}$$

$$CA = \cos X_{3p}$$

$$SB = \sin X_{3e}$$

$$CB = \cos X_{3e}$$

$$SC = \sin (X_{5p} - X_{5e})$$

$$CC = \cos (X_{5p} - X_{5e})$$

again,

$$\dot{\Omega}_{T_f} = \left(\frac{\partial \Omega}{\partial T} + \frac{\partial \Omega}{\partial X} \dot{X} \right)_{T_f} = (\Omega_x f)_{T_f}$$

was formed by matrix multiplication within the computer program.

Appendix C.

Plots of Trajectory 1

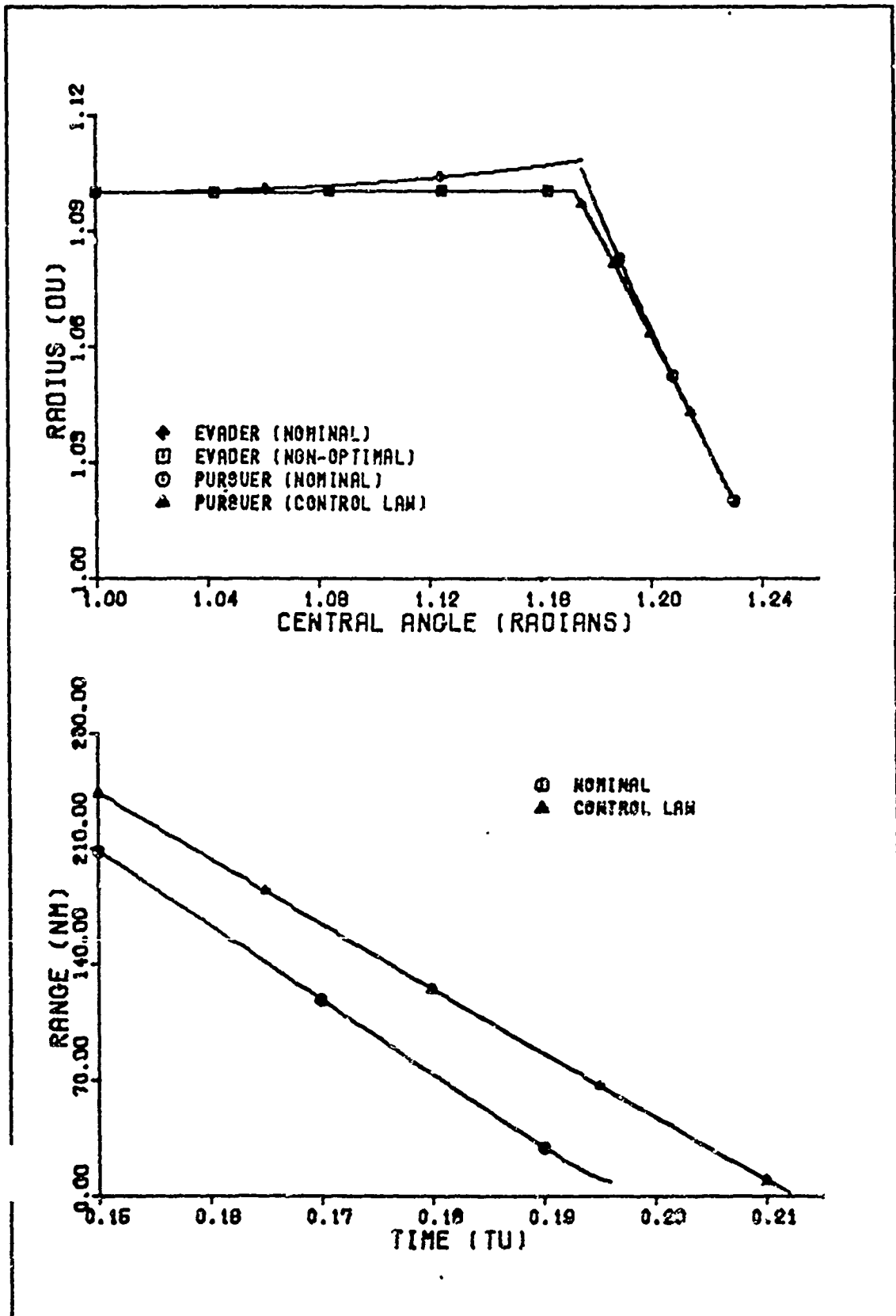


Fig. C-1. Trajectory 1, Backward Sweep Method.
 $V = 3.0$, Sampling Interval = 0.012 TU.

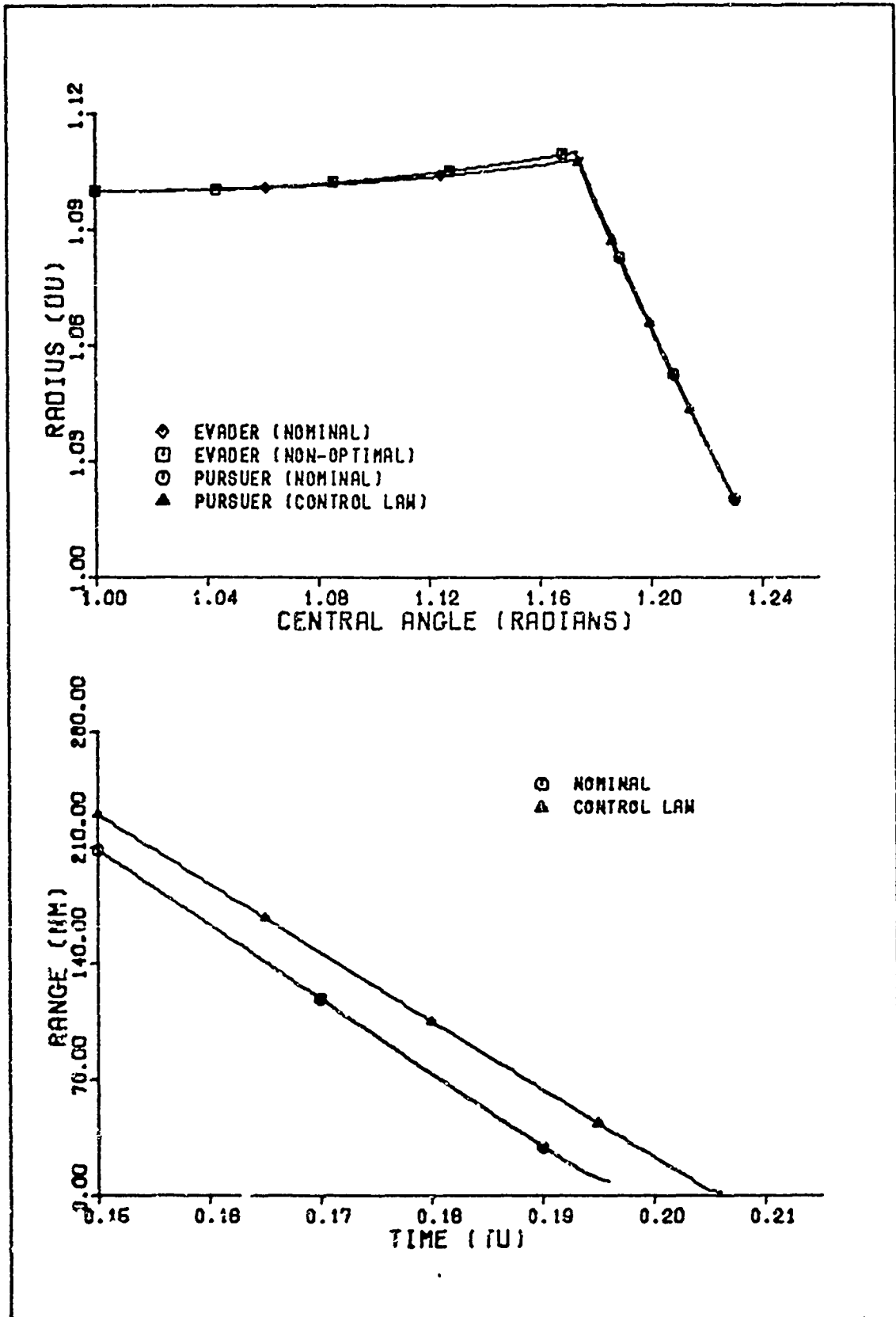


Fig. C-2. Trajectory 1, Backward Sweep Method.
 $V = 2.0$, Sampling Interval = 0.012 TU.

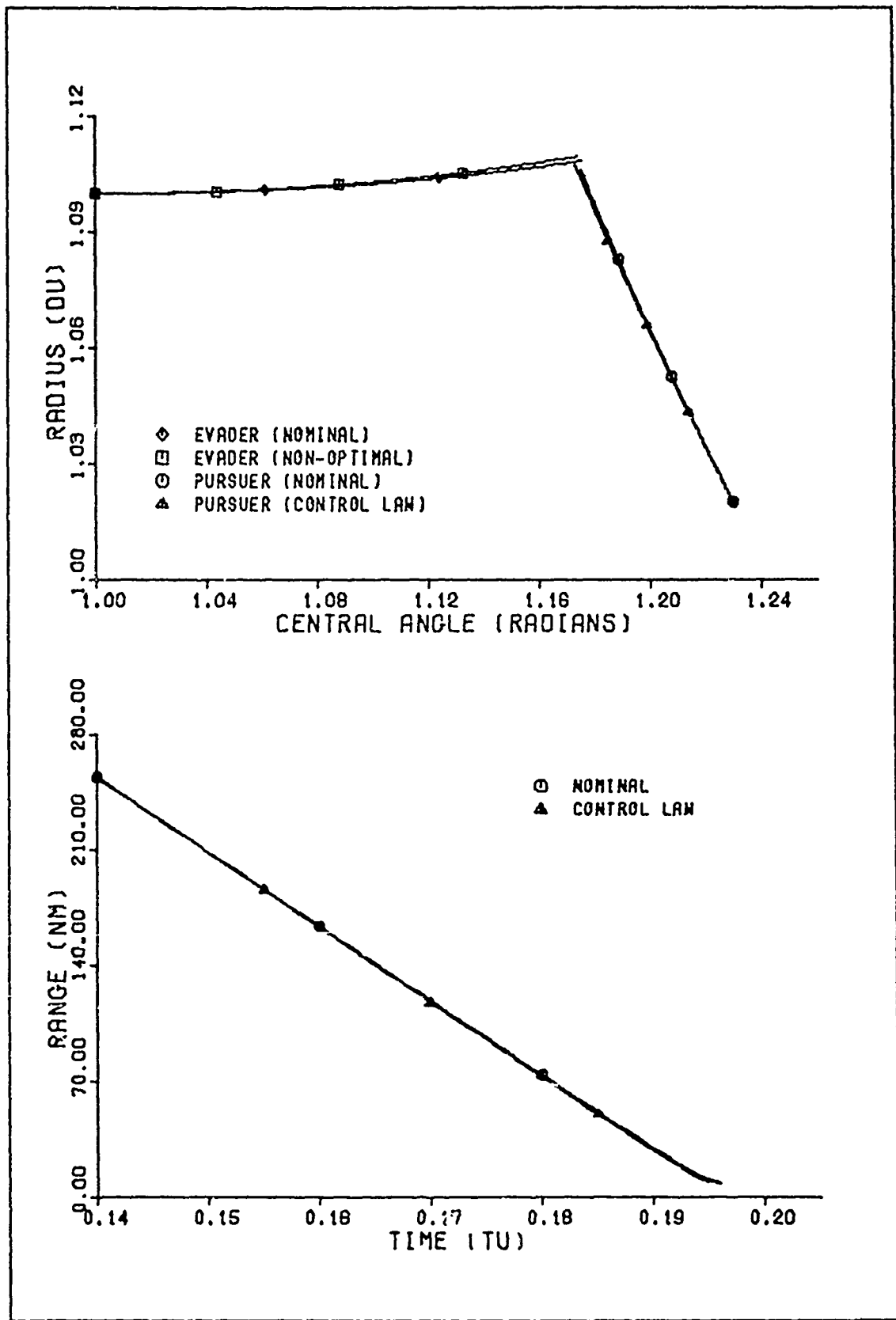


Fig. C-3. Trajectory 1, Backward Sweep Method.
 $V = 1.0$, Sampling Interval = 0.008 TU.

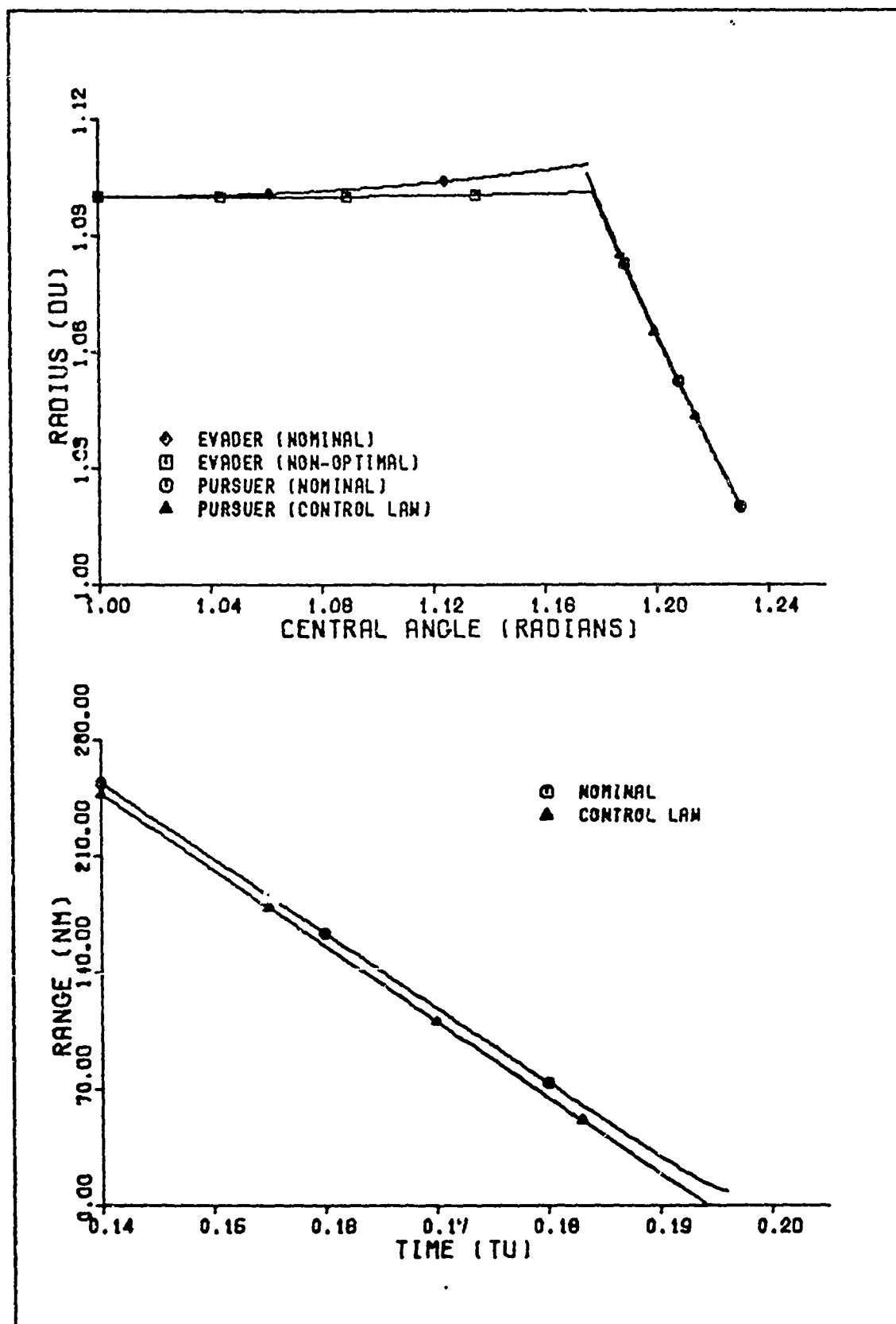


Fig. C-4. Trajectory 1, Backward Sweep Method.
 $V = 0.0$, Sampling Interval = 0.012 TU.

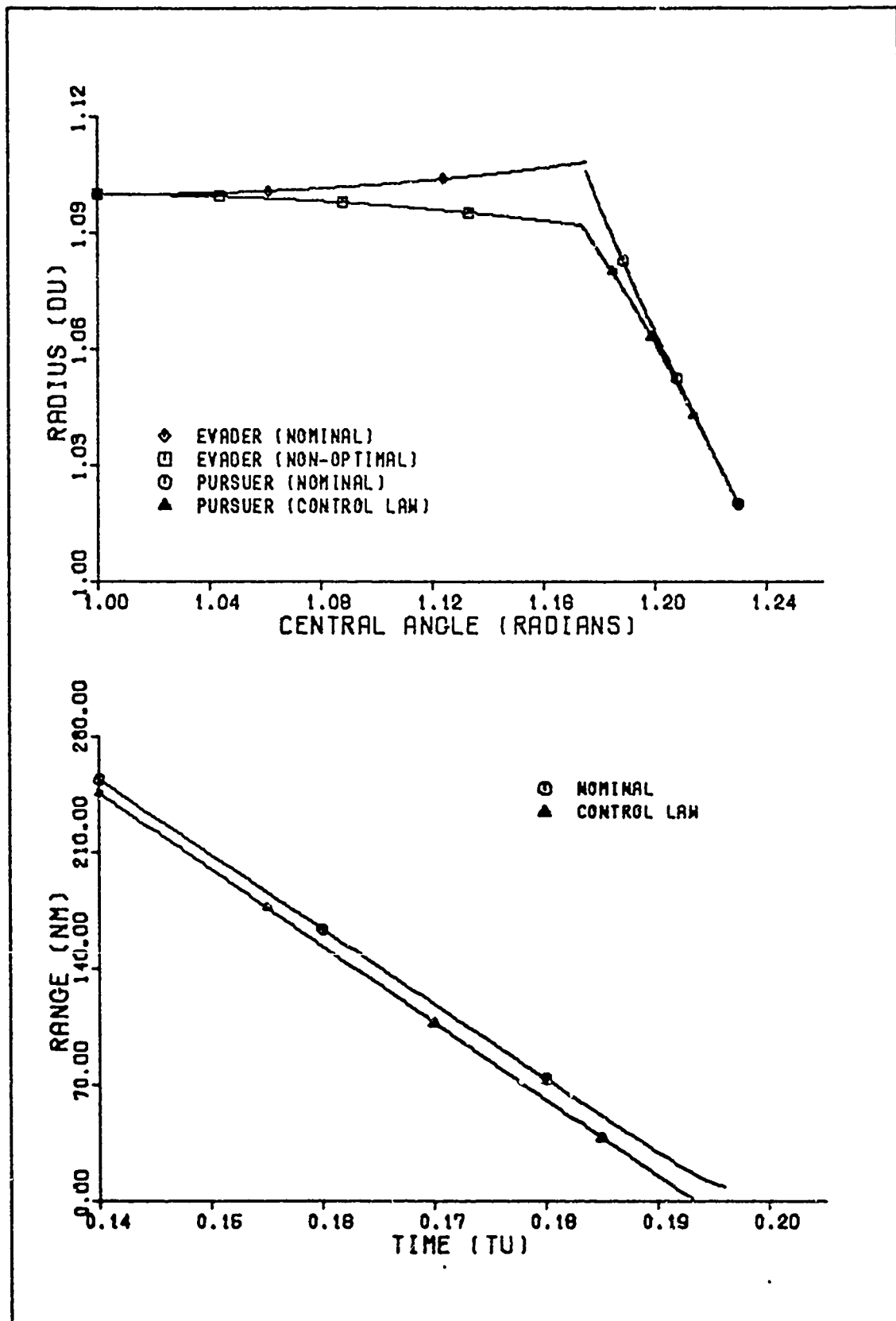


Fig. C-5. Trajectory 1, Backward Sweep Method.
 $V = -1.0$, Sampling Interval = 0.012 TU.

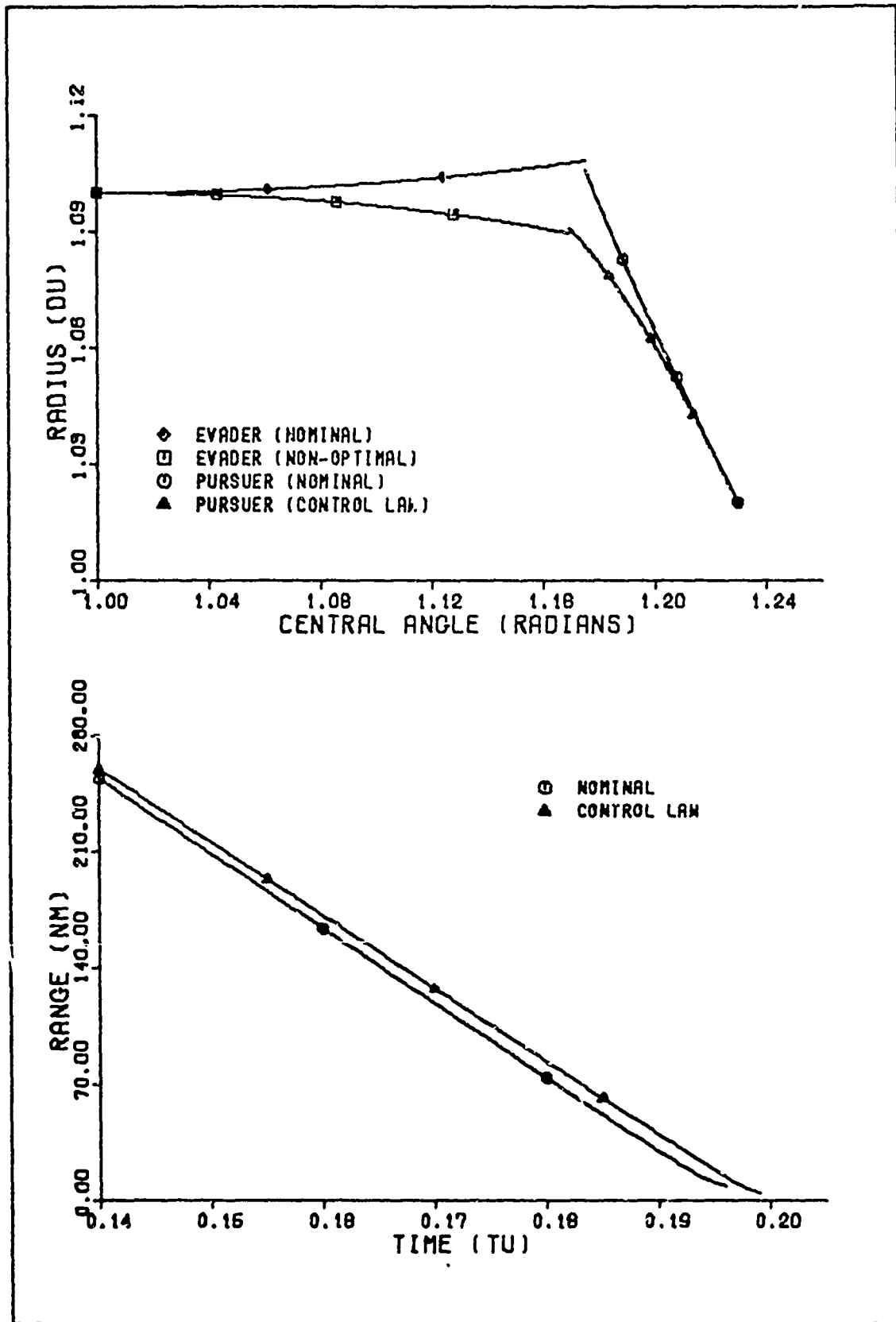


Fig. C-6. Trajectory 1, Backward Sweep Method.
 $V = -2.0$, Sampling Interval = 0.012 TU.

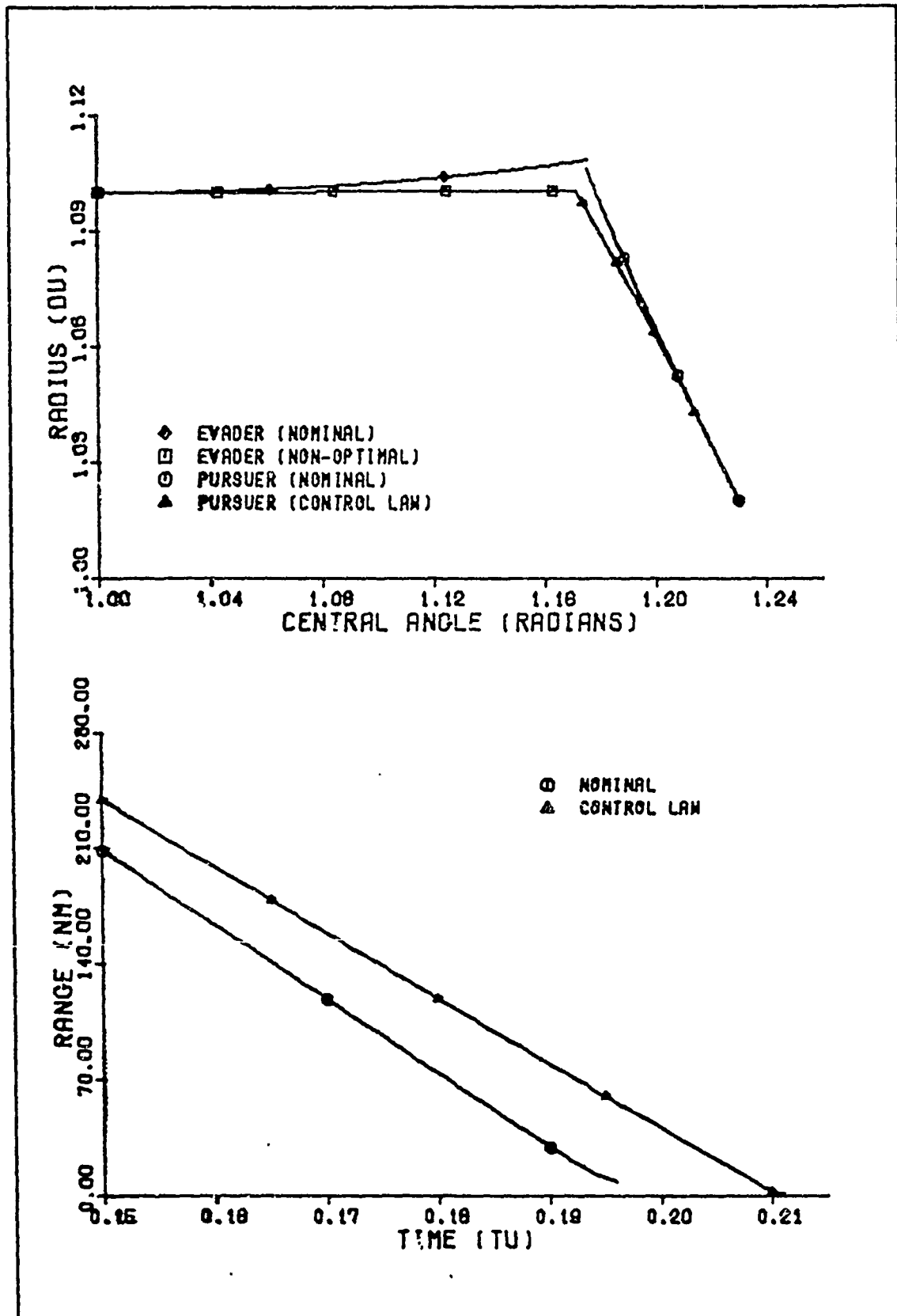


Fig. C-7. Trajectory 1, Backward Sweep Method.
 $V = -3.0$, Sampling Interval = 0.012 TU.

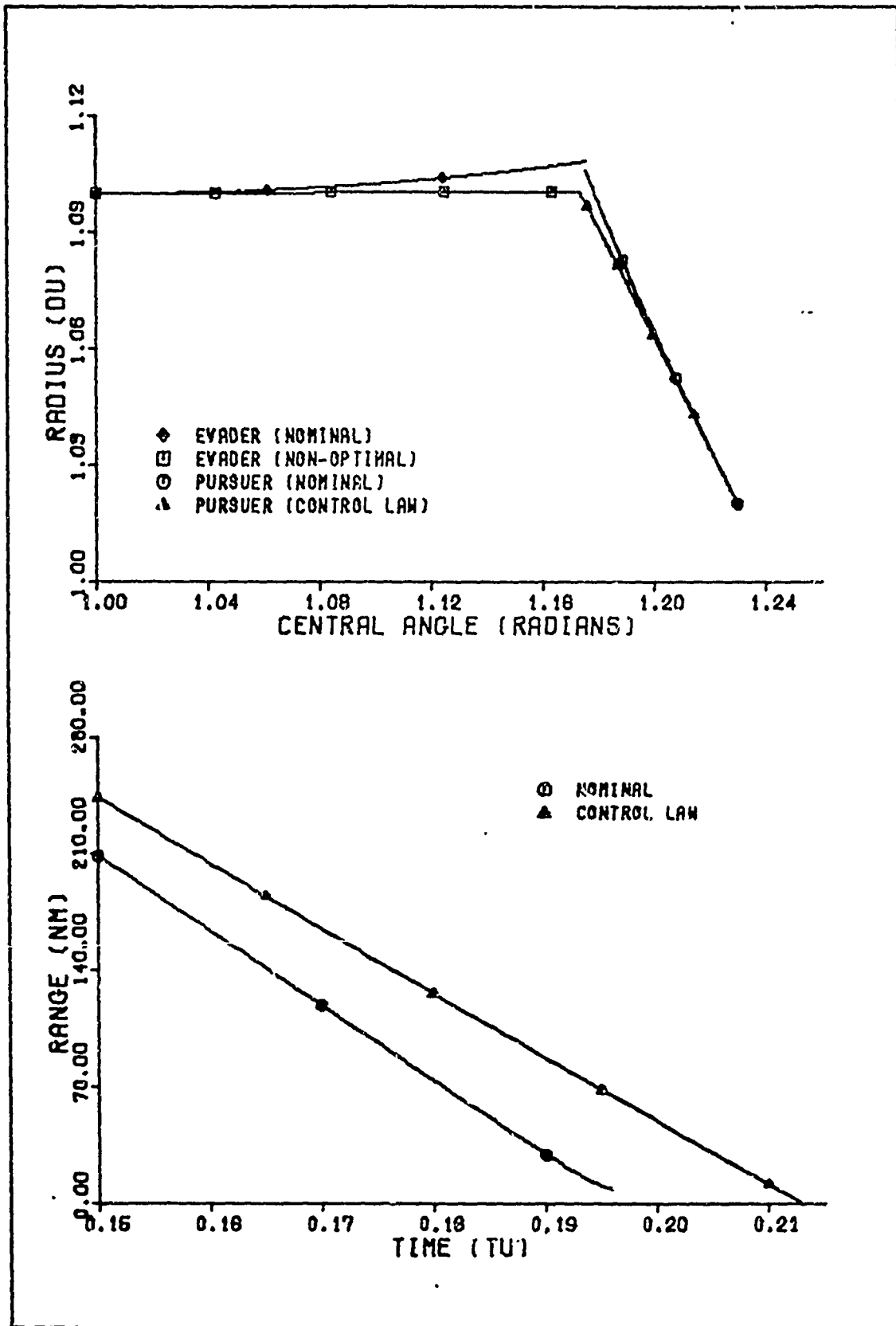


Fig. C-8. Trajectory 1, Transition Matrix Method.
 $V = 3.0$, Sampling Interval = 0.012 TU.

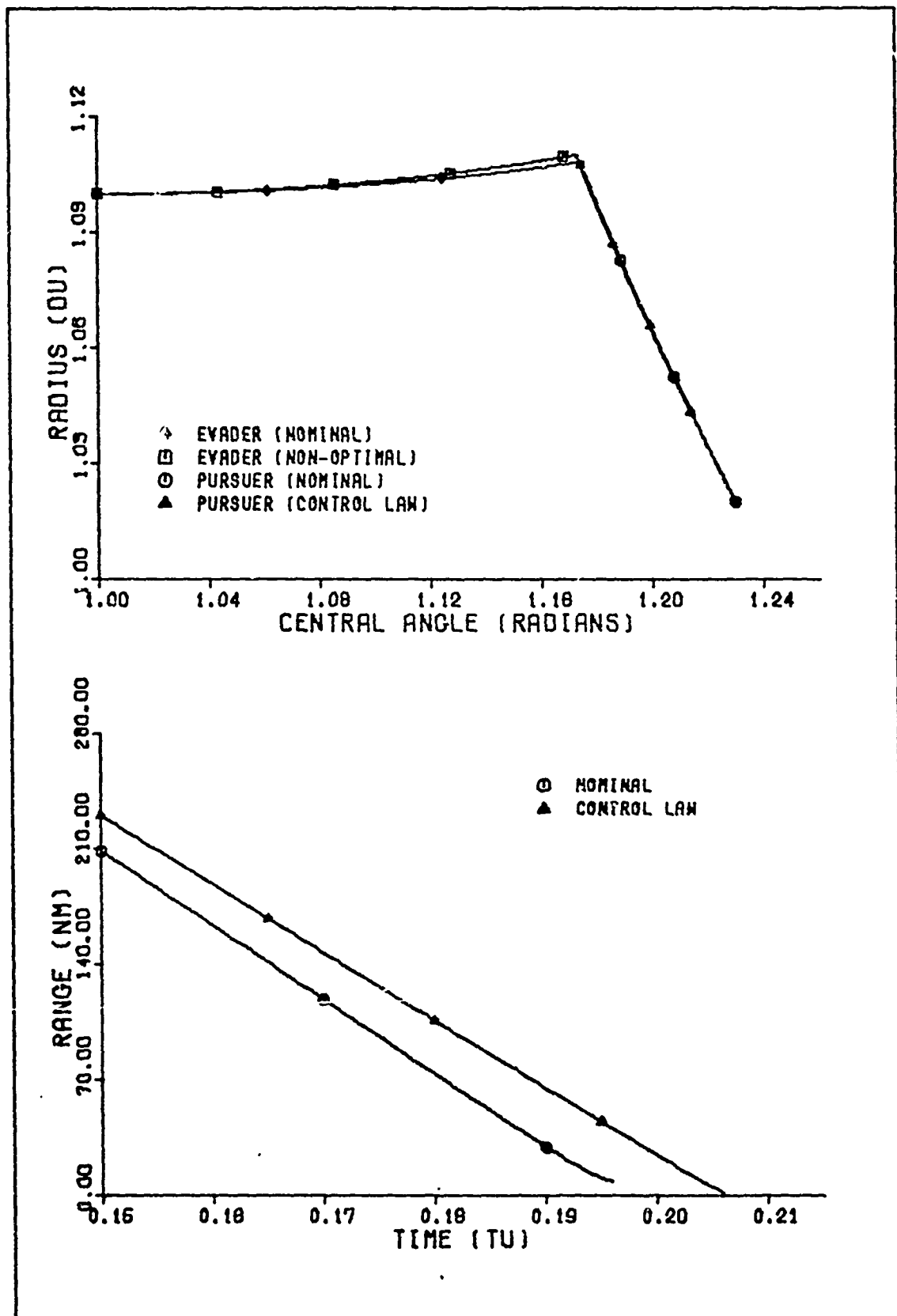


Fig. C-9. Trajectory 1, Transition Matrix Method.
 $V = 2.0$, Sampling Interval = 0.012 TU.

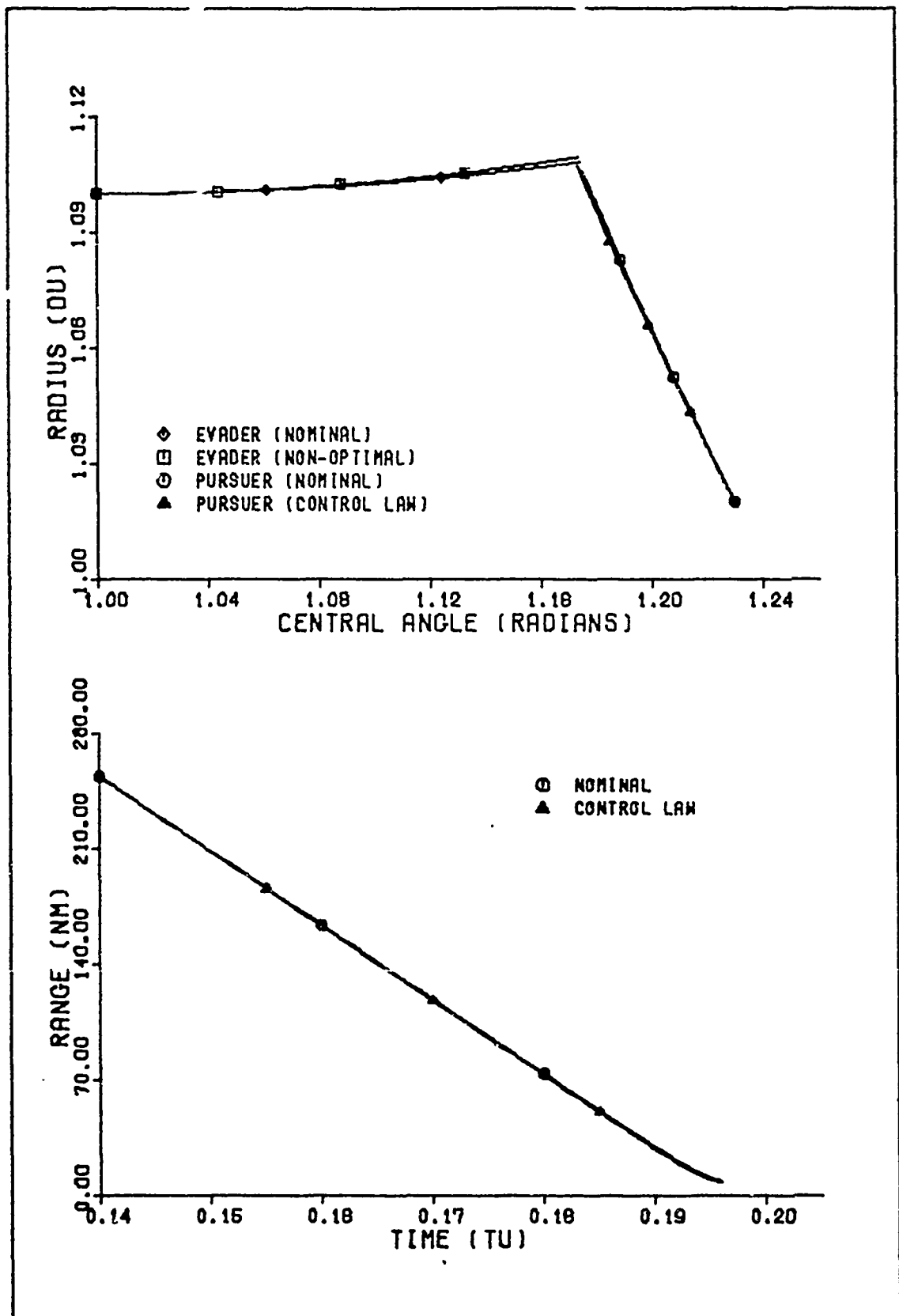


Fig. C-10. Trajectory 1, Transition Matrix Method.
 $V = 1.0$, Sampling Interval = 0.012 TU.

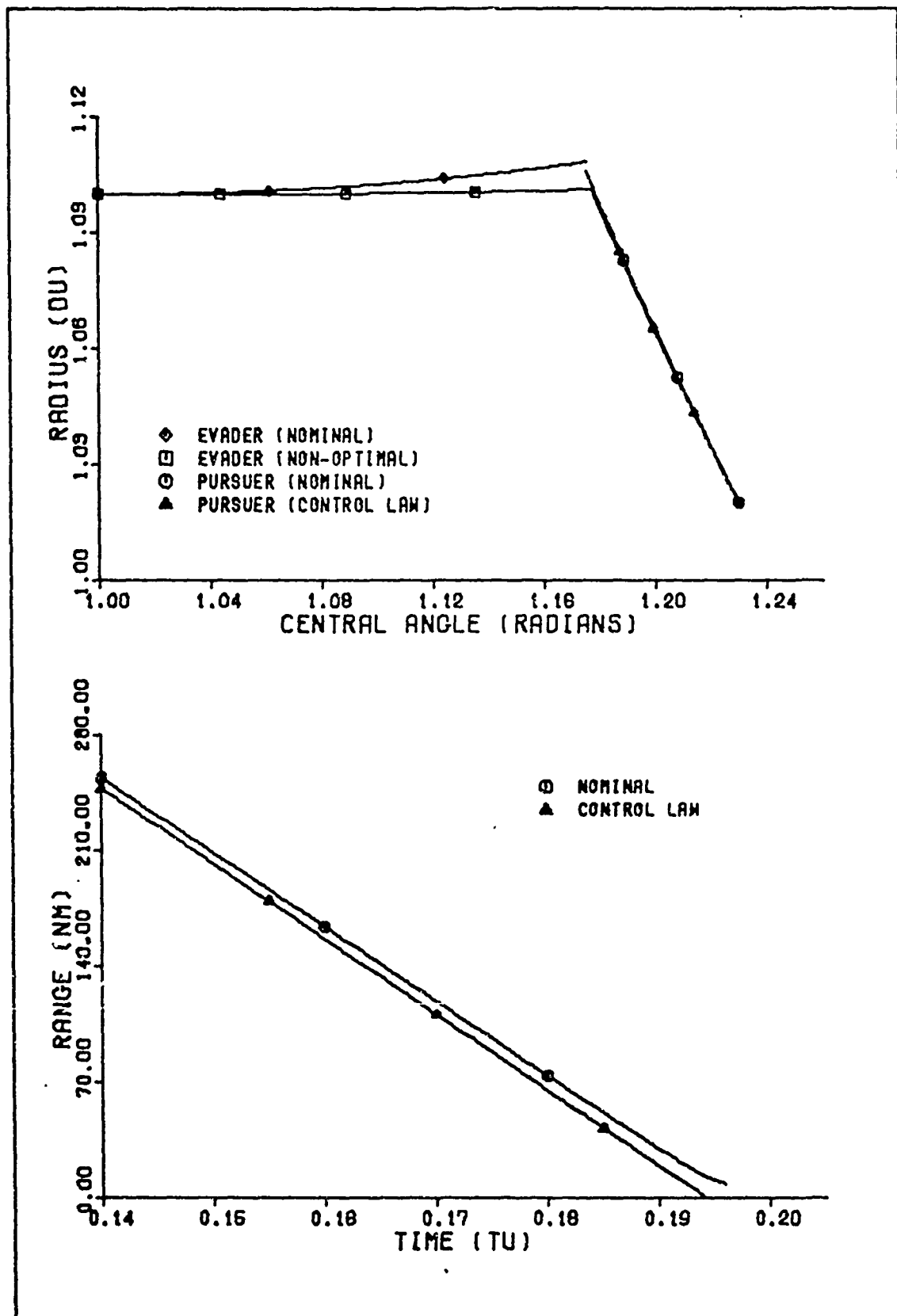


Fig. C-11. Trajectory 1, Transition Matrix Method.
 $V = 0.0$, Sampling Interval = 0.012 TU.

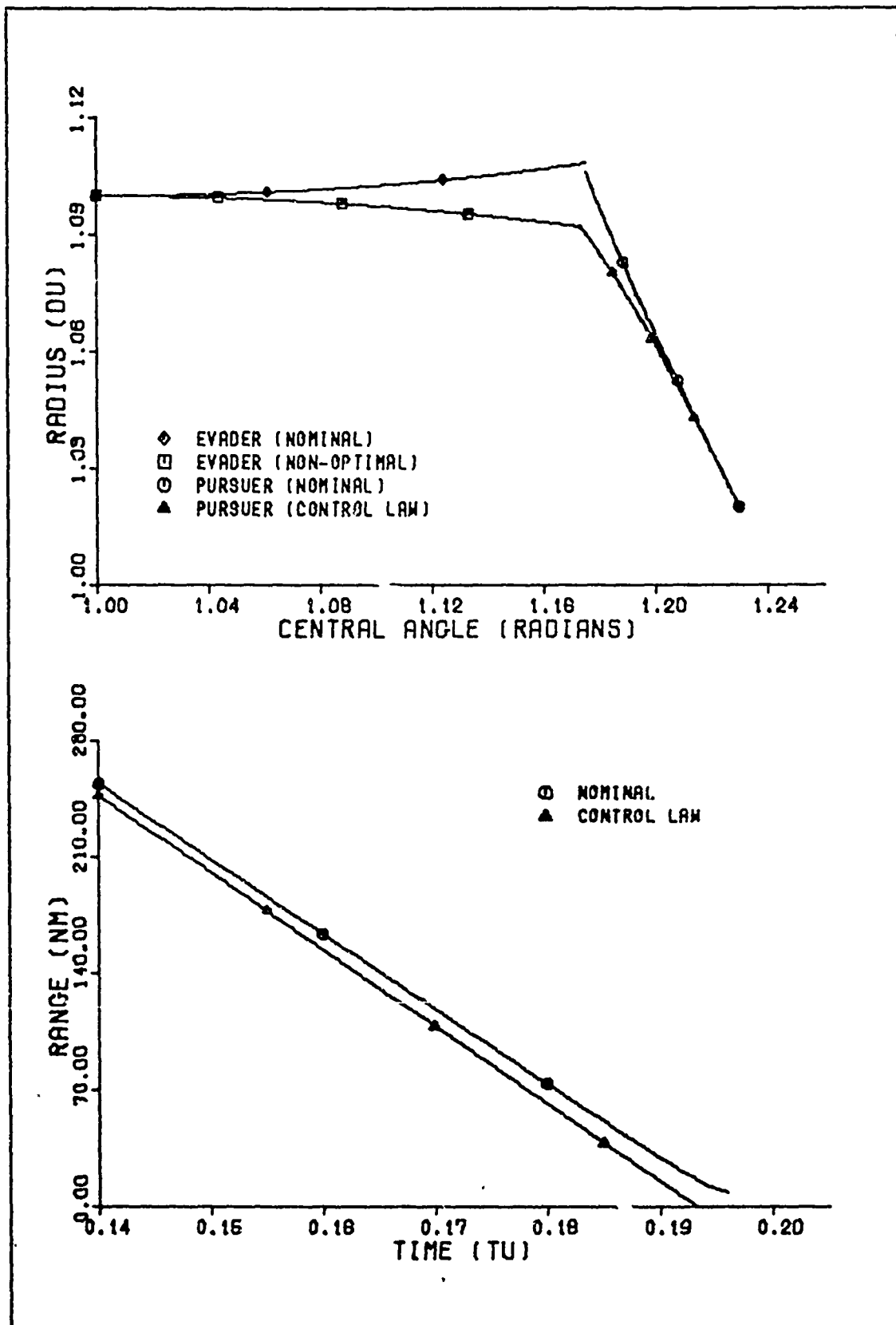


Fig. C-12. Trajectory 1, Transition Matrix Method.
 $V = -1.0$, Sampling Interval = 0.012 TU.

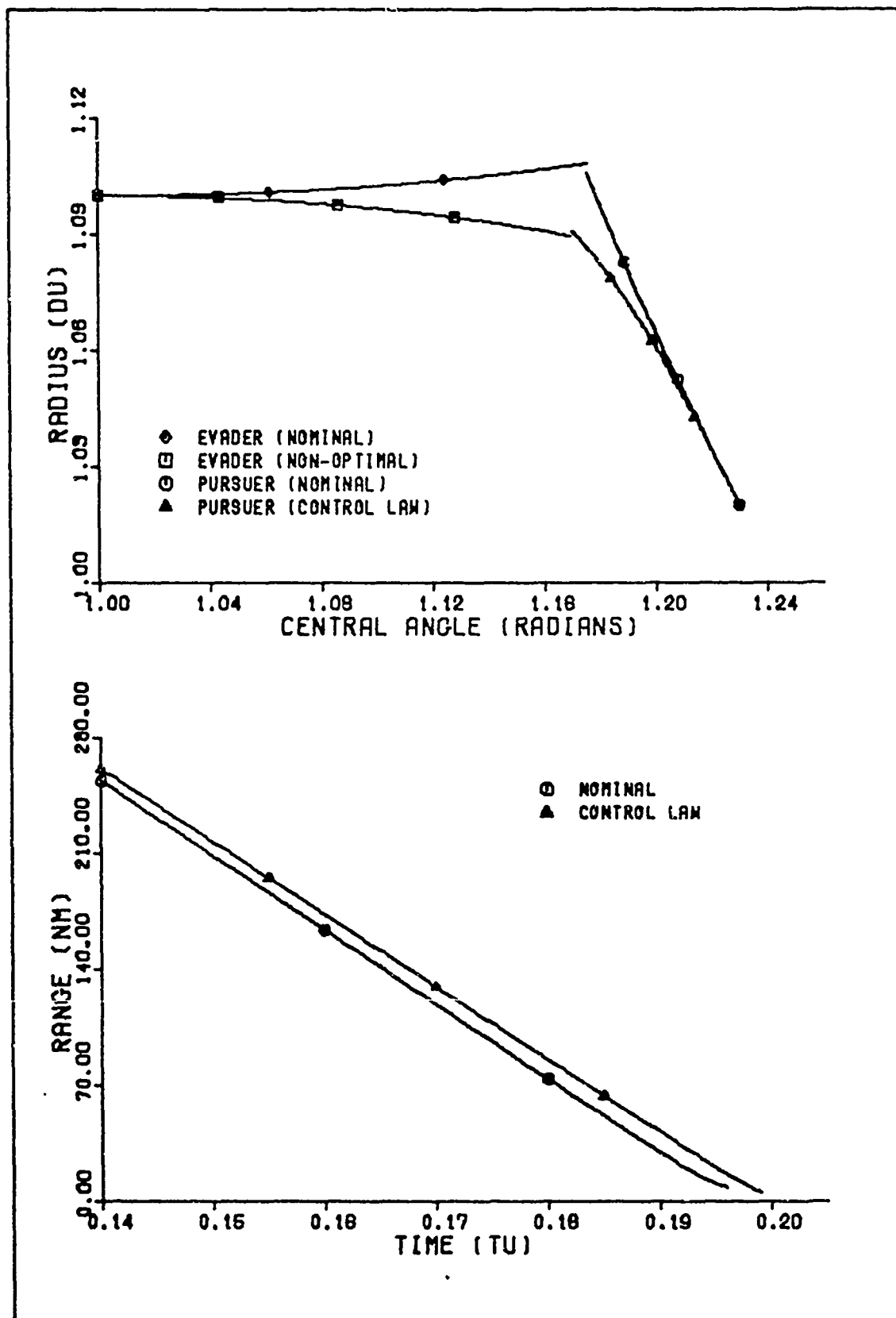


Fig. C-13. Trajectory 1, Transition Matrix Method.
 $V = -2.0$, Sampling Interval = 0.012 TU.

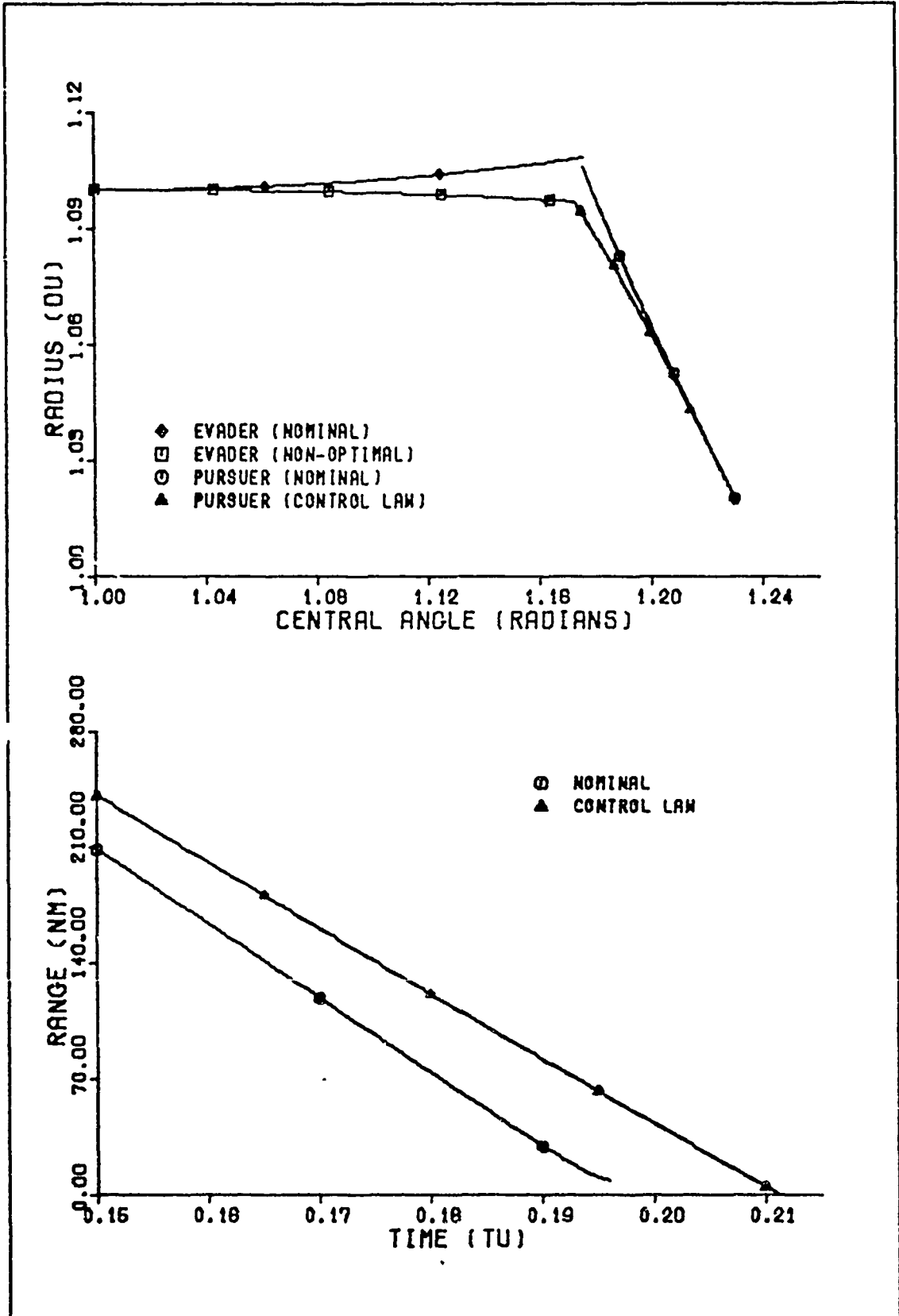


Fig. C-14. Trajectory 1, Transition Matrix Method.
 $V = -3.0$, Sampling Interval = 0.012 TU.

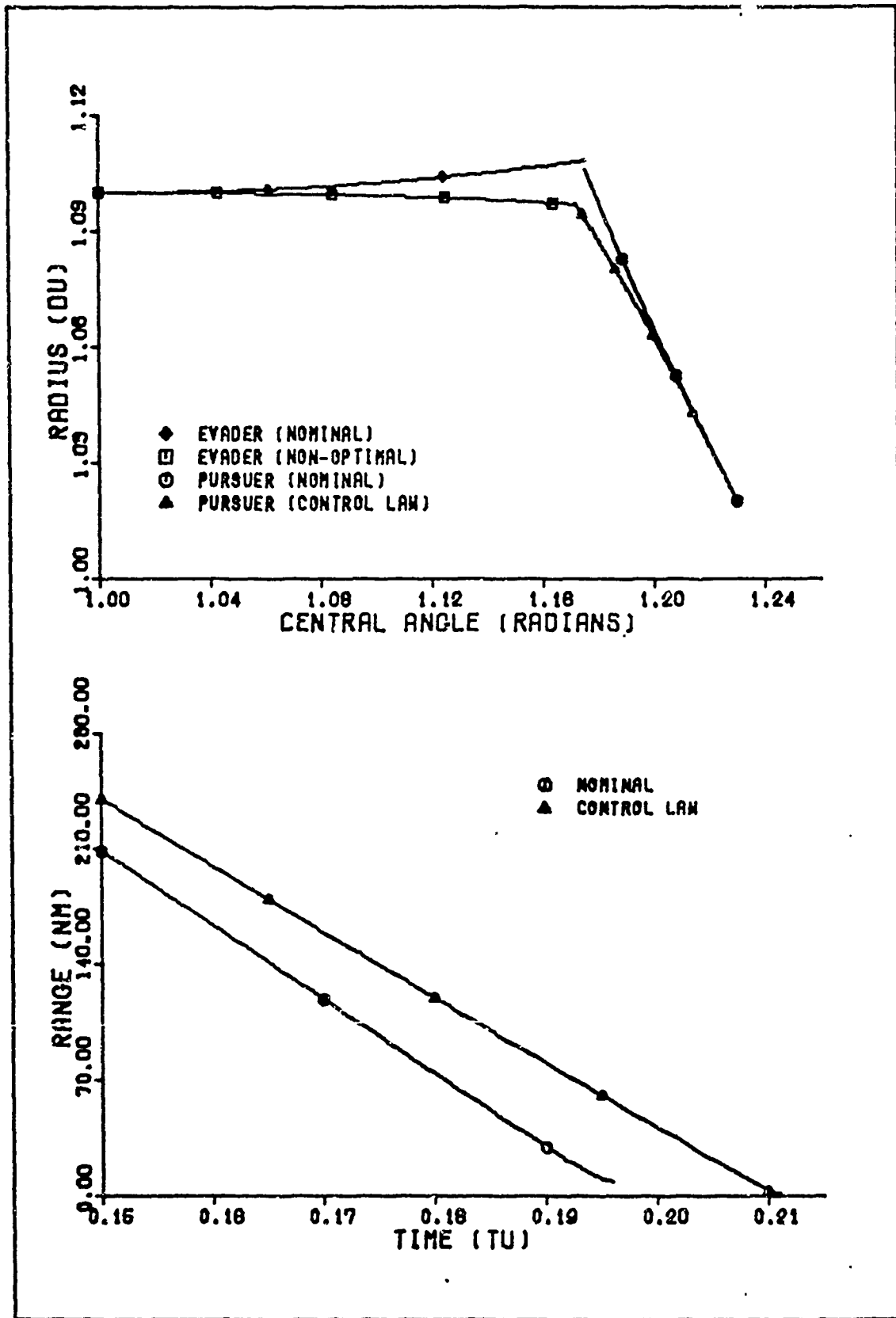


Fig. C-15. Trajectory 1, Backward Sweep Method.
 $V = 3.0$, Sampling Interval = 0.016 TU.

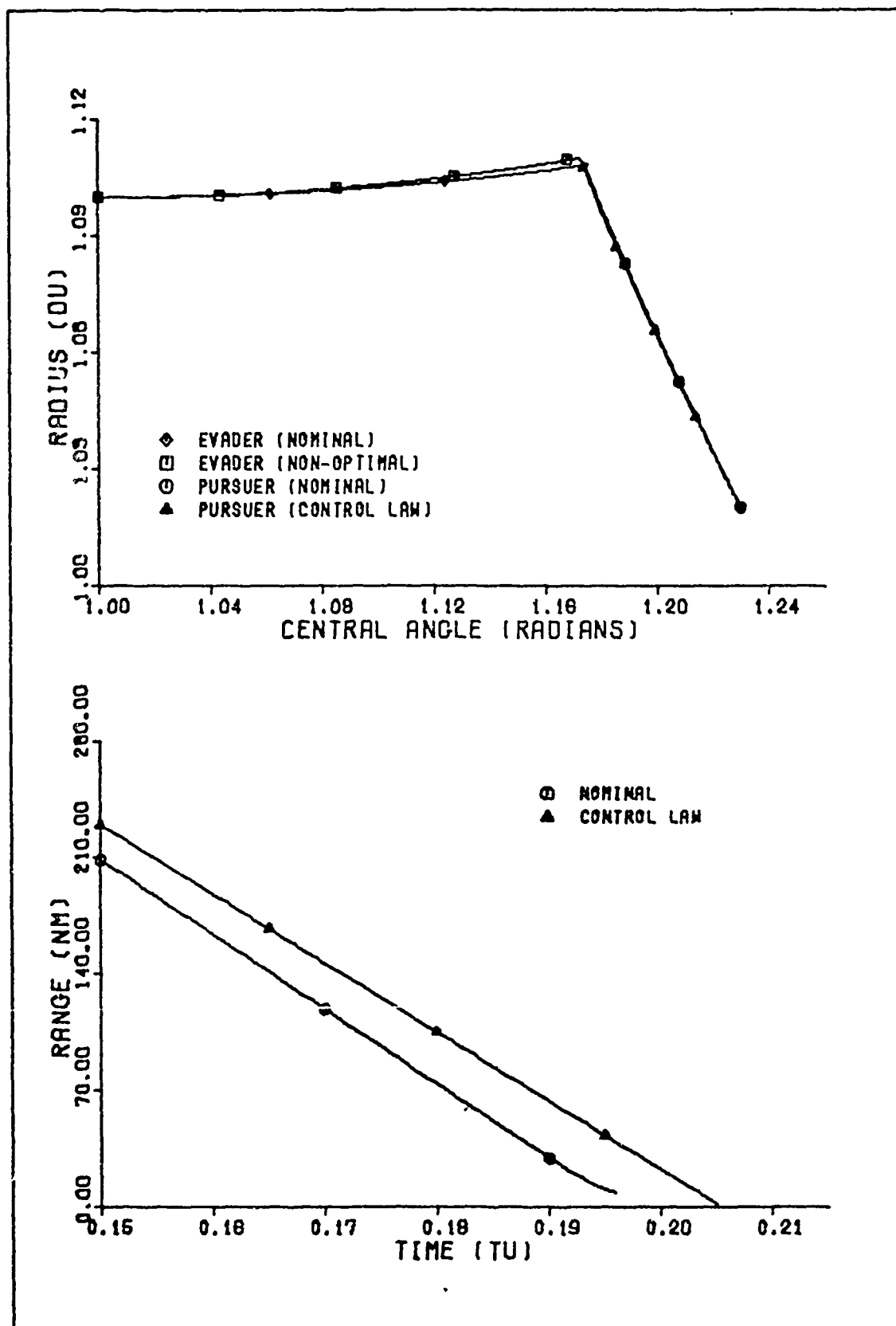


Fig. C-16. Trajectory 1, Backward Sweep Method.
 $V = 2.0$, Sampling Interval = 0.016 TU,

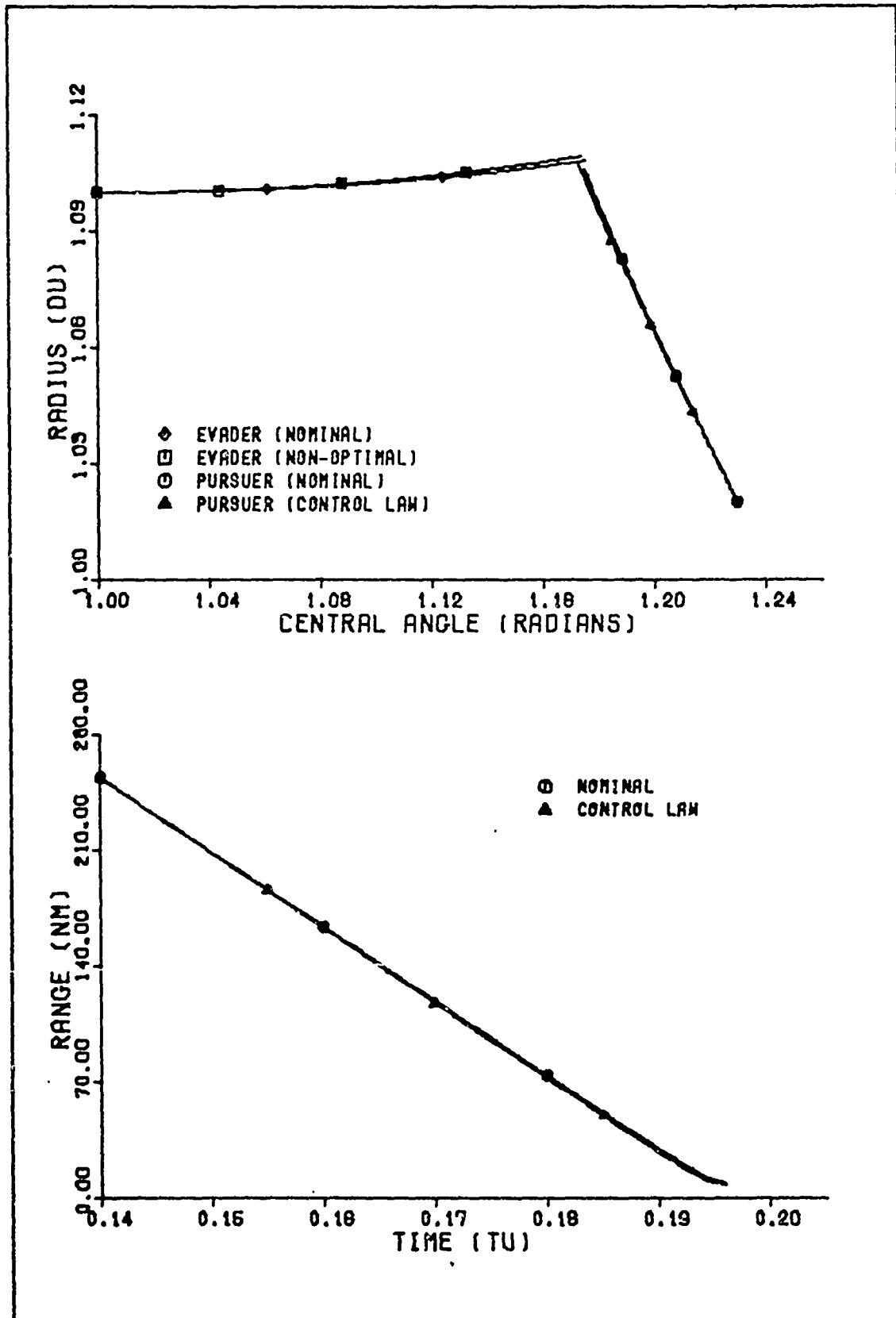


Fig. C-17. Trajectory 1, Backward Sweep Method.
 $V = 1.0$, Sampling Interval = 0.016 TU.

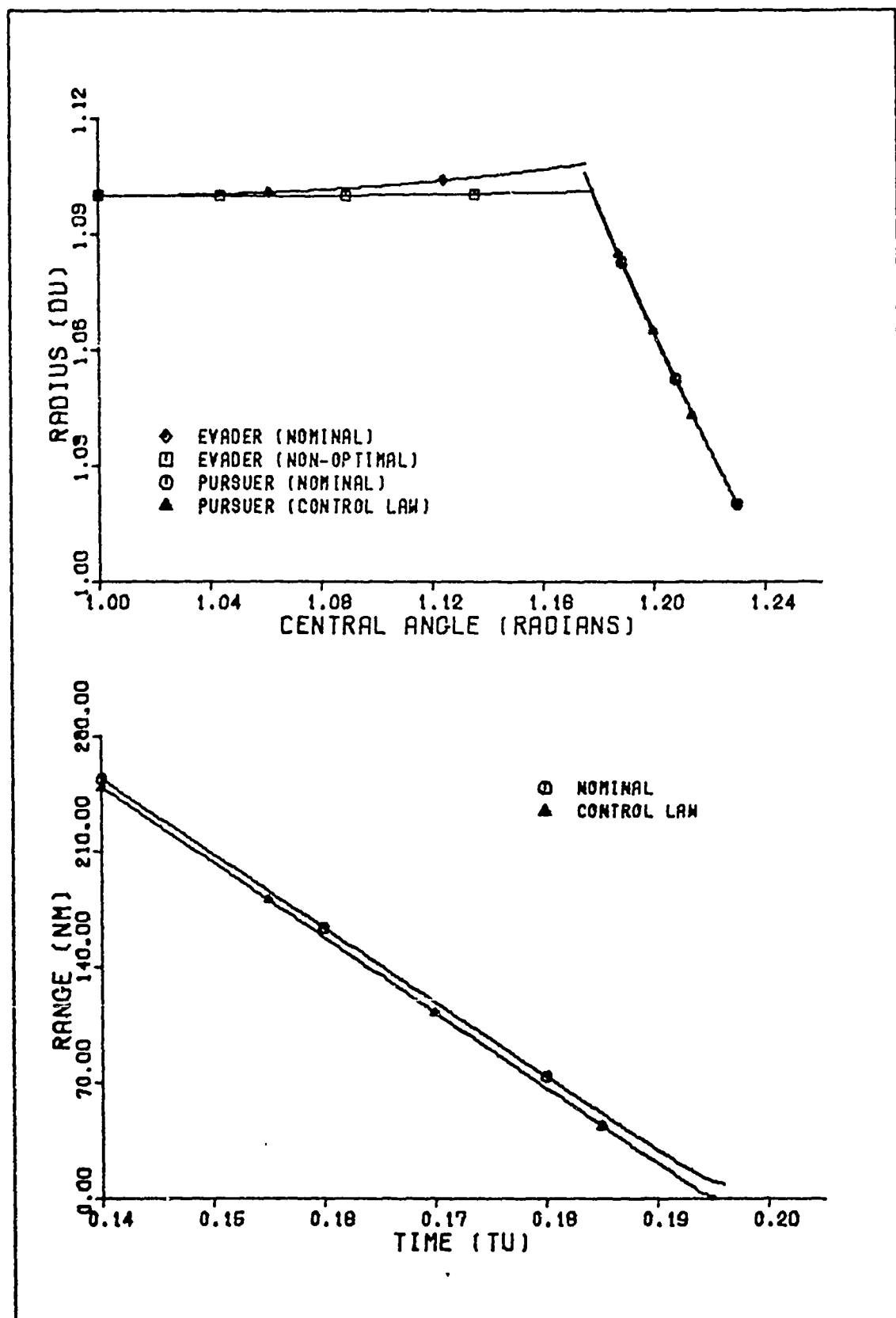


Fig. C-18. Trajectory 1, Backward Sweep Method.
 $V = 0.0$, Sampling Interval = 0.016 TU.

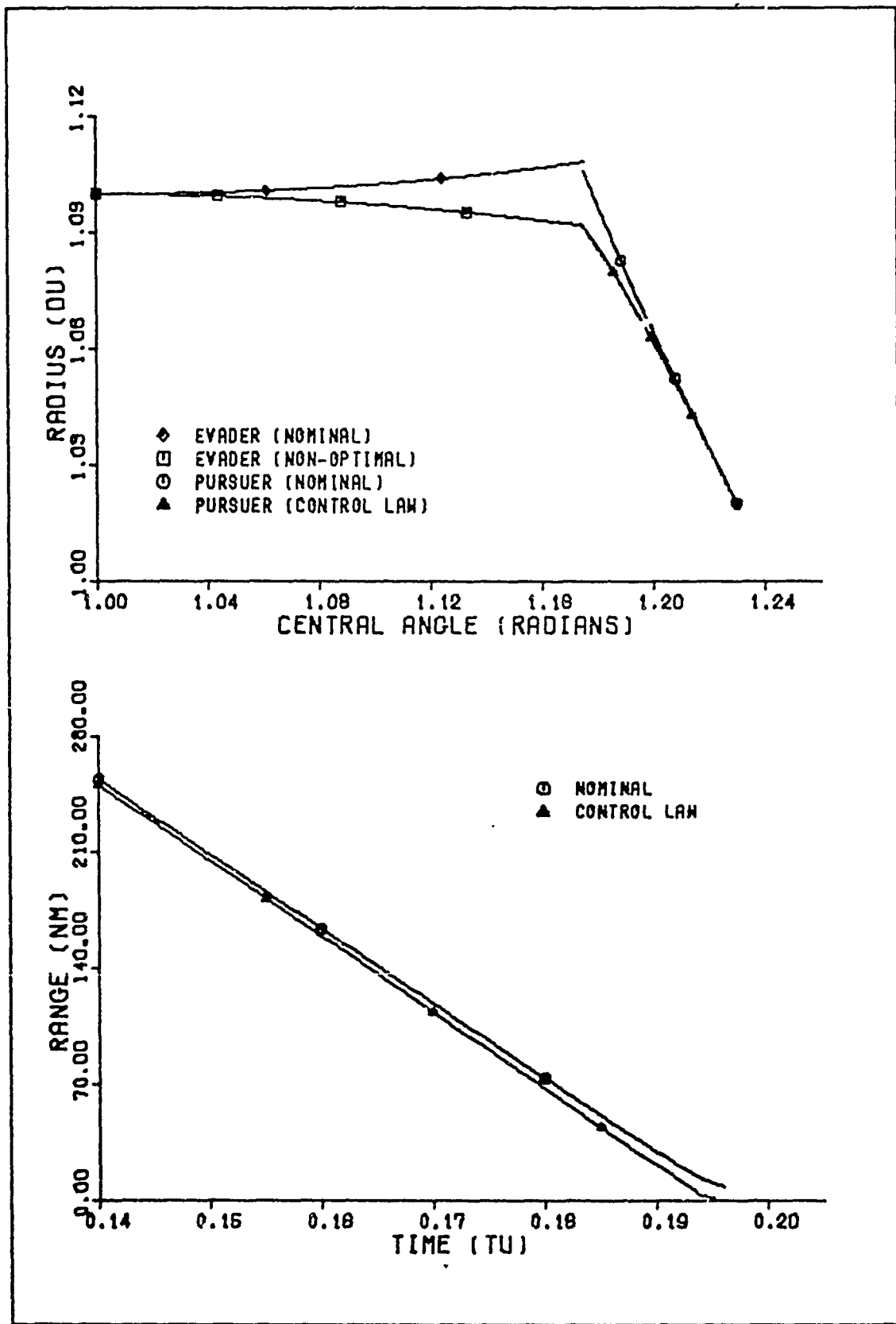


Fig. C-19. Trajectory 1, Backward Sweep Method.
 $V = -1.0$, Sampling Interval = 0.016 TU.

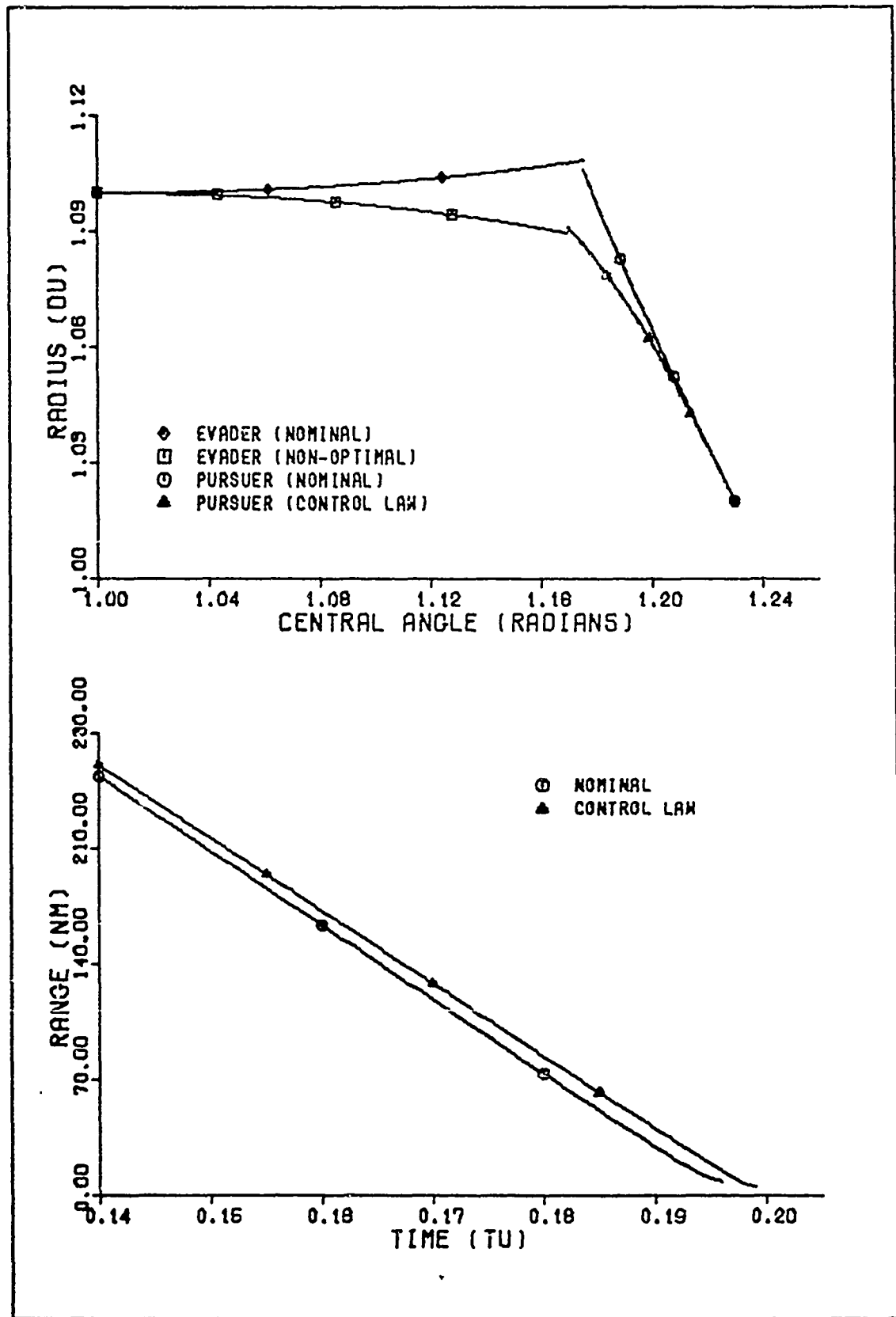


Fig. C-20. Trajectory 1, Backward Sweep Method. $V = -2.0$, Sampling Interval = 0.016 TU.

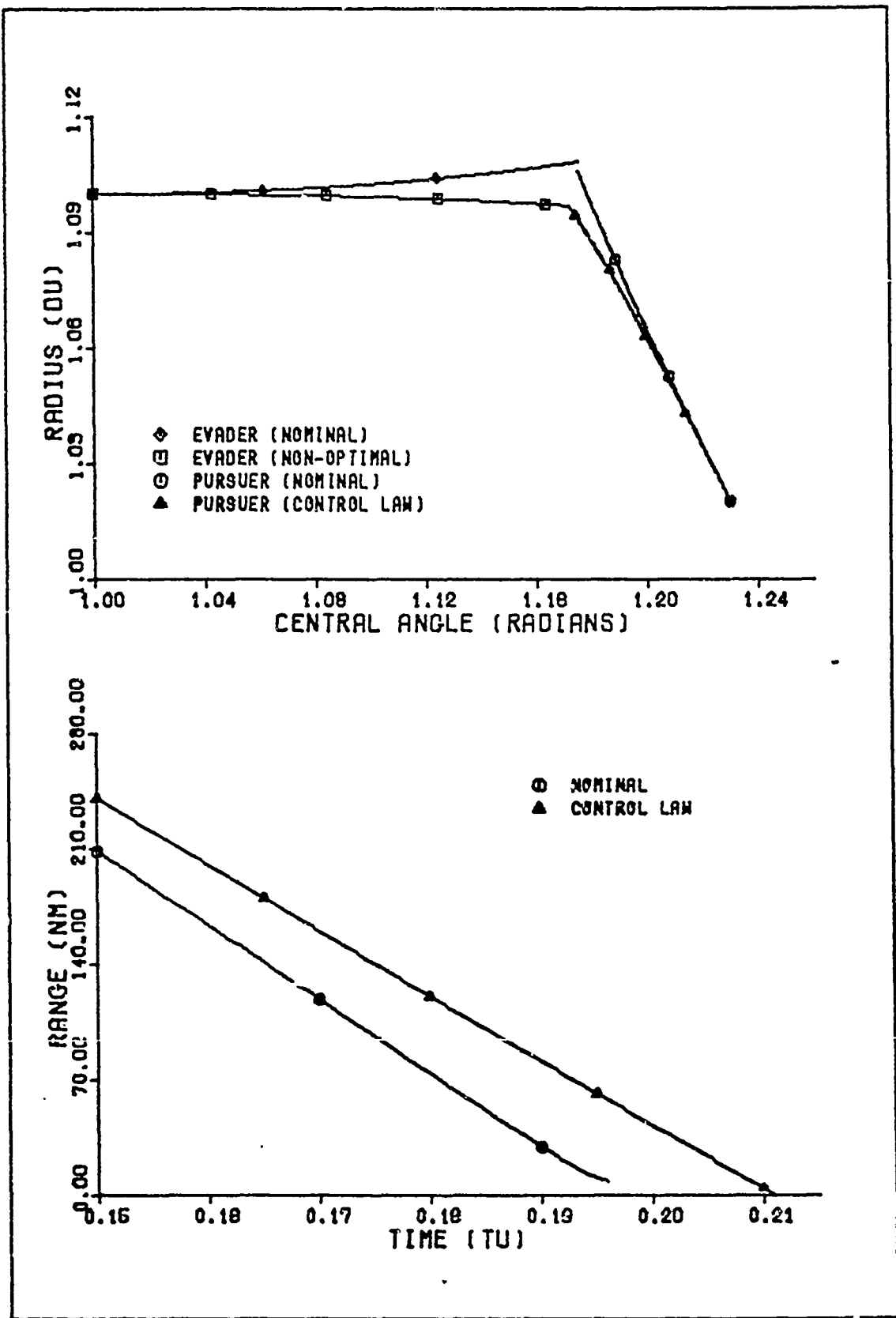


Fig. C-21. Trajectory 1, Backward Sweep Method.
 $V = -3.0$, Sampling Interval = 0.016 TU.

Appendix D

Plots of Trajectory 2

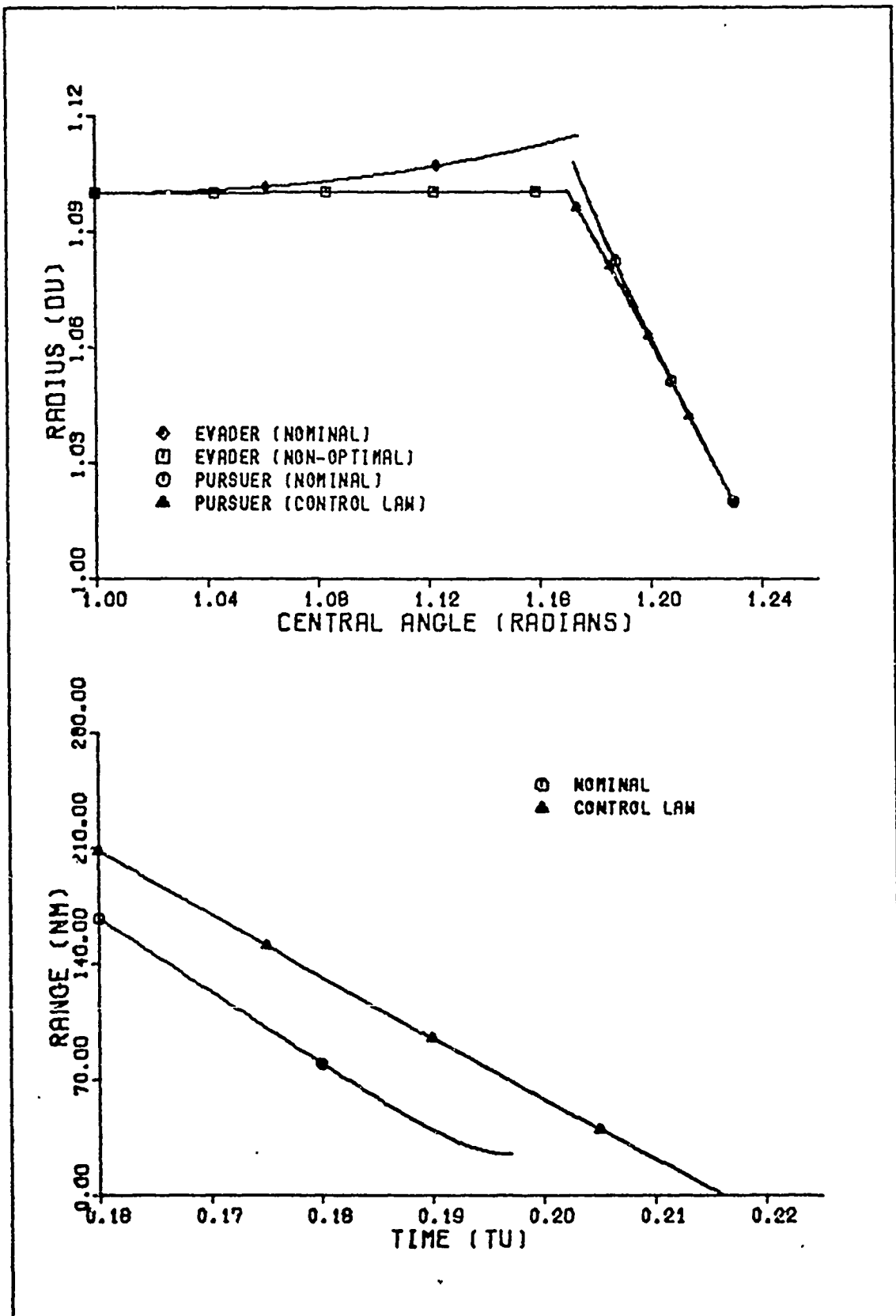


Fig. D-1. Trajectory 2, Backward Sweep Method.
 $V = 3.0$, Sampling Interval = 0.012 TU.

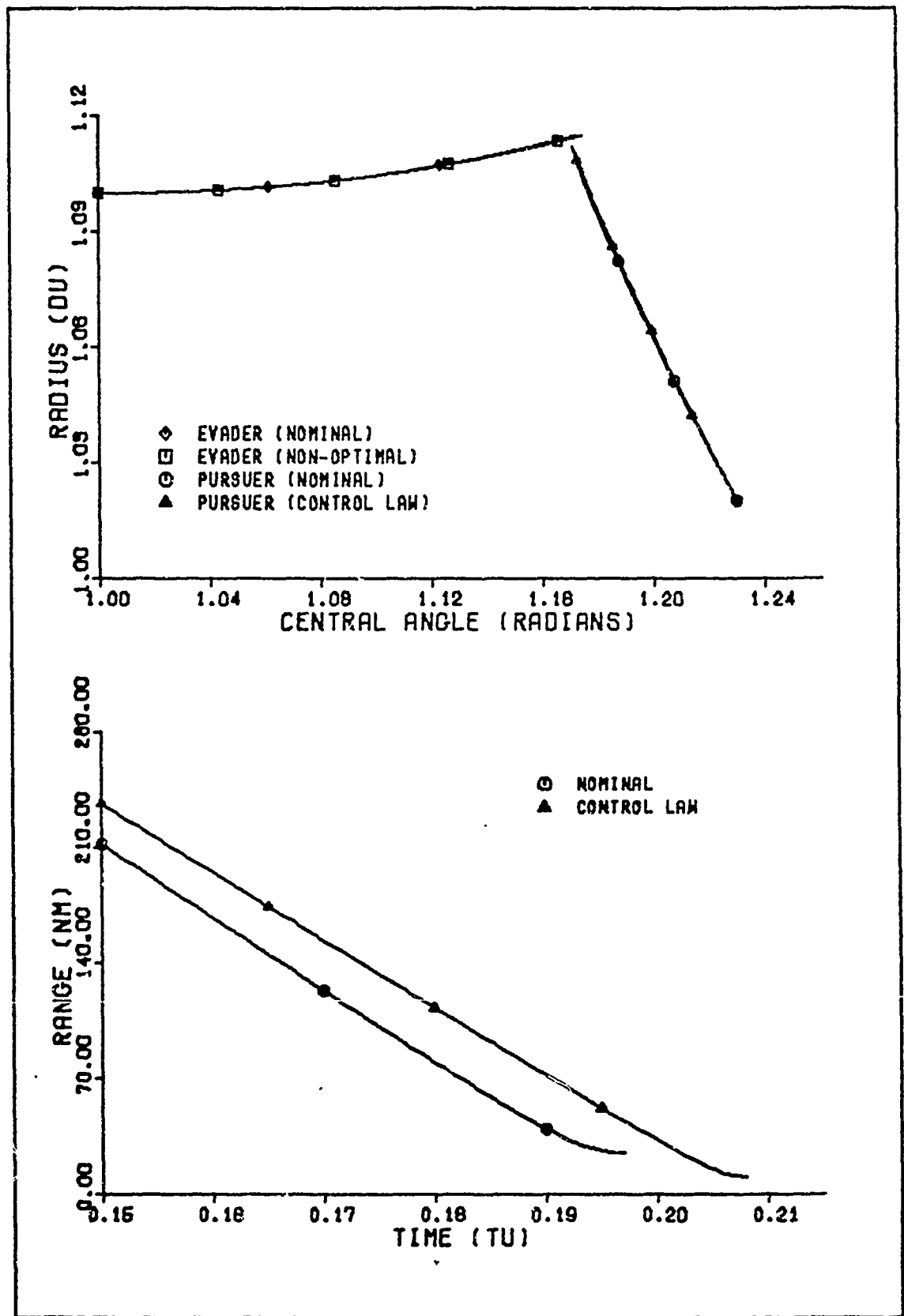


Fig. D-2. Trajectory 2, Backward Sweep Method.
 $V = 2.0$, Sampling Interval = 0.012 TU.

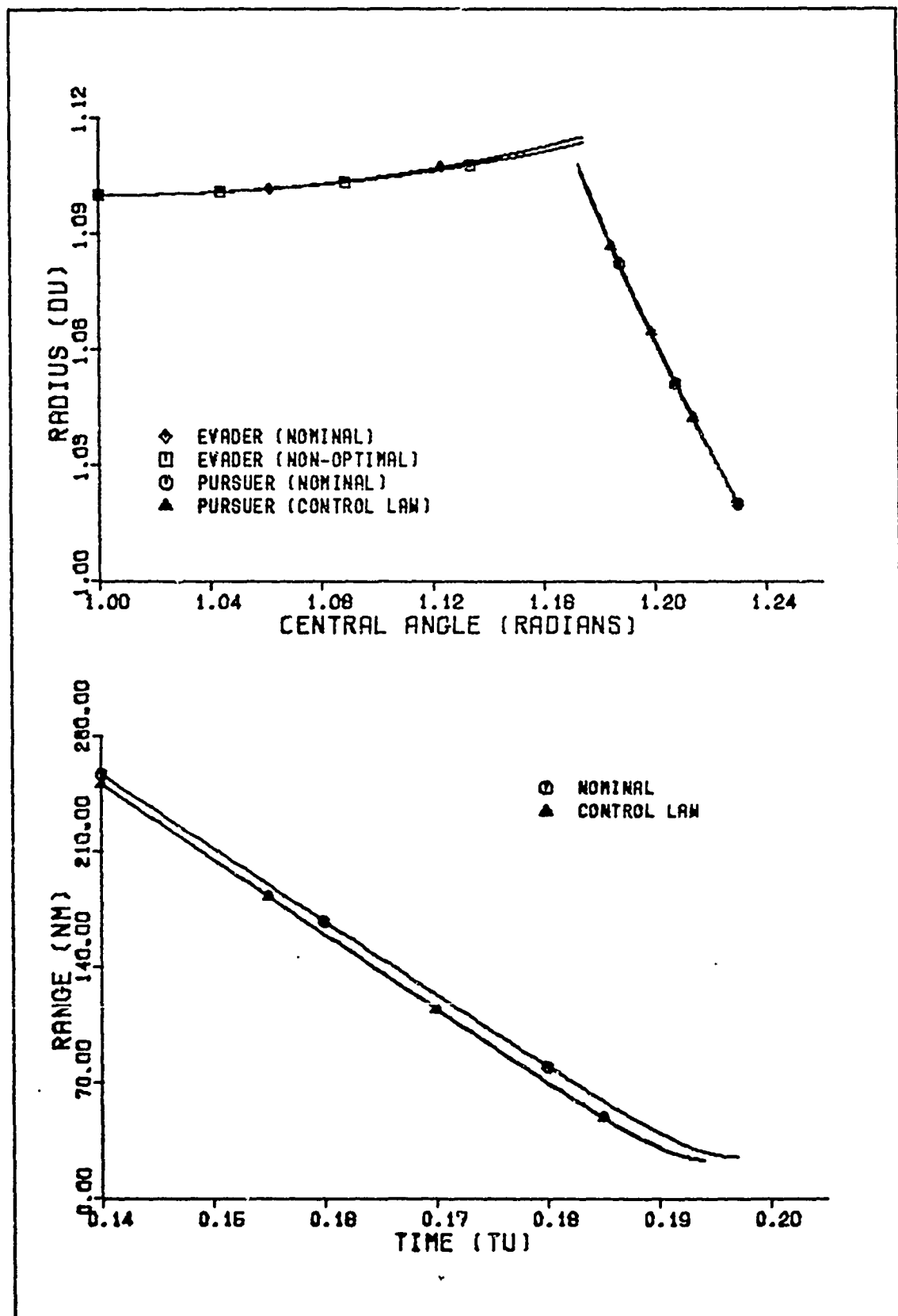


Fig. D-3. Trajectory 2, Backward Sweep Method.
 $V = 1.0$, Sampling Interval = 0.012 TU.

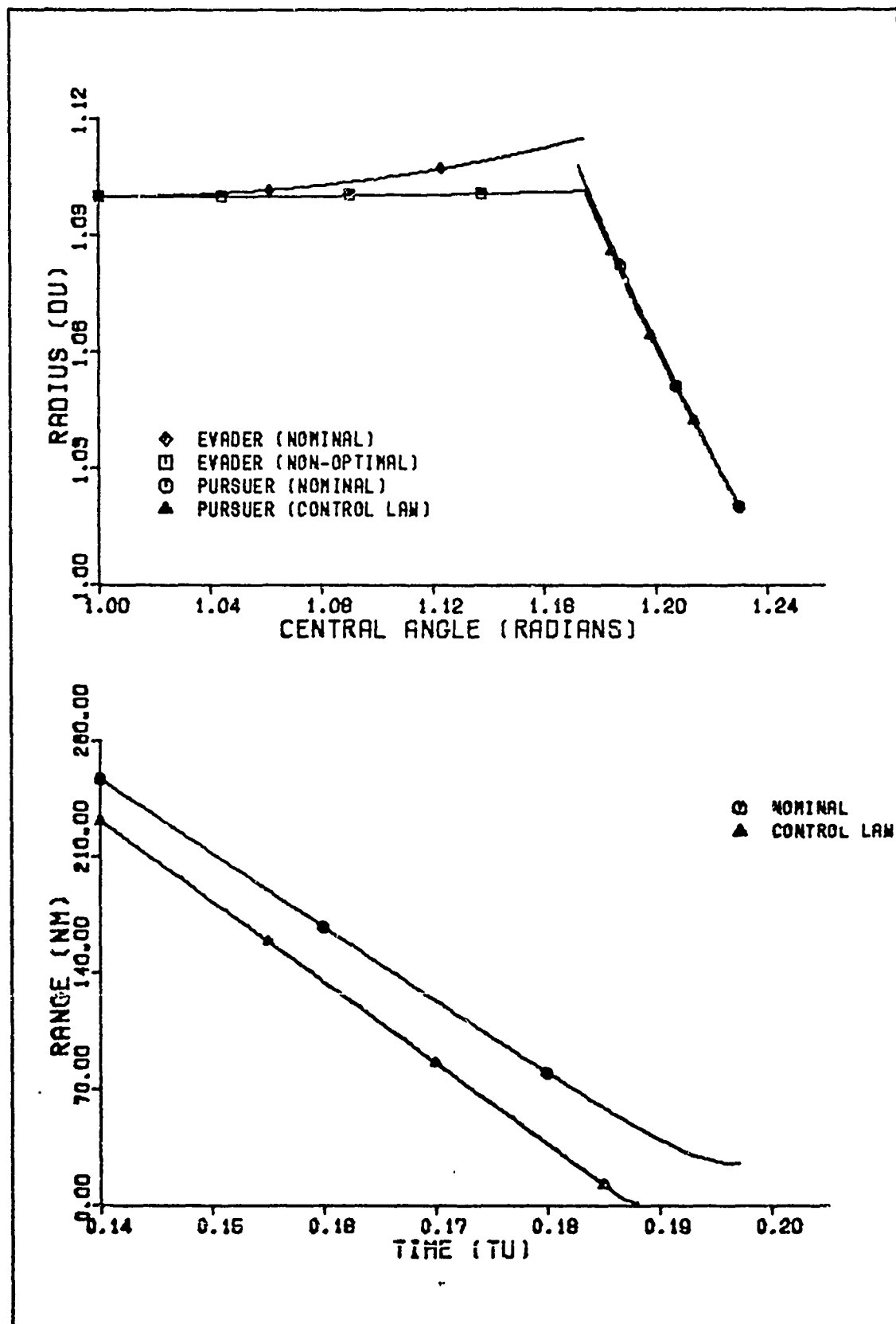


Fig. D-4. Trajectory 2, Backward Sweep Method.
 $V = 0.0$, Sampling Interval = 0.012 TU.

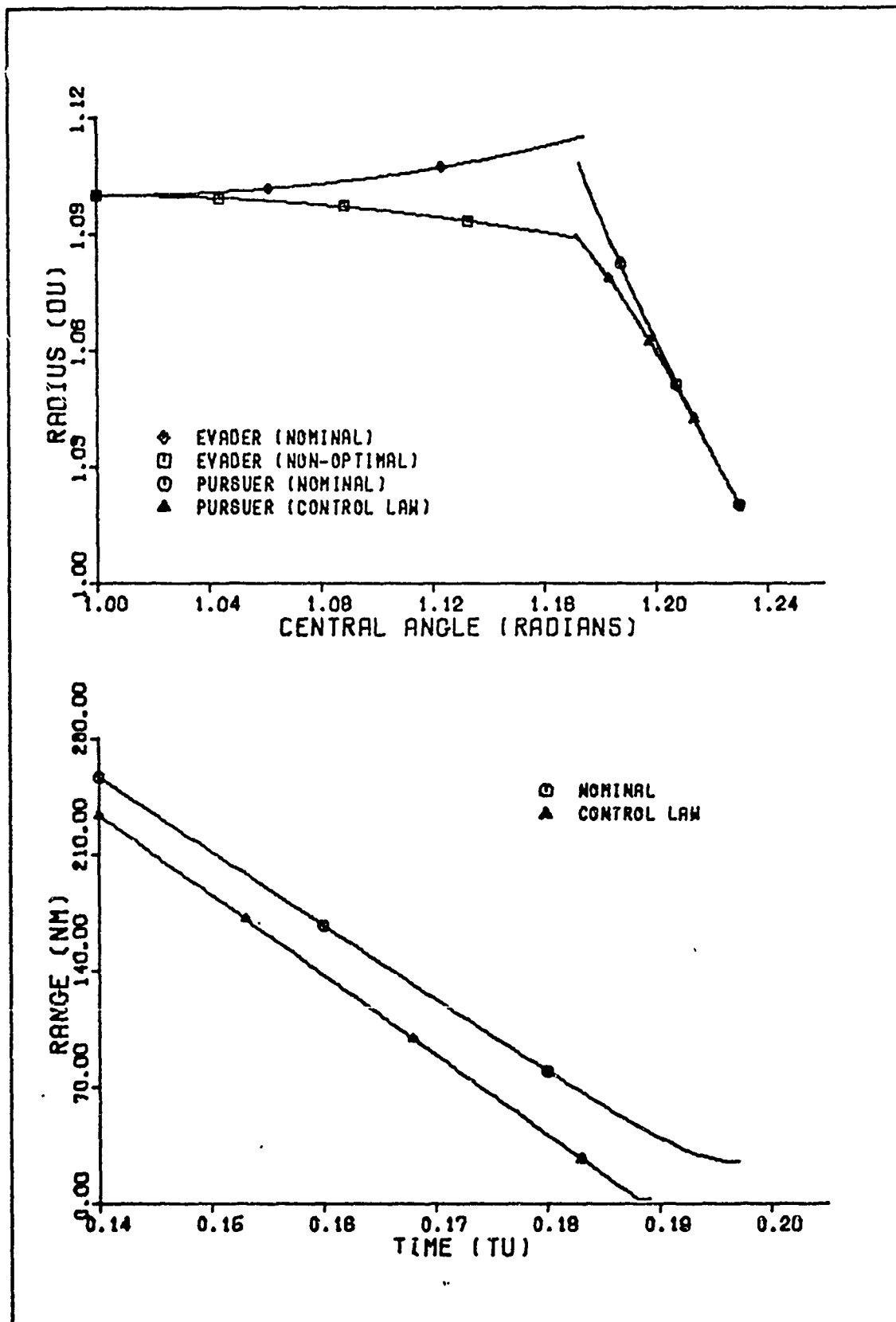


Fig. D-5. Trajectory 2, Backward Sweep Method.
 $V = -1.0$, Sampling Interval = 0.012 TU.

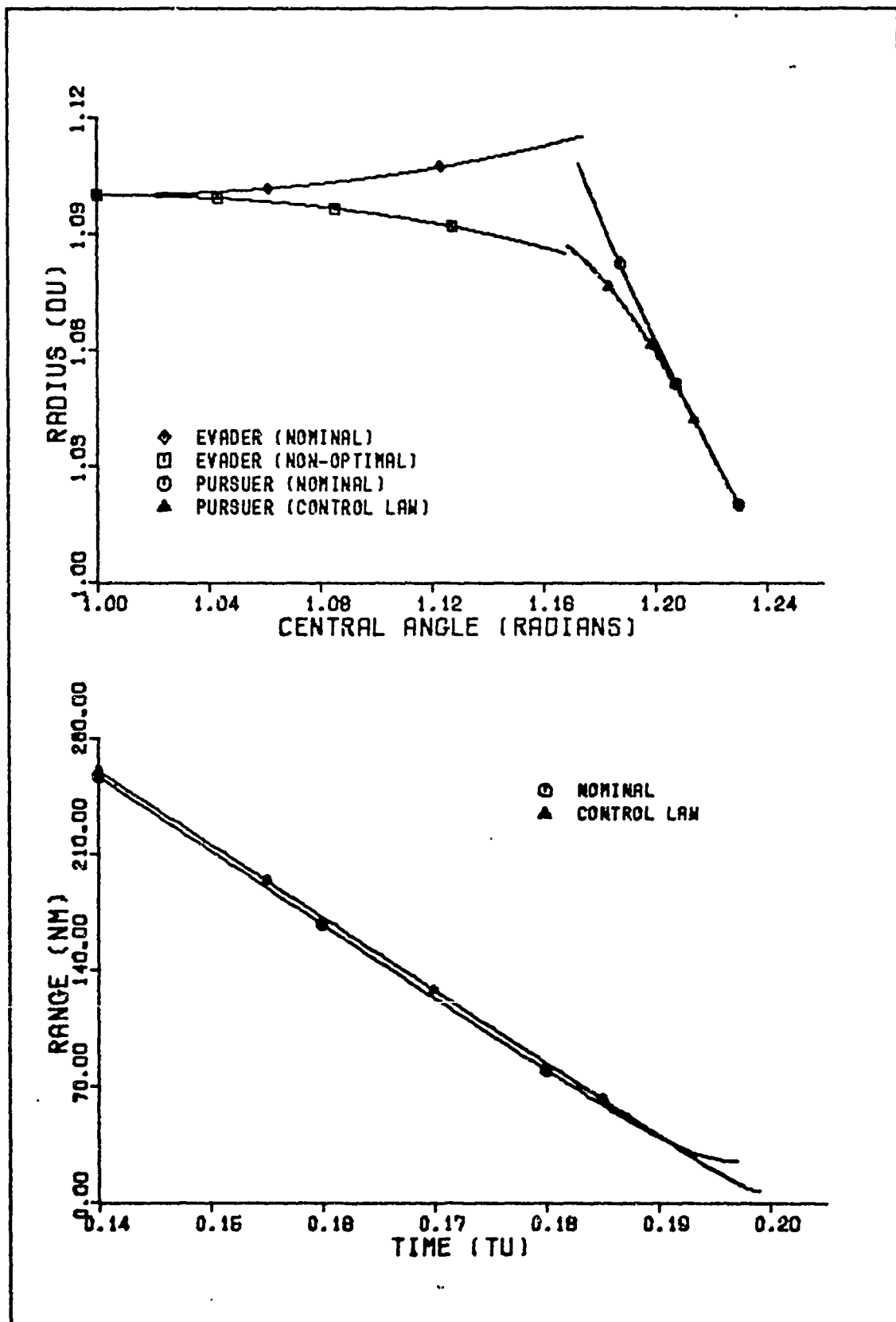


Fig. D-6. Trajectory 2, Backward Sweep Method.
 $V = -2.0$, Sampling Interval = 0.012 TU.

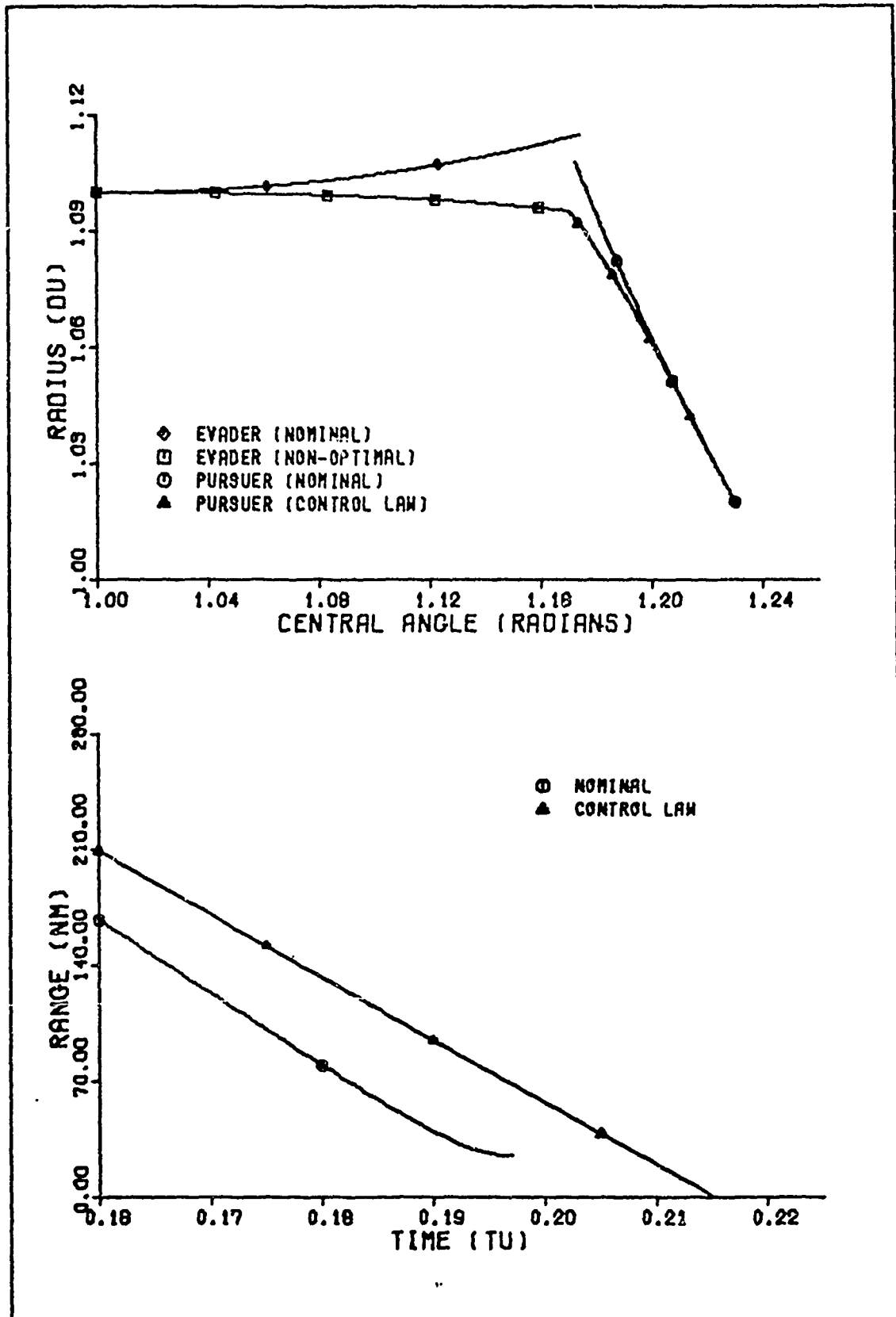


Fig. D-7. Trajectory 2, Backward Sweep Method.
 $V = -3.0$, Sampling Interval = 0.012 TU.

Appendix E

Plots of Trajectory 3

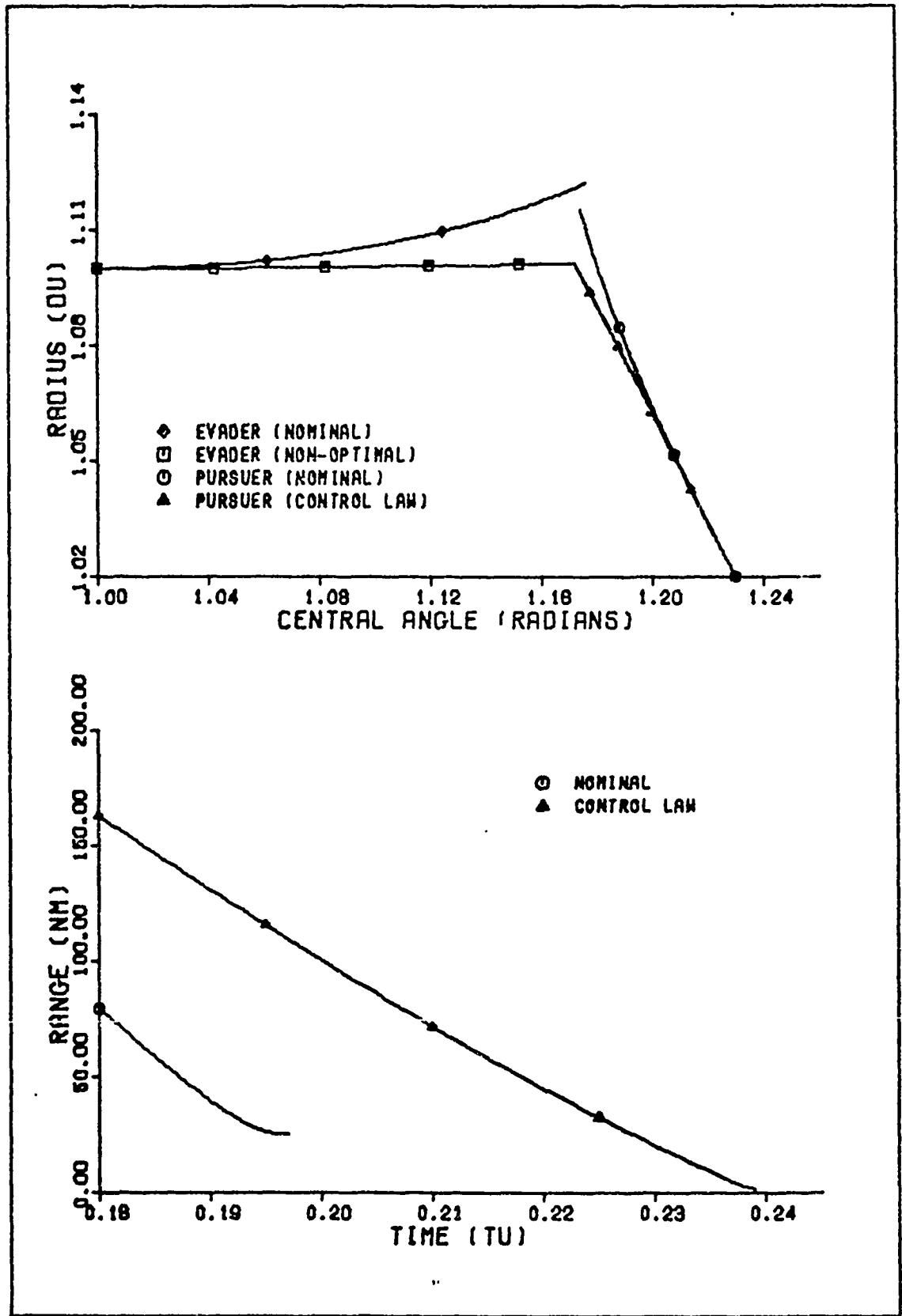


Fig. E-1. Trajectory 3, Transition Matrix Method.
 $V = 3.0$, Sampling Interval = 0.012 TU.

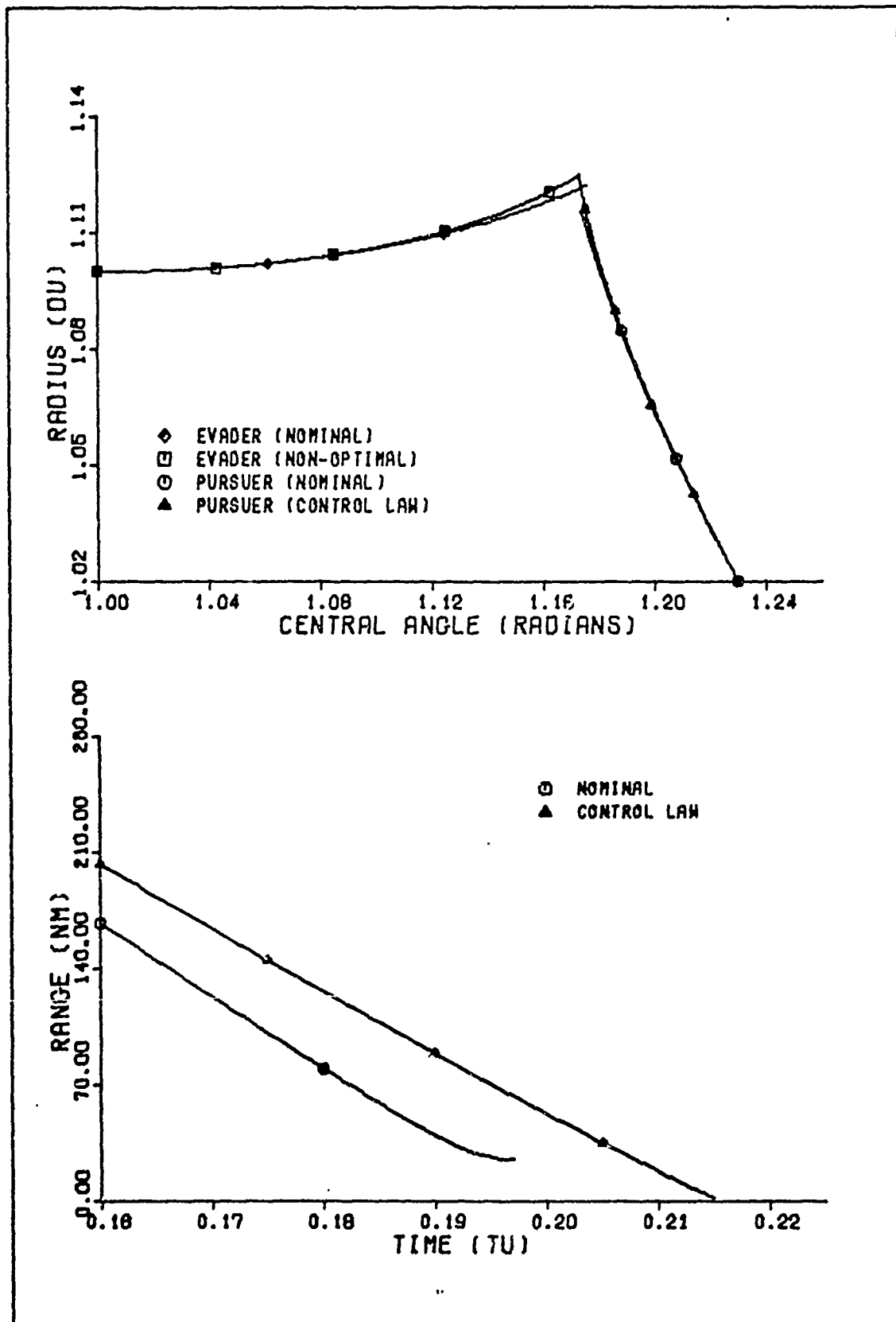


Fig. E-2. Trajectory 3, Transition Matrix Method.
 $V = 2.0$, Sampling Interval = 0.012 TU.

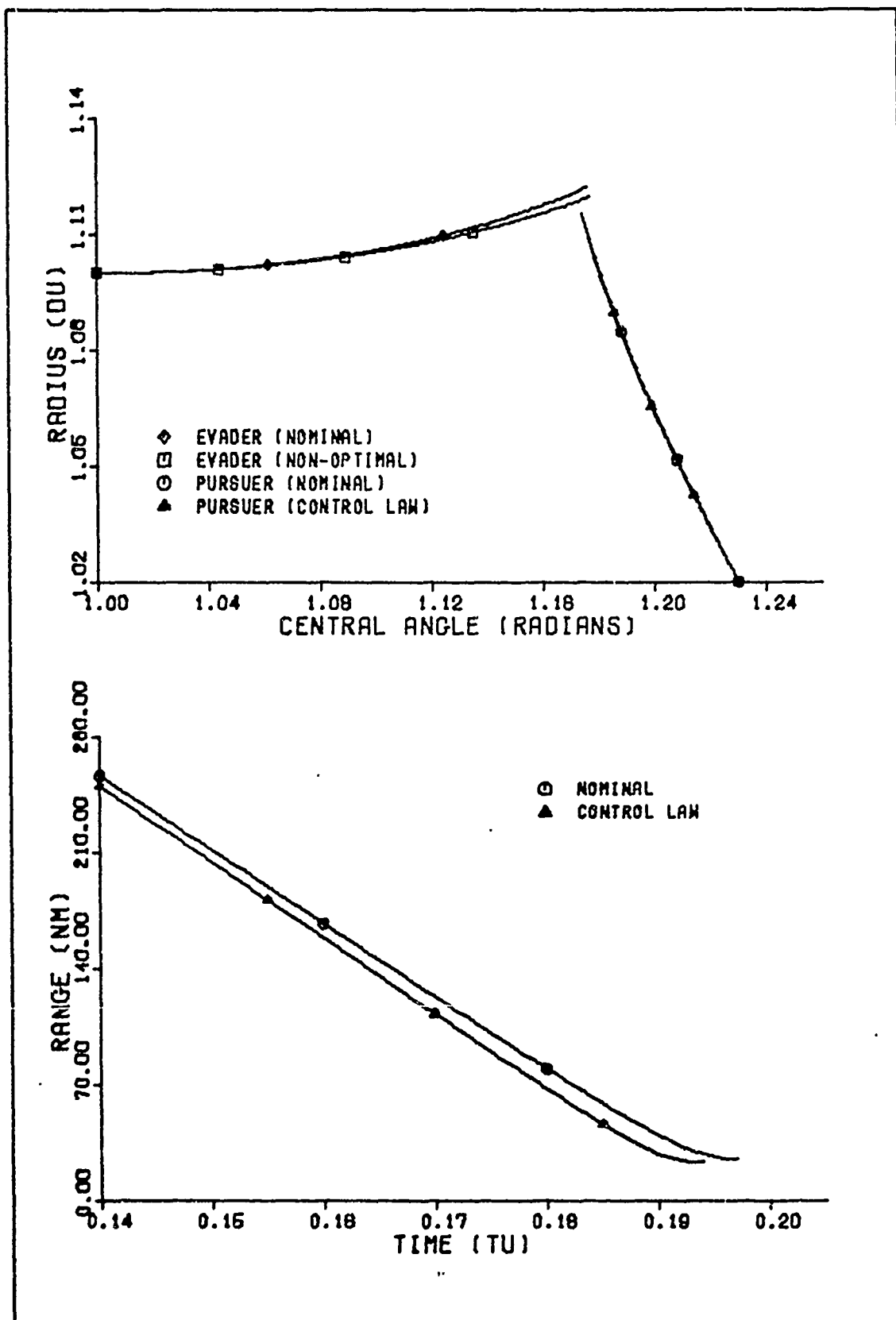


Fig. E-3. Trajectory 3, Transition Matrix Method.
 $V = 1.0$, Sampling Interval = 0.012 TU.

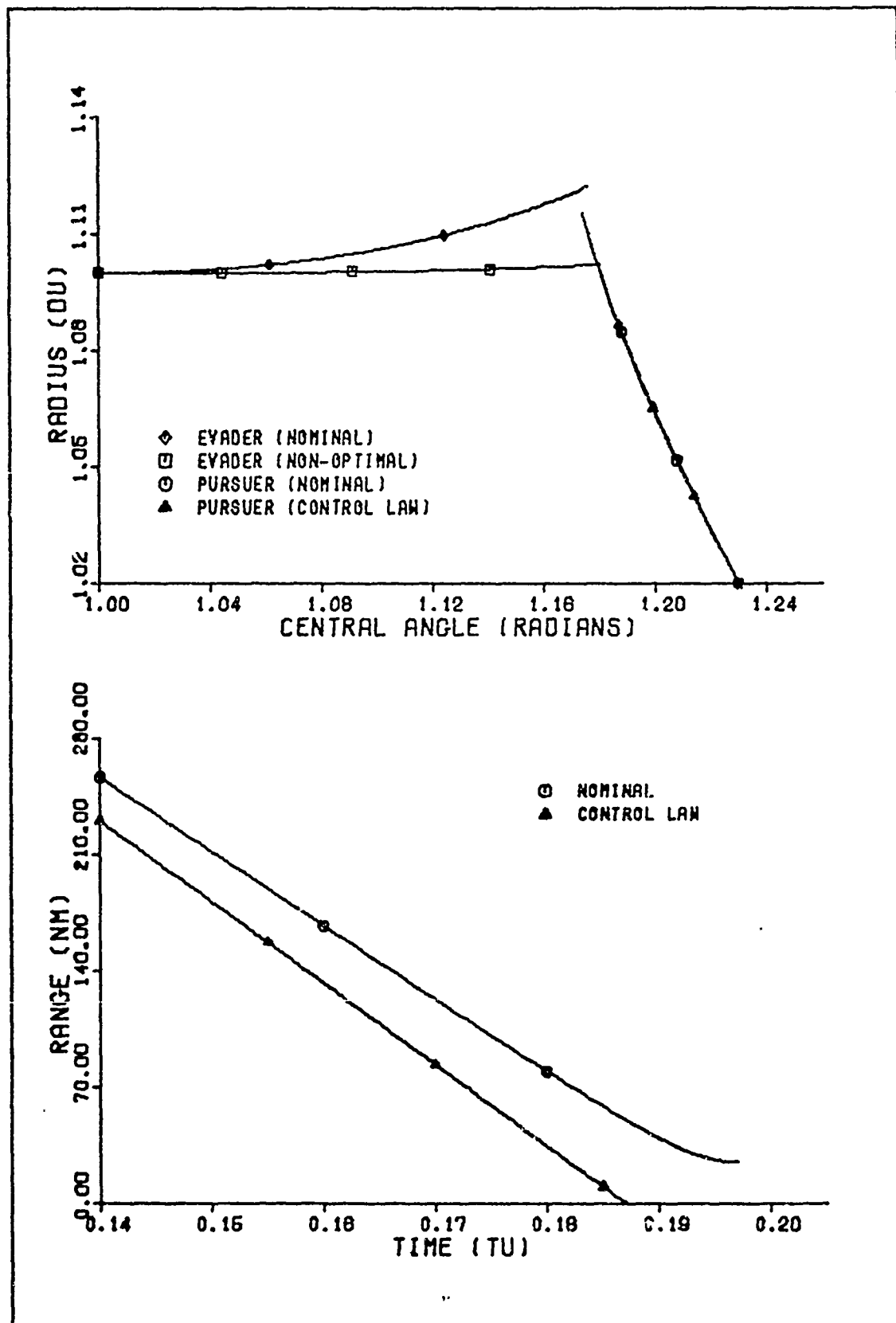


Fig. E-4. Trajectory 3, Transition Matrix Method.
 $V = 0.0$, Sampling Interval = 0.012 TU.

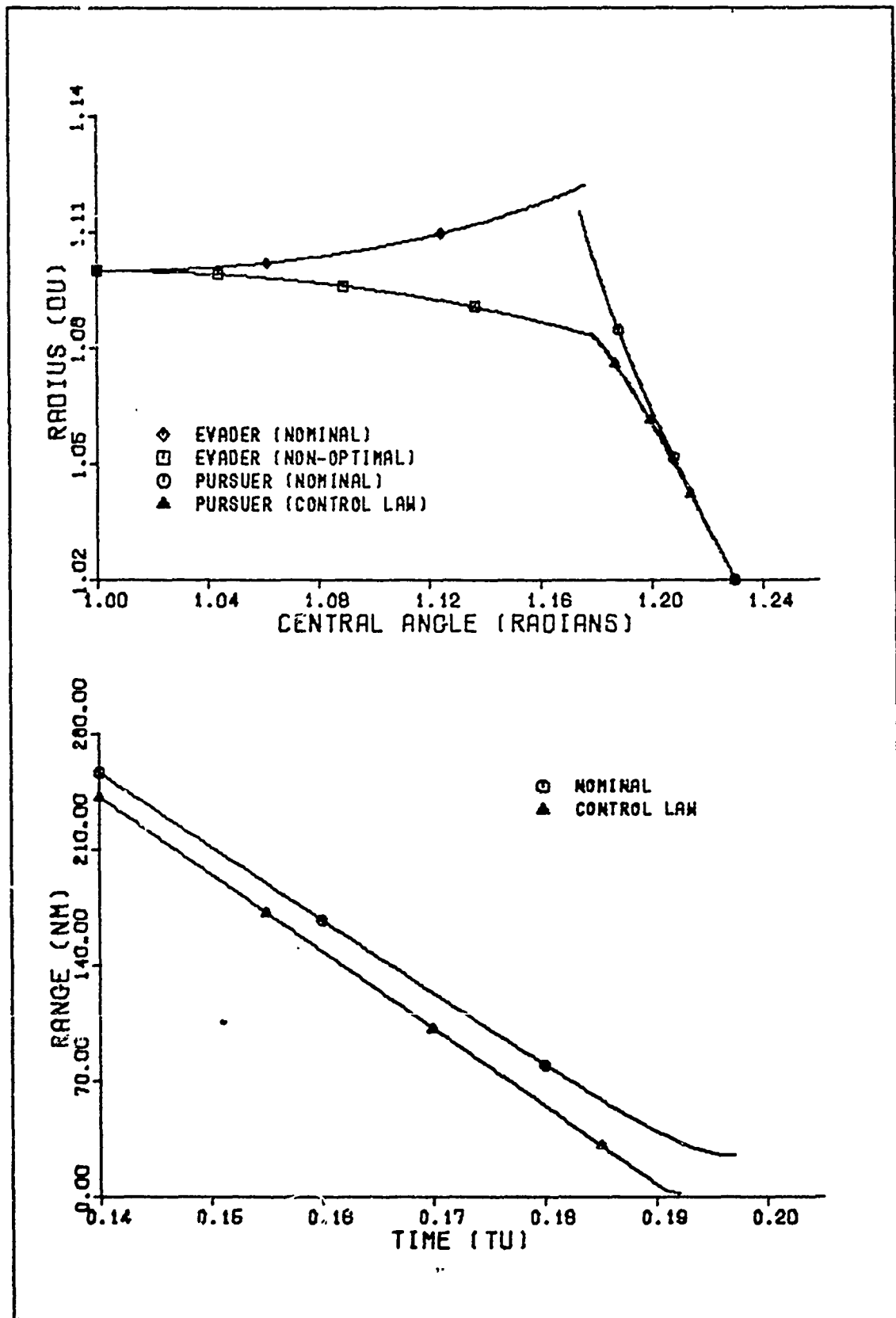


Fig. E-5. Trajectory 3, Transition Matrix Method.
 $V = -1.0$, Sampling Interval = 0.012 TU.

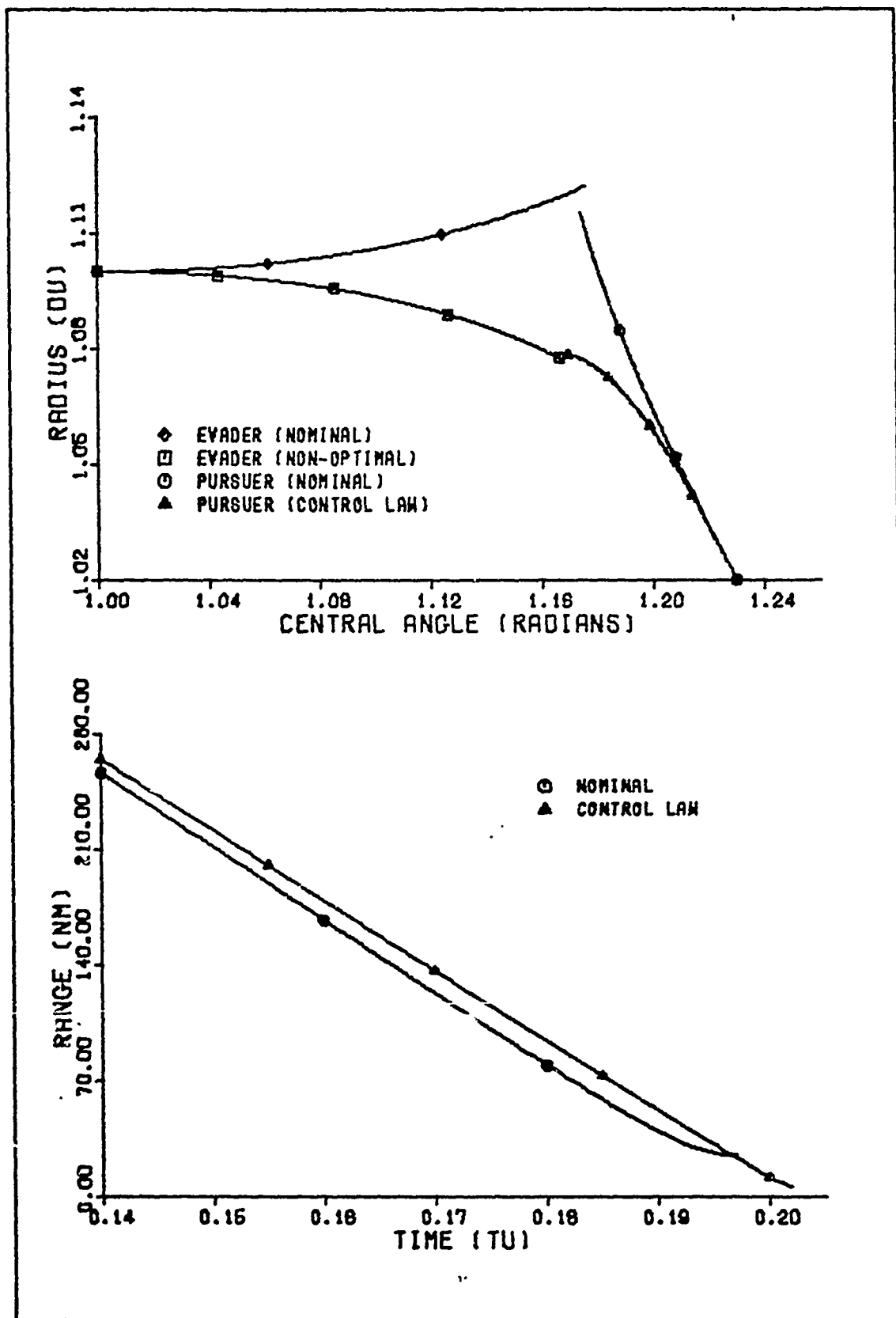


Fig. E-6. Trajectory 3, Transition Matrix Method.
 $V = -2.0$, Sampling Interval = 0.012 TU.

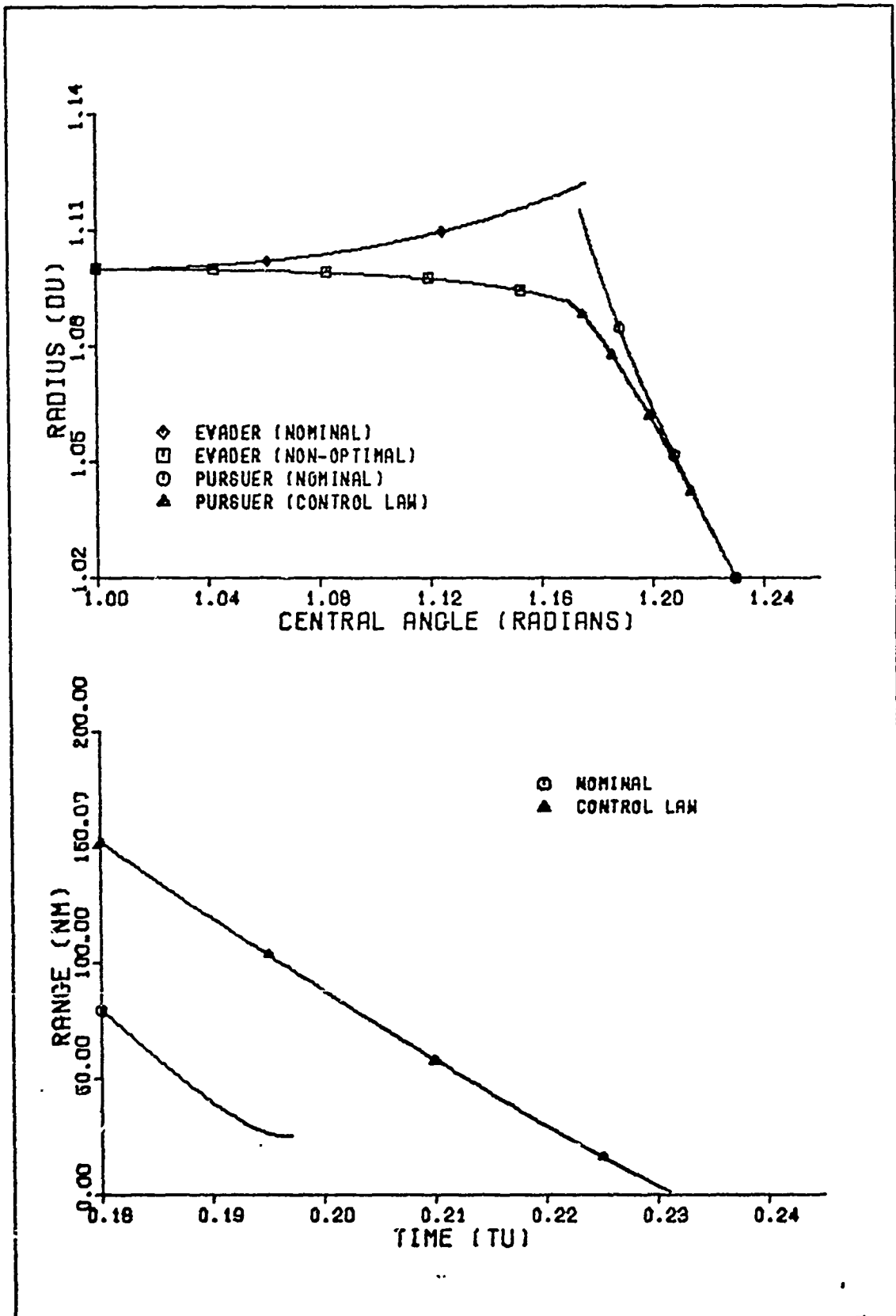


Fig. E-7. Trajectory 3, Transition Matrix Method.
 $V = -3.0$, Sampling Interval = 0.012 TU.

Appendix F

Plots of Trajectory 4

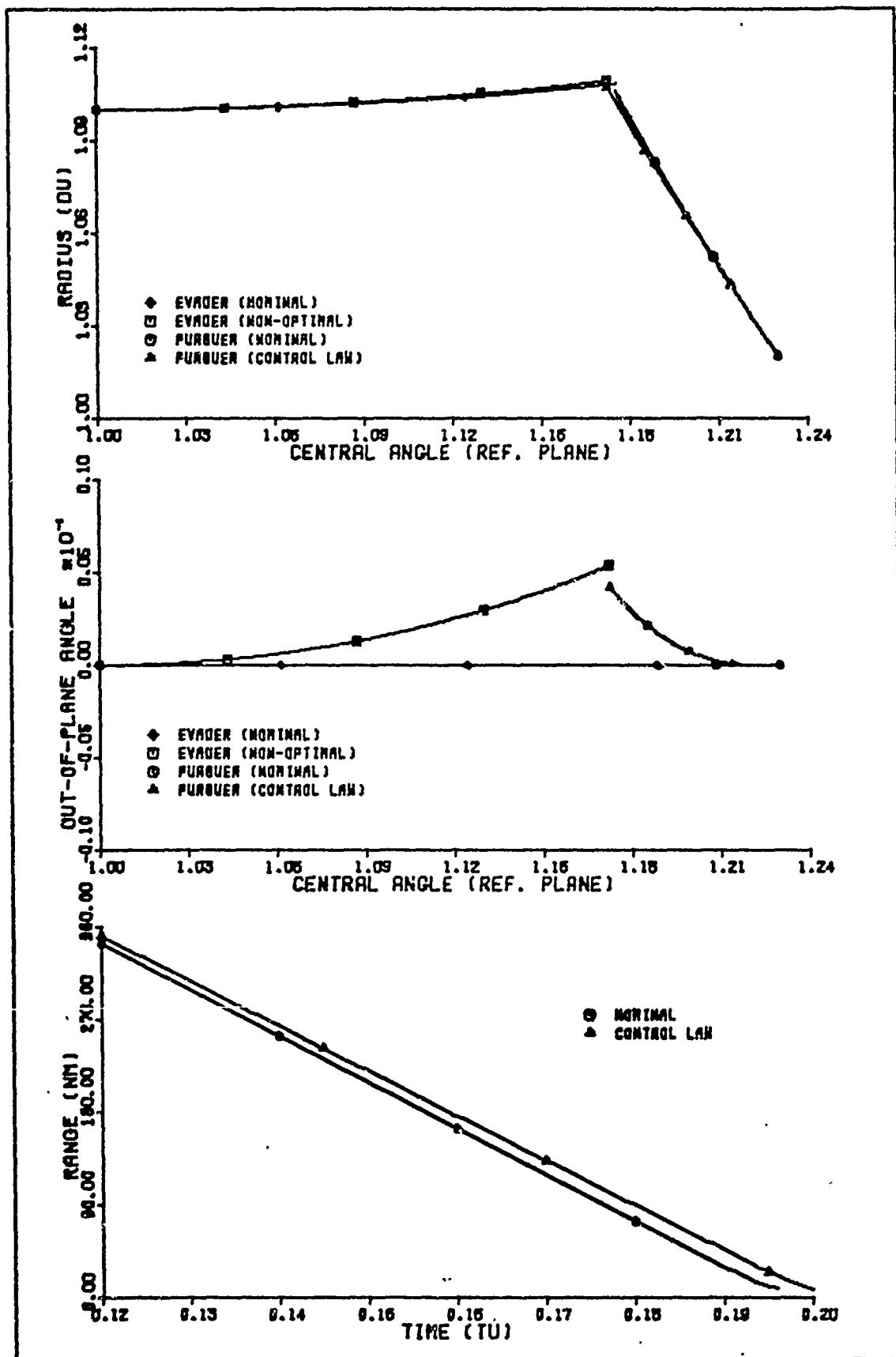


Fig. P-1. Trajectory 4, Backward Sweep Method.
 $V_1 = 0.0$, $V_2 = 1.0$, Sampling Interval = 0.024 TU.

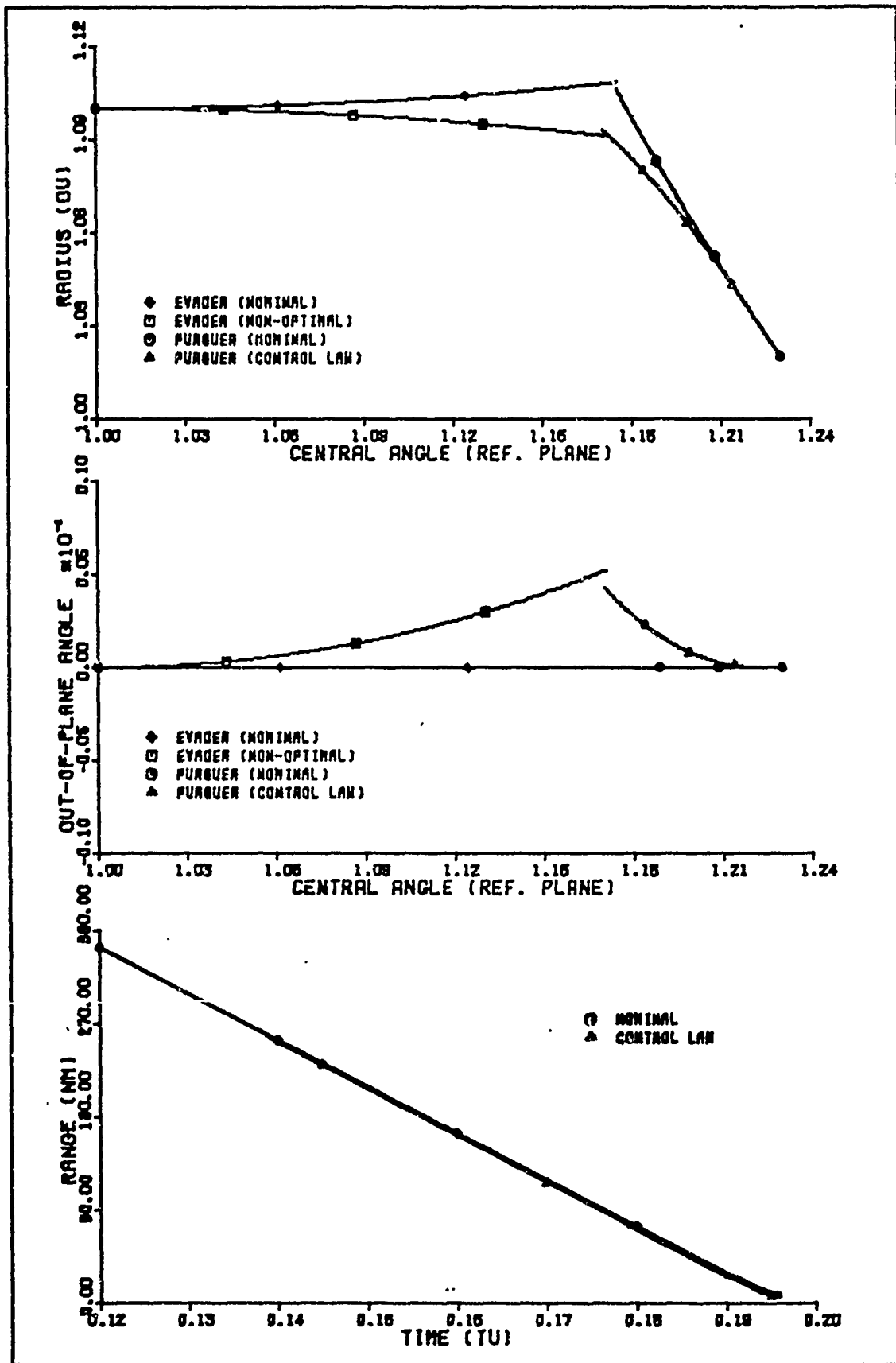


Fig. F-2. Trajectory 4, Backward Sweep Method.
 $V_1 = 0.0$, $V_2 = -1.0$, Sampling Interval = 0.024 TU.

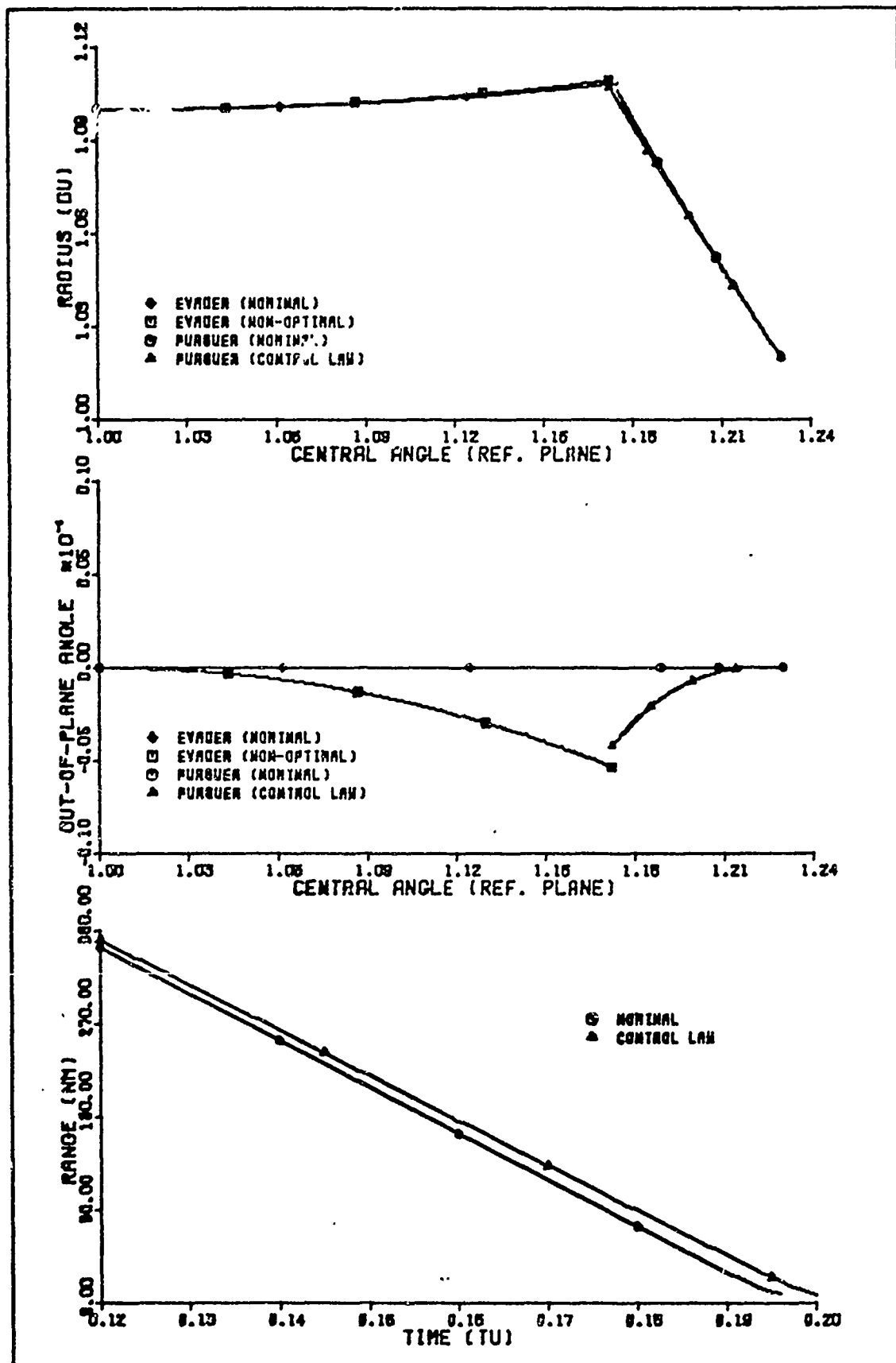


Fig P-3. Trajectory 4, Backward Sweep Method.
 $V_1 = 3.14$, $V_2 = 1.0$, Sampling Interval = 0.024 TU.

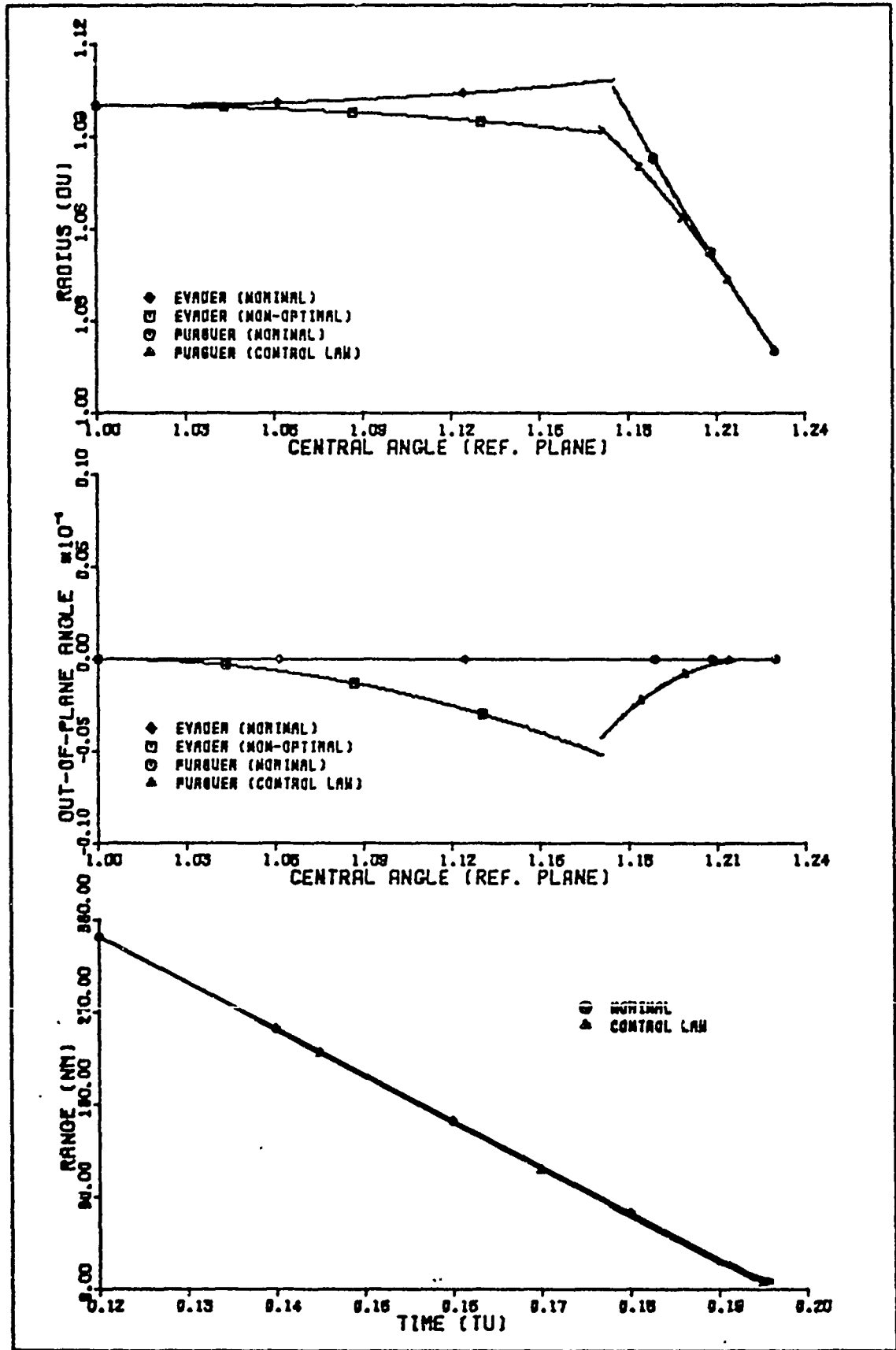


Fig. F-4. Trajectory 4, Backward Sweep Method.
 $V_1 = 3.14$, $V_2 = -1.0$, Sampling Interval = 0.024 TU.

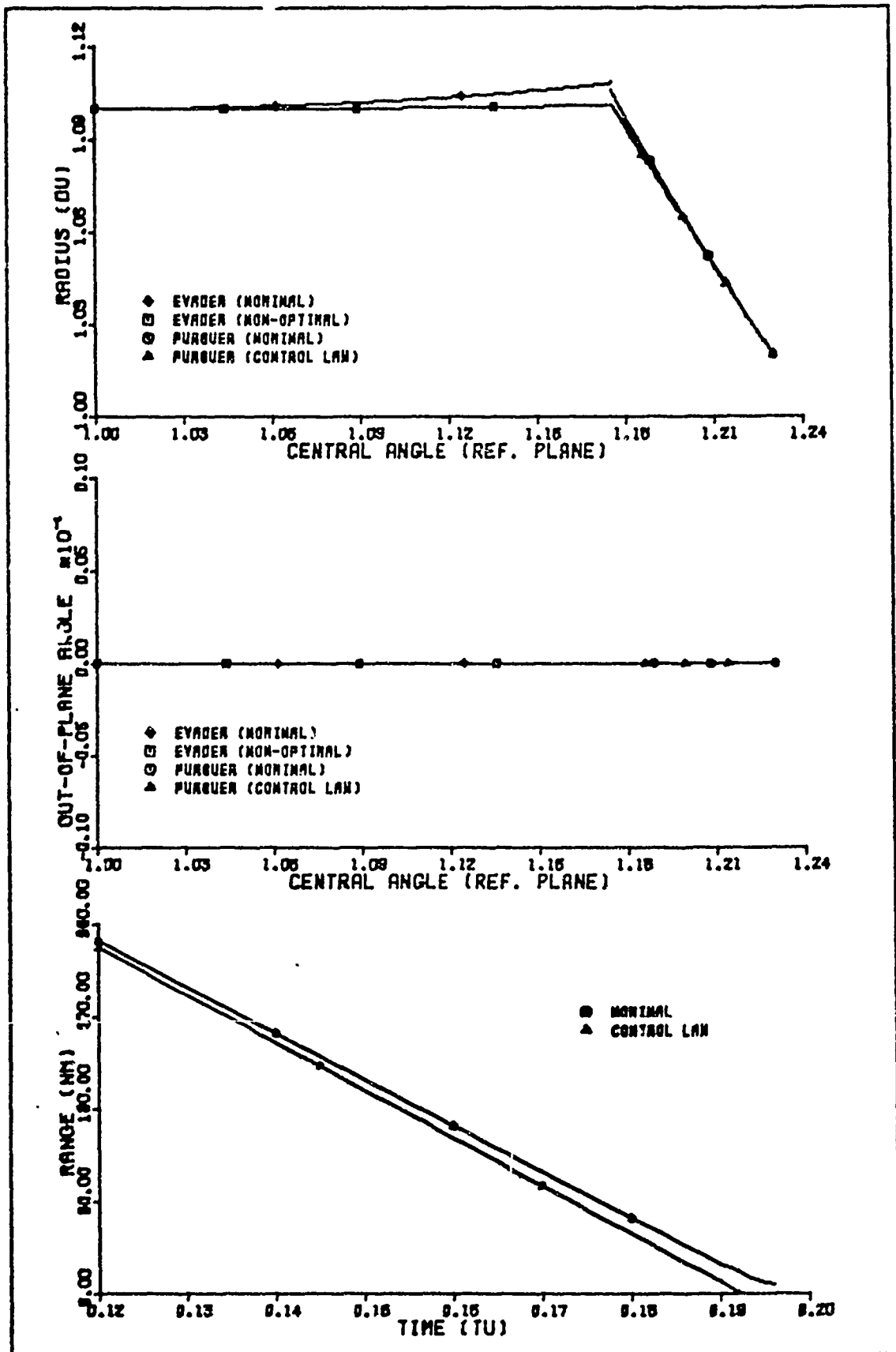


Fig. F-5. Trajectory 4, Backward Sweep Method.
 $V_1 = 1.571$, $V_2 = 0.0$, Sampling Interval = 0.024 TU.

Appendix G

Plots of Trajectory 5

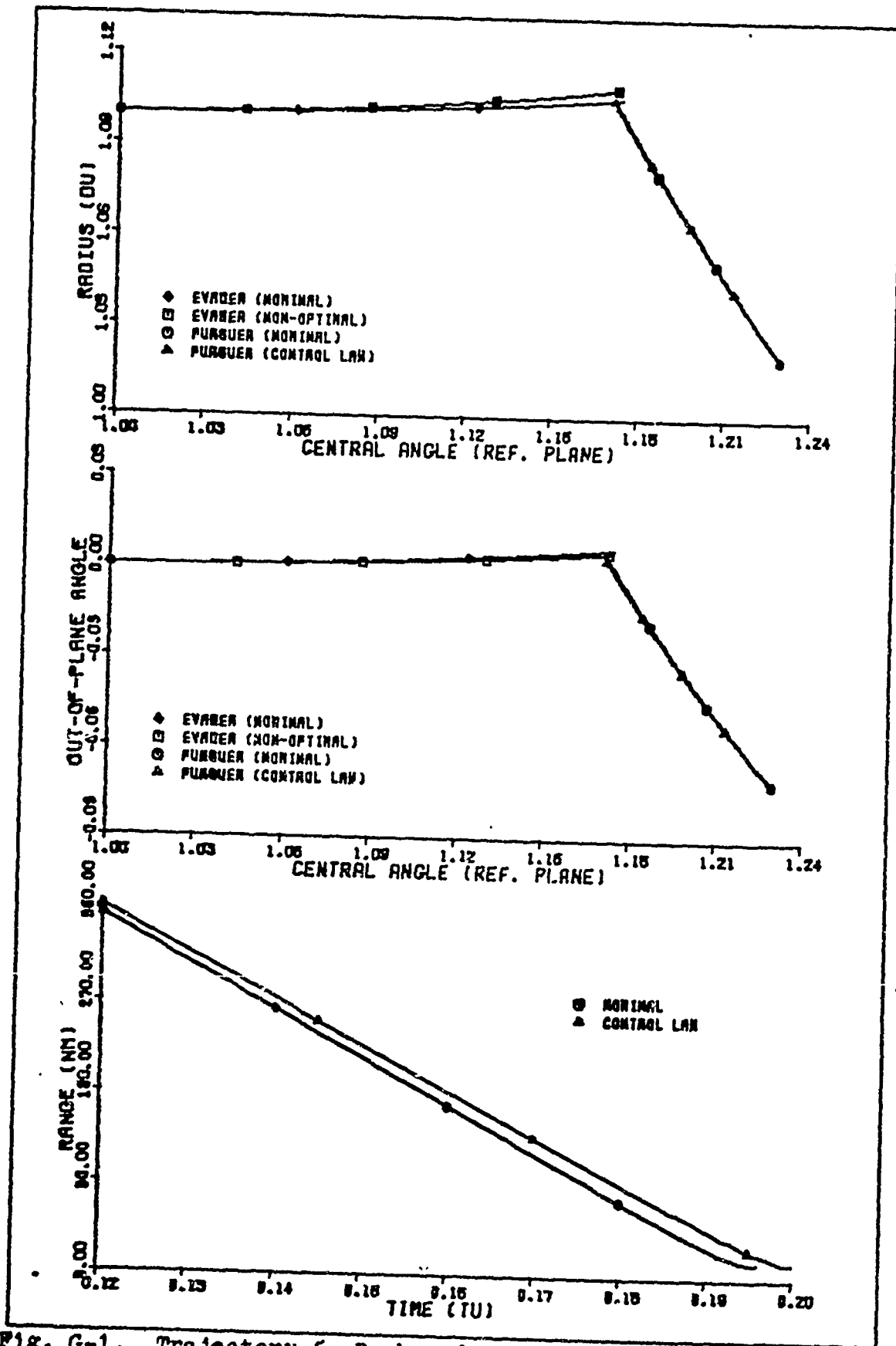


Fig. G-1. Trajectory 5, Backward Sweep Method.
 $V_1 = 0.0$, $V_2 = 1.0$, Sampling Interval = 0.012 TU.

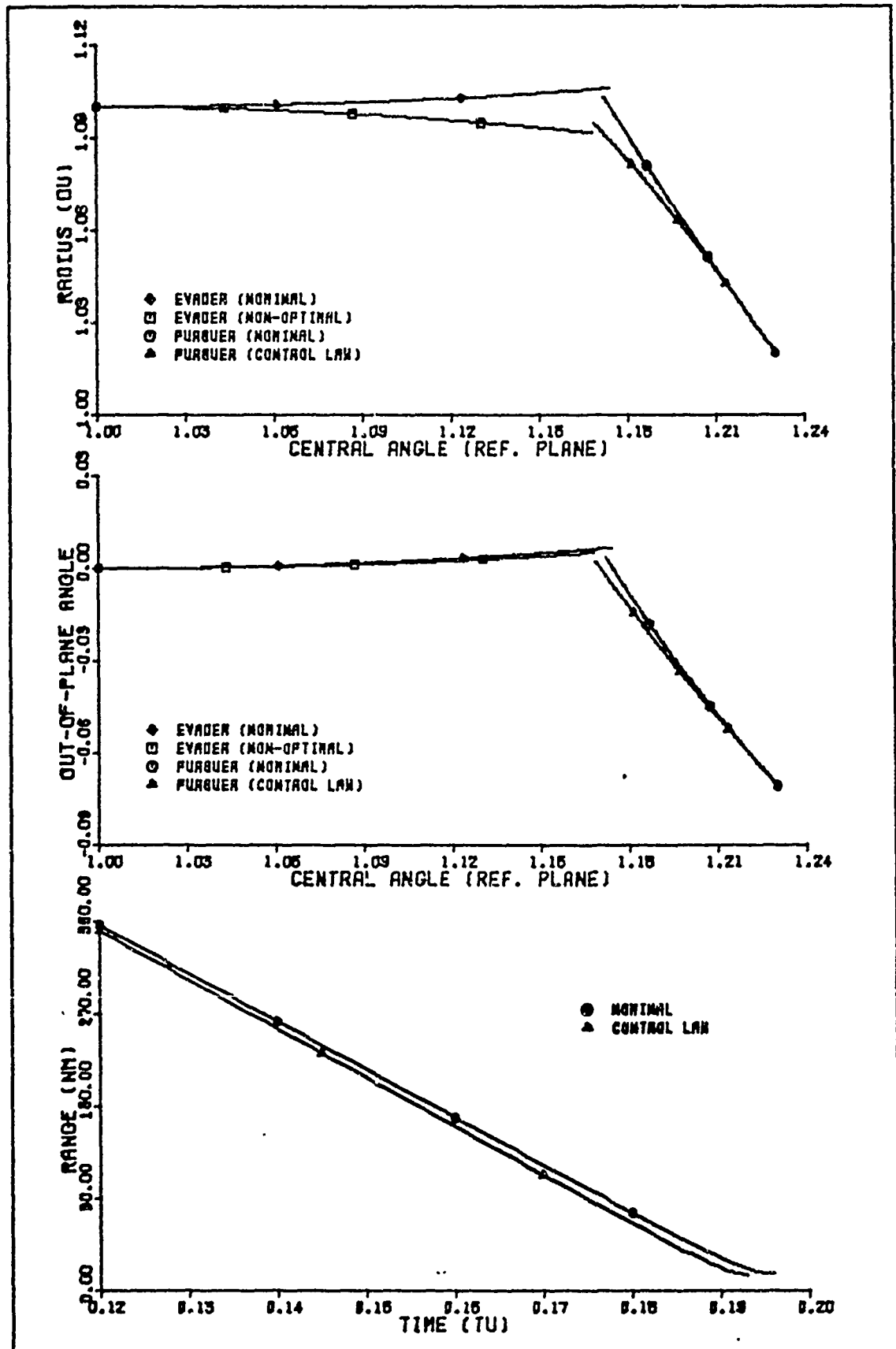


Fig. G-2. Trajectory 5, Backward Sweep Method.
 $V_1 = 0.0$, $V_2 = -1.0$, Sampling Interval = 0.024 TU.

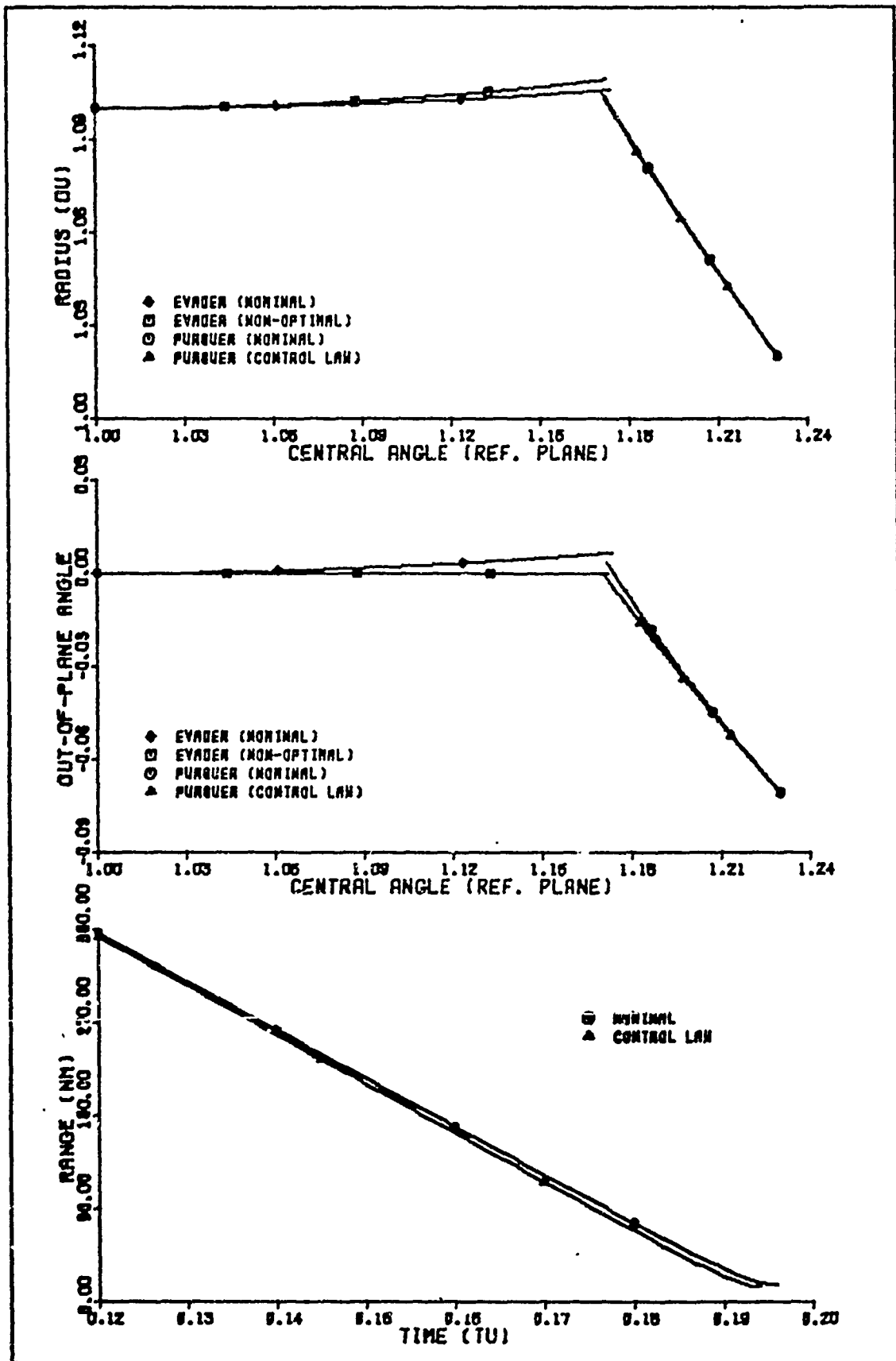


Fig. G-3. Trajectory 5, Backward Sweep Method.
 $V_1 = 1.571$, $V_2 = 1.0$, Sampling Interval = 0.016 TU.

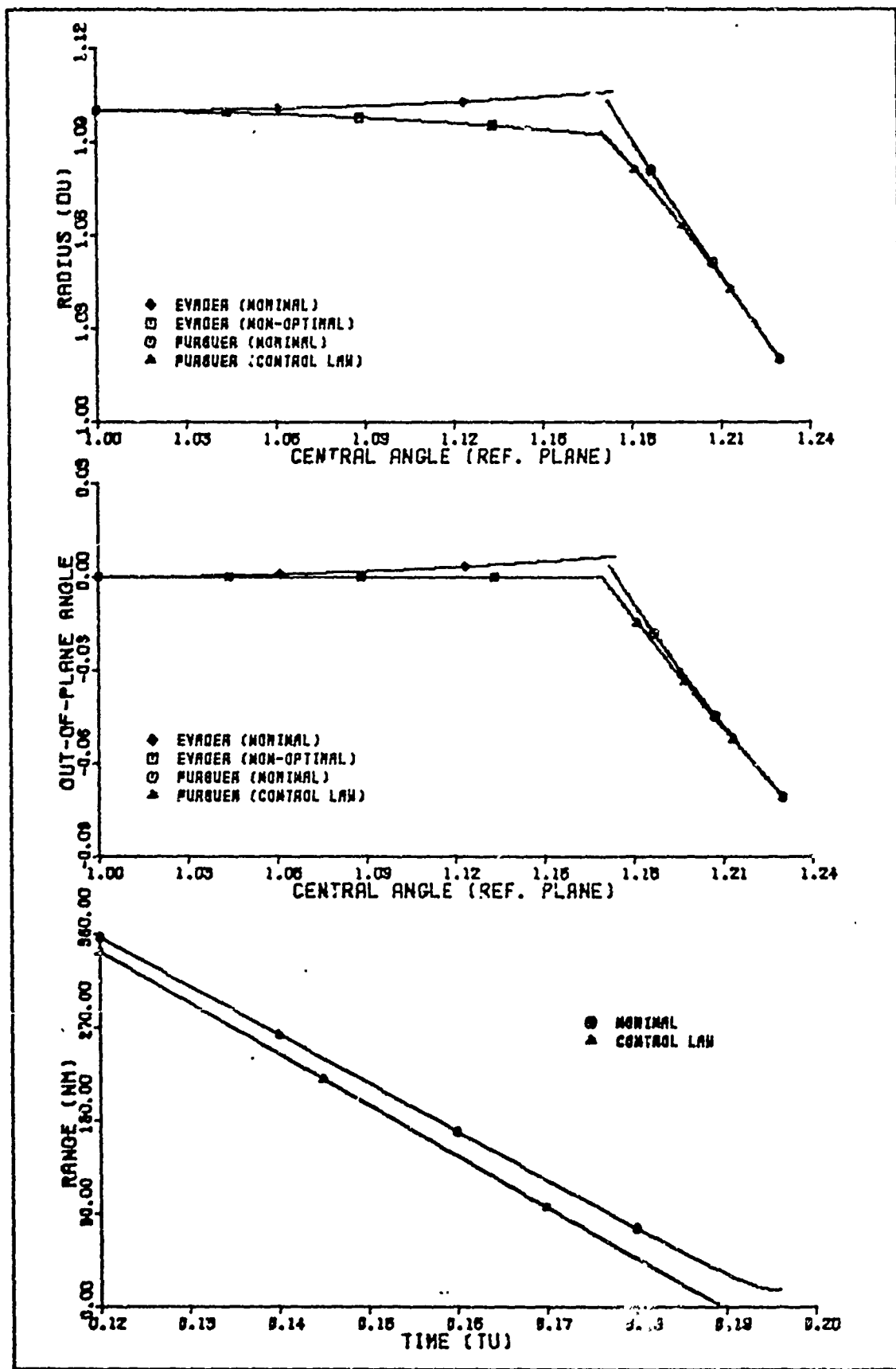


Fig. G-4. Trajectory 5, Backward Sweep Method.
 $V_1 = 1.571$, $V_2 = -1.0$, Sampling Interval = 0.024 TU.

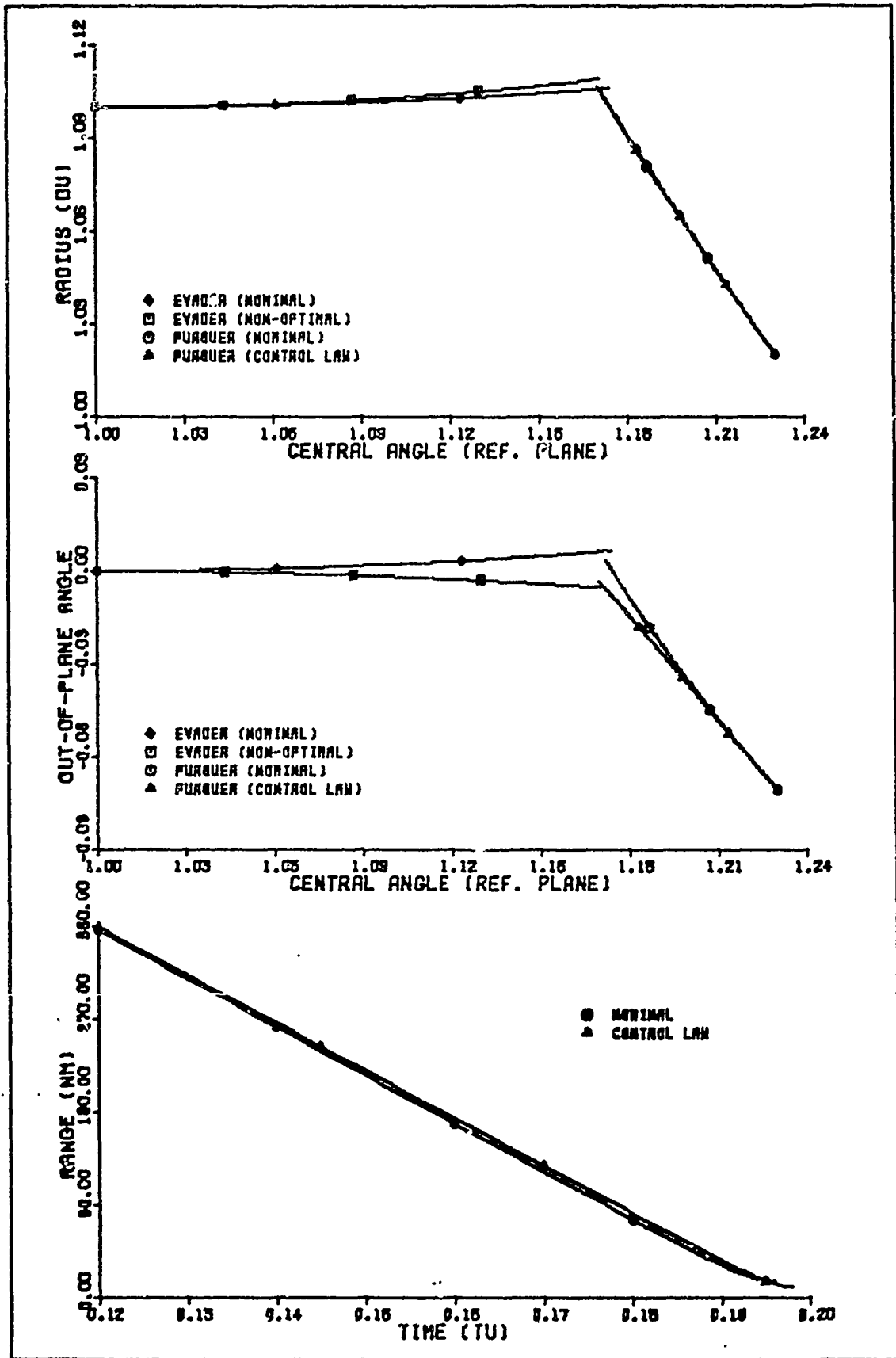


Fig. G-5. Trajectory 5, Backward Sweep Method.
 $V_1 = 3.14$, $V_2 = 1.0$, Sampling Interval = 0.024 TU.

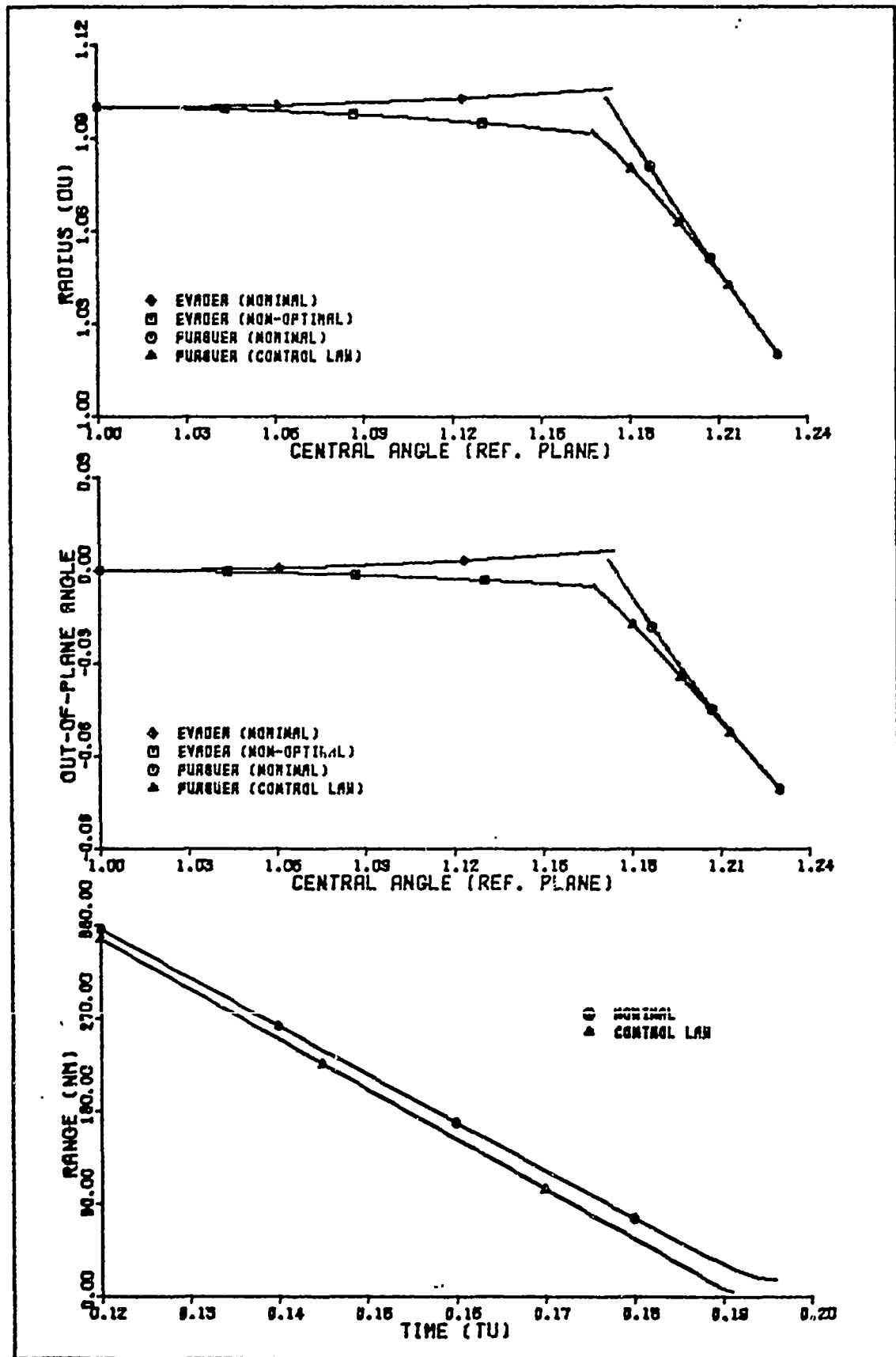


Fig. G-6. Trajectory 5, Backward Sweep Method.
 $V_1 = 3.14$, $V_2 = -1.0$, Sampling Interval = 0.024 TU.

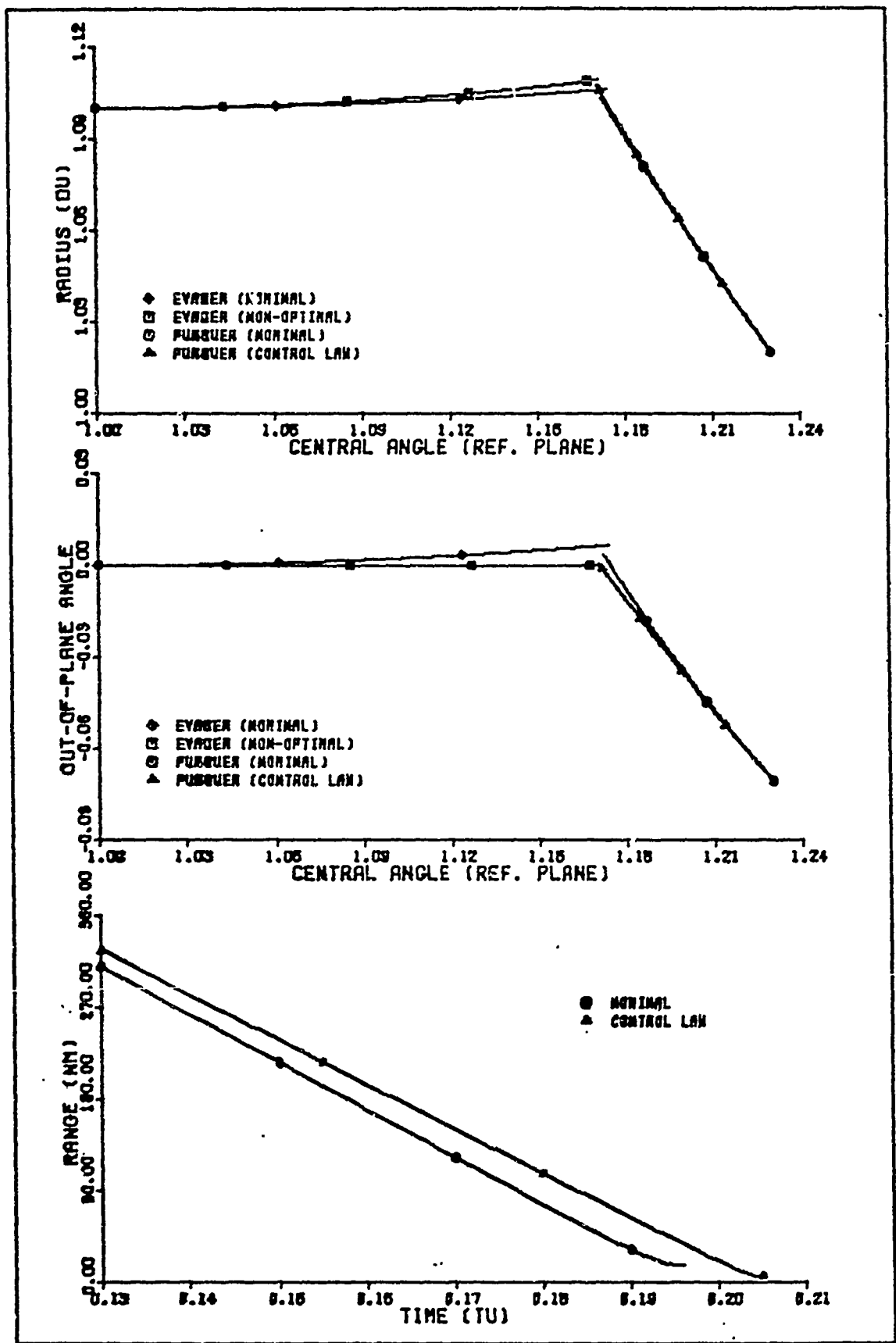


Fig. G-7. Trajectory 5, Backward Sweep Method.
 $V_1 = 4.71$, $V_2 = 1.0$, Sampling Interval = 0.024 TU.

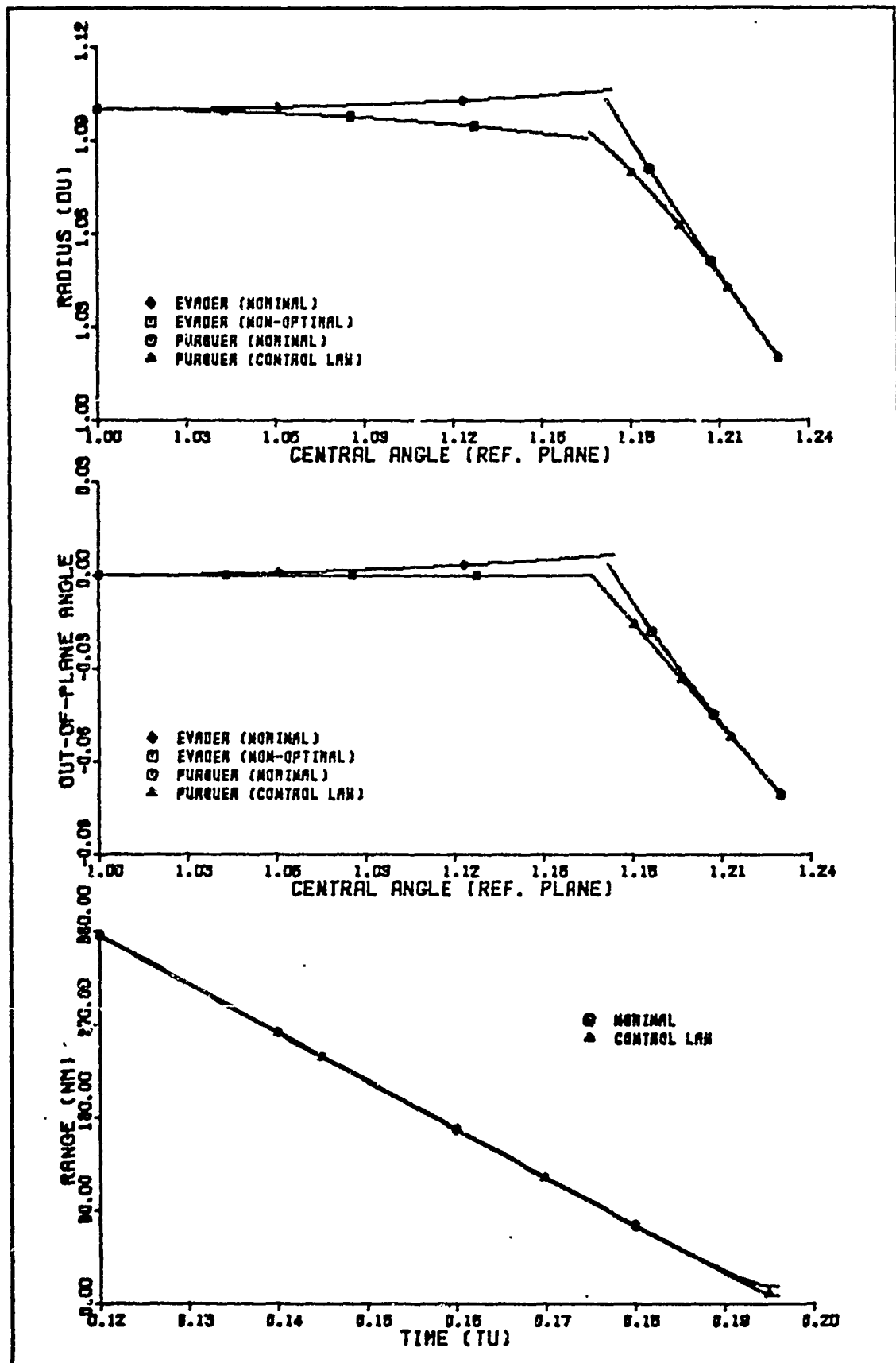


Fig. G-8. Trajectory 5, Backward Sweep Method.
 $V_1 = 4.71$, $V_2 = -1.0$, Sampling Interval = 0.024 TU.

Vita

Gary D. Bohn [REDACTED]
[REDACTED]

He attended Kansas State University where he earned a Bachelor of Science degree in Electrical Engineering. Upon graduation in 1967, he was commissioned through the USAF ROTC program and was assigned to USAF Undergraduate Pilot Training. Following completion of pilot training, he served as a squadron pilot in the F-102 in Germany; as a Forward Air Controller and flight instructor in the O-2A in Southeast Asia; as flight instructor in the T-38; and as a Wing Operations Staff Officer. In June, 1974, he entered the Graduate Astronautical Engineering program at the Air Force Institute of Technology.